THE POWER QUALITY IMPACT FROM THE PHOTOVOLTAIC ROOFTOP TO THE GRID DISTRINUTION SYSTEM USING PSCAD/EMTDC

NATTAPAN THANOMSAT

A DISSERTATION SUBMITTED IN PARTIAL FULLFILLMENT OF THE
REQUIREMENT FOR THE DEGREE OF DOCTOR OF ENGINEERING
PROGRAM IN ENERGY AND MATERIALS ENGINEERING
(INTERNATIONAL PROGRAM)
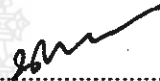FACULTY OF ENGINEERING
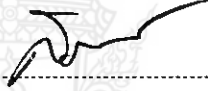RAJAMANGALA UNIVERSITY OF TECHNOLOGY THANYABURI
ACADEMIC YEAR 2018
COPYRIGHT OF RAJAMANGALA UNIVERSITY
OF TECHNOLOGY THANYABURI

THE POWER QUALITY IMPACT FROM THE PHOTOVOLTAIC ROOFTOP
TO THE GRID DISTRINUTION SYSTEM USING PSCAD/EMTDC

NATTAPAN THANOMSAT

A DISSERTATION SUBMITTED IN PARTIAL FULLFILLMENT OF THE
REQUIREMENT FOR THE DEGREE OF DOCTOR OF ENGINEERING
PROGRAM IN ENERGY AND MATERIALS ENGINEERING
(INTERNATIONAL PROGRAM)
FACULTY OF ENGINEERING
RAJAMANGALA UNIVERSITY OF TECHNOLOGY THANYABURI
ACADEMIC YEAR 2018

Dissertation Title	The Power Quality Impact from the Photovoltaic Rooftop
	to the Grid Distribution System Using PSCAD/EMTDC
Name-Surname	Mr. Nattapan Thanomsat
Program	Energy and Materials Engineering
Dissertation Advisor	Associate Professor Boonyang Plangklang, Dr.-Ing.
Academic Year	2018

DISSERTATION COMMITTEE

.... Chairman

(Assistant Professor Wirachai Roynarin, Ph.D.)

.... Committee

(Associate Professor Napaporn Phuangpornpitak, D.Eng.)

.... Committee

(Assistant Professor Sorapong Pavasupree, Ph.D.)

.... Committee

(Associate Professor Krischonme Bhumkittipich, Ph.D.)

.... Committee

(Associate Professor Boonyang Plangklang, Dr.-Ing.)

Approved by the Faculty of Engineering, Rajamangala University of Technology Thanyaburi in Partial Fulfillment of the Requirement for the Degree of Doctor of Engineering

.... Dean of Faculty of Engineering

(Assistant Professor Sivakorn Angthong, Ph.D.)

October 29, 2018

Dissertation Title	The Power Quality Impact from the Photovoltaic Rooftop to the Grid Distribution System Using PSCAD/EMTDC
Name-Surname	Mr. Nattapan Thanomsat
Program	Energy and Materials Engineering
Dissertation Advisor	Associate Professor Boonyang Plangklang, Dr.-Ing.
Academic Year	2018

ABSTRACT

The general trend in the past 10 years of increasing PV system efficiency, low PV system prices, attractive government motivation programs, and other interesting factors have joined synergistically to reduce the block of access for PV systems to have an influence in the market and to develop their commitment to the worldwide vitality portfolio. In the same way, the abnormal situations of power quality which link the PV systems to the distribution network are becoming an important problem as the PV penetration level is increasing continually.

This thesis proposes an impact analysis of power quality from PV rooftop systems integrated with a very small power producer (VSPP) installed capacity of 1 MW, which was associated with the Provincial Electricity Authority (PEA's) distribution network. The power quality information is collected by the power quality analyzer at the Point Common Coupling (PCC) of PEA distribution line 22 kV by 7 days then the design, modeling, and analysis of PV rooftop system connected to the distribution system based on real data from measurement were performed in the PSCAD/EMTDC software simulation. In addition, the simulations in ferroresonance abnormal cases were also implemented. The simulation system comprises of the PV rooftop system, capacitance in long line, nonlinear saturated distribution transformer core, and a single phase switching breaker connected to the grid distribution system.

From the monitored data, it was found that the highest power yield was 778.125 kW while the simulation result was 815 kW. Moreover, based on the PEA standard EN 50160 with the cumulative percentile at 95% of power quality measurement for PV rooftop system, the measured data showed that the power quality of the PV rooftop system passed the PEA regulations for its distribution network connecting system. From the simulation result, it showed that the ferroresonance phenomenon will occur if a single phase switching breaker was switched one by one and the transformer core was saturated causing the overvoltage, overcurrent, and the destruction of the distribution transformer and other apparatus in the distribution network. This important phenomenon can help the operators for future maintenance and operations to protect the disrupted distribution network.

Keywords: power quality, PV rooftop systems, ferroresonance, PSCAD/EMTDC

Acknowledgements

First of all, I would like to acknowledge and thank the help, support and consultation from my academic advisor, Associate. Prof. Dr.-Ing. Boonyang Plangklang, he gave to me which showed the clear guidance and encouragement through my studies. He has been valuable to me through his comments, and suggestions which have always been a source of knowledge for me.

Secondly, I would like to thank the committee members of both the proposal and thesis defense for their useful comments and suggestions including: Asst. Prof. Dr. Wirachai Roynarin, Associate. Prof. Dr. Napaporn Phuanpornpitak, Asst. Prof. Dr. Sorapong Pavasupree, Associate. Prof. Dr. Krischonme Bhumkittipich, and Prof. Dr. Eng. Hideaki OHGAKI who showed me the successful and useful way toward completion of this work. Moreover, many thanks go to Faculty of Engineering, Rajamangala University of Techonology Thanyabui, for the assistance, support, and the provision of facilities.

Thirdly, I would like to thank to the Faculty of Engineering, Burapa university that provide scholarships for my doctoral education.

Finally, I would like to thank to my family for all love, all support and encouragement.

Nattapan Thanomsat

Table of Contents

Table of Contents (Continued)

List of Tables

List of Figures

List of Figures (Continued)

List of Figures (Continued)

List of Figures (Continued)

CHAPTER 1

INTRODUCTION

1.1 Background and Statement of the Problems

In 20 Century, the power system is look like Traditional industrial conception of the electrical energy supply. The large power plant generates the electricity, normally located near to the primary energy source (for example: coal mines) and distantly from the end user centers. The electrical energy is transferred to the end user using a large transmission line infrastructure, which ties high voltage (HV), medium voltage (MV) and low voltage (LV) networks. These networks are designed to operate radially. The power can flow in one direction: from high voltage levels down-to low voltage to the end users situated along the radial lines. In this process, there are three stages to be sent over before the power reaching the final user, that call "generation, transmission and distribution" as show in Figure 1.1. The distribution is the final stage which is the most important part of the power system, as the final power quality depends on its reliability [1].
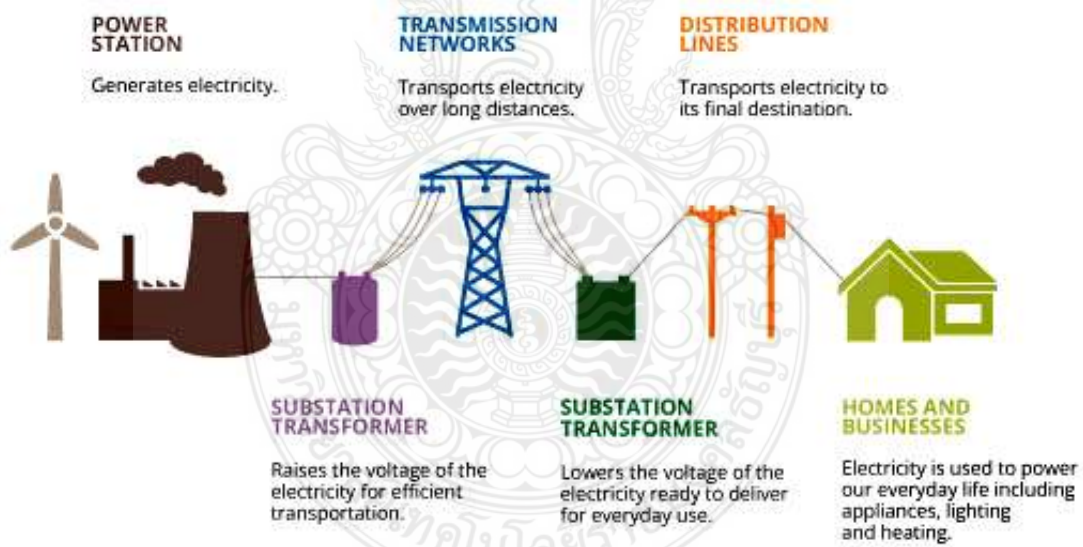
Figure 1.1 Traditional industrial conception of the electrical energy supply [2].

In present, power system is decentralization generation. A lot of small power plant with used renewable energy source such as photovoltaic (PV) Farm, Wind Farm are installed in the distribution system [3]. In the new conception, the generation electrical energy is not specific to large power station. Therefore, some of the electrical energy demand is supplied by the centralized generation and another part is produced by

decentralization generation as show in Figure 1.2. The electrical energy is going to be produced near to the customers or produced by the customers [4], [5].
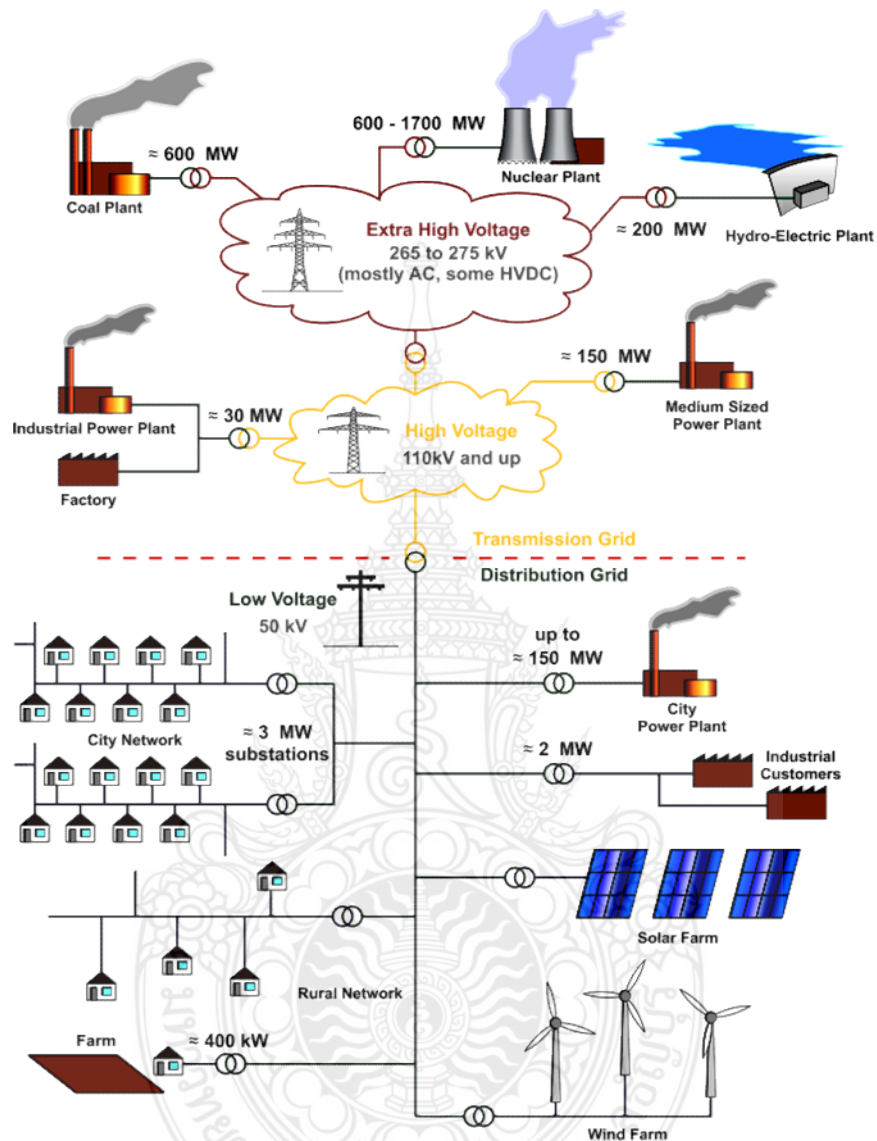
Figure 1.2 New industrial conception of the electrical energy supply [3]

In Thailand, the power system of the Provincial Electricity Authority (PEA) is stable in the distribution system. The government is encouraging people to play a role and invest in electrical energy generation [6]. The decentralization generation in the form of PV rooftop system (PVRS), which are connected to the distribution network of PEA in the low voltage distribution system 380/220 V. The result of PVRS connected to the distribution system of PEA has contributed to the power quality (PQ) in the system that is likely to change in the direction of better or worse. The PQ is very important in distribution network. It is defined as the characteristic of the voltage, current and frequency of the power supply in normal conditions. Poor PQ can cause damage to

electrical equipment and distribution component. Therefore, it is essential to study, analysis, and review from research paper and academic paper that relates both positive and negative impacts, as well as solutions to potential problems of electrical energy generation [7] - [9]. These are for technical information for planning purposes, promote and use as design information and configure system. This thesis addresses the issues incurred impact of PQ, in case that a number of PVRS are connected to a radial system.

1.2 Purpose of the dissertation

The objectives of the dissertation are as follows:

1.2.1 To measured PQ from real PVRS under PEA's grid code condition.

1.2.2 To study the PQ issues such as voltage, current, frequency, active power, reactive power, voltage and current fluctuations, and harmonic distortion of voltage and current from real PVRS.

1.2.3 To study an impact PV rooftop connected to the distribution system with simulation under normal and abnormal case condition.

1.3 Scope and Limitations

The scope and limitations of this research are as follows:

1.3.1 Measure PQ from real PV rooftop system under PEA's grid code condition.

1.3.2 Analyze the PQ issues such as voltage, current, frequency, active power, reactive power, voltage and current fluctuations, and harmonic distortion of voltage and current from real PVRS.

1.3.3 The PQ impact of PV rooftop connected to the distribution system with simulation by PSCAD/EMTDC will be investigate under normal and abnormal case condition.

1.4 Outline of the dissertation

This thesis contains 5 chapters and one appendix. It is organized as follows:

CHAPTER 1: INTRODUCTION

This chapter is a brief introduction of the background and general statement of the problem, purpose, scope, and utilization of the thesis.

CHAPTER 2: THEORETICAL AND LITERATURE REVIEW

This chapter will include a summary of the theoretical relevant to this thesis and previous research that needed to explain the parameters to gain more understanding of PVRS, PQ standard and PEA grid code.

CHAPTER 3: IMPLEMENTATION

This chapter describes the overall methodology, techniques, and simulation for analysis of the PQ impact from the PV rooftop on Distribution Networks.

CHAPTER 4: THE MEASUREMENT AND SIMULATION RESULTS

This chapter describes the measurement results of the evaluation of the power quality measurements of the large PV Rooftop capacity 1 MW and the simulation results of the effect of PVRS grid connected that will investigate under abnormal situation using PSCAD/EMTDC.

CHAPTER 5: CONCLUSIONS AND FURTURE WORK

The conclusions are presented in this chapter. The chapter ends naming some of the works that can be done in the future with reference to the work presented in this thesis.

Appendix

It presents Data sheet of solar cell, PSCAD application note and list of Publications.

1.5 Utilization of the dissertation

1.5.1 To obtain the information and insight about the PQ from the PVRS, that are connected to the distribution system of PEA.

1.5.2 To have a better understanding the impact of the potential quality problems and to be able to solve them.

1.5.3 To obtain improving PVRS that could increase the penetration level of PV rooftop system in the distribution system.

CHAPTER 2

THEORITICAL AND LITERATURE REVIEW

This chapter describes the basic theories for Photovoltaic Rooftop System (PVRS), the Power Quality (PQ) and the simulation software PSCAD. Firstly, each major equipment is explained as well as the details of PV rooftop fundamental component and their functions. Secondly, the PQ affecting the operation and efficiency of based power systems are also given. Thirdly, impacts of grid-connected PV system on grid networks are explained. Fourthly, commercial simulation software tool is explained. And finally, literature reviews are fully given.

2.1 Overview of PV system

The free energy resource to generate electrical energy is one of the essential works for research. Conversion of energy from radiation of sunlight to direct current through a solar cell has become an extensive. Advantage of solar cell applications because of free, reliable and efficient energy source is forecasted to increase in coming year [10]. In addition, the number of PVRS on the residential homes connected to the distribution network has increased very interesting.

In a grid connected PVS, also known as a "on-grid", or "grid-tied" PVS, the solar panels or PV array are electrically connected or "tied" to the main distribution network which transfers electrical energy back into the grid system. The PV system Grid connected always have a connection to the distribution network by a suitable inverter because the solar panel or PV array only transfer DC power. The system is shown in Figure 2.1.
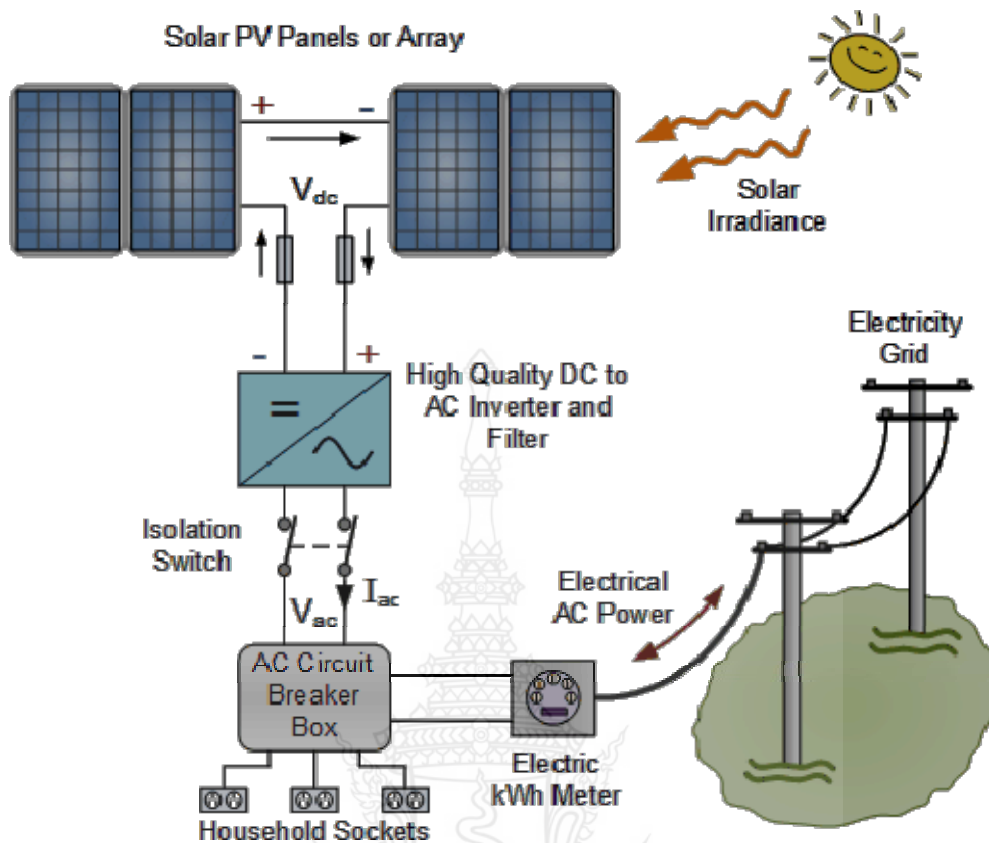
Figure 2.1 The simplified grid connected PV System [11].

2.2 The main of Grid connected Photovoltaic Rooftop system

The main of PV rooftop system, as seen in Figure 2.1, comprises of solar cell converting sunlight into direct current and its control system, the PV inverter are AC converters used to convert the DC input into a sinusoidal AC output with variable frequency and amplitude, and the filter mechanism which is an imperative implementation block to keep the harmonic of voltage and current within joint standard. This section describes about them.

2.2.1 Solar Cell or PV module

The PV array, made up of single solar modules, is the main component in PVS. The photons in the sunlight energize electrons in the semiconductor material after a solar cell is exposed to light. Since material properties of the semiconductor, the positively charged "holes" and the negatively charged electrons which they leave behind are separated. These consigns a voltage across the solar module, which creates it possible to obtain a current flowing through a connected load [12]. The function of a solar cell is shown in Figure 2.2

17
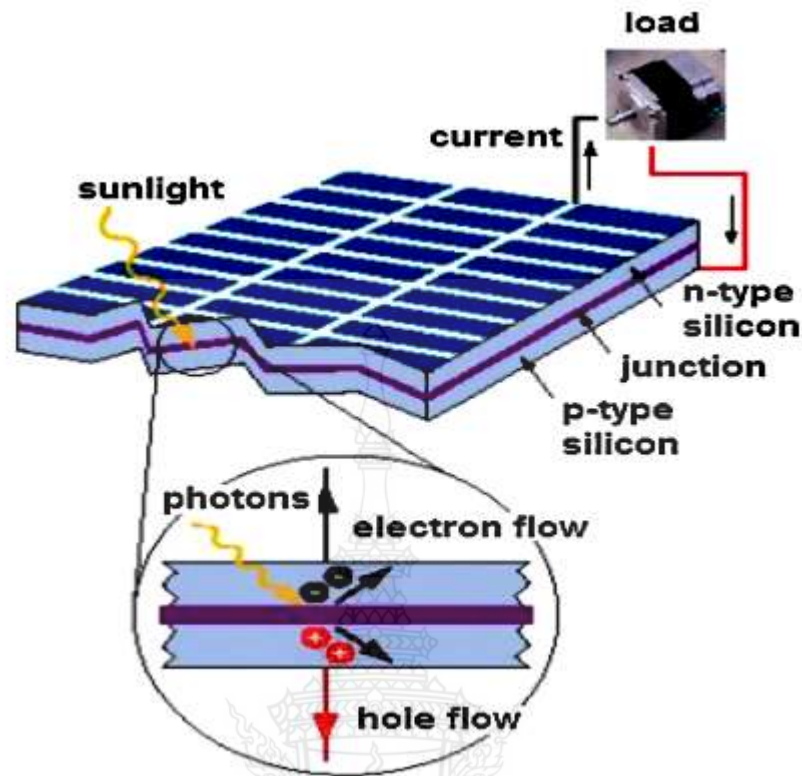
Figure 2.2 The function of a solar cell [12].

When the energy is high enough, both electrons and holes will run to match together. The electrons run to the n-type layer and the holes run to the p-type layer. All electrons run together at the Front Electrode and all holes run together at the Back Electrode. The electrical circuit from the Front Electrode and Back Electrode is complete, it will generate electricity because both electrons and holes run to match. The intensity of light and temperature are important variables that contribute to solar cell efficiency.

2.2.2 Types of solar cells

The crystalline silicon and amorphous silicon (thin film) are the two major types of solar cell materials used. There are three general types of solar cell, that made from silicon. First, monocrystalline silicon, second, polycrystalline silicon, and the last, thin film silicon [13].

2.2.2.1 Monocrystalline silicon

It is a single crystalline type with higher purity of silicon than poly crystalline. The monocrystalline is more expensive than polycrystalline and high efficiency about 18%. The monocrystalline solar cells have been improved and

18

developed by reduce reflecting solar radiation inside of the cell and is exposed to light most at n-layer. That mean, solar cell can increase the efficiency up to 25%.

2.2.2.2 Polycrystalline silicon

The polycrystalline silicon has less purity of silicon than the monocrystalline silicon. The performance of polycrystalline silicon is lower than the monocrystalline silicon but higher than amorphous silicon. The efficiency is between 12% and 15%. The polycrystalline silicon Solar cell is silver mixed with other minerals that are attached.

2.2.2.3 Amorphous silicon (thin film)

Due to their non-single crystal structure, requiring larger sized cells. The thin film solar cells suffer from poor cell conversion efficiency and has been implemented efficiency about 6-10%.

2.2.3 The solar irradiance and temperature that affects solar cells

The solar cells have more efficient in converting solar energy into electricity in Cold temperature and it works better than in high temperature. Solar cells are electronic devices that produce electricity from the sun. Some mechanisms are not conducive to working in high temperature conditions. But in winter, solar cells can generate electricity less than in summer, because the daylight in winter is shorter than in summer. Moreover, there are a lot of cloud motion in winter.

2.2.4 Characteristics of a solar cell

A circuit equivalent one-diode model display normally a solar cell, that shown in Figure 2.3. This circuit can be applied for a single solar cell, a PV module comprise of a number of cells, or an PV array comprise of several modules [13].
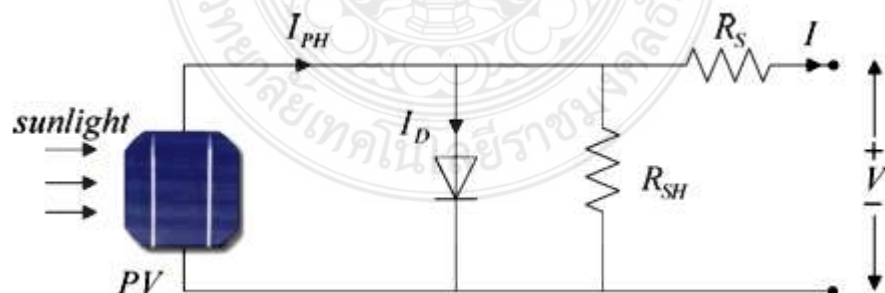
Figure 2.3 A ciruit equivalent of solar cell [13].

This circuit that shown in Figure 2.3 comprise of a current source or photocurrent, I_{PH}, one diode, and a series resistance R_S, which shows the resistance

inside each cell. The diode has also an internal shunt resistance. The net current, I, is the difference between the photocurrent I_{PH}, and the normal diode current I_D, given by [13]:

$$I = I_{PH} - I_D - \frac{V + IR_S}{R_{SH}} = I_{PH} - I_0 \left[\exp(\frac{e(V + IR_S)}{kT_C}) - 1 \right] - \frac{V + IR_S}{R_{SH}} \qquad (2.1)$$

It should be noticed, in the event that the shunt resistance is normally much bigger than a load resistance, and the series resistance is much smaller than a load resistance. Therefore, it can be ignoring these two resistances. Then the net current, I, given by

$$I = I_{PH} - I_D = I_{PH} - I_0 \left[\exp(\frac{eV}{kT_C}) - 1 \right] \qquad (2.2)$$

where

k is Boltzmann's gas constant, 1381×10^{-23} J/K;

T_C is absolute temperature of the cell (K);

e is electronic charge, 1602×10^{-19} J/E;

V is voltage imposed across the cell (V);

I_0 is dark saturation current, which depends strongly on temperature (A).

Another main equation is for open circuit voltage V_{OC} equation, that given by

$$V_{OC} = \frac{kT}{q} \ln(\frac{I_{PH}}{I_0} + 1) \approx \frac{kT}{q} \ln(\frac{I_{PH}}{I_0}) \qquad (2.3)$$

The amount of solar irradiance and temperature of the solar cell influence the output power of the solar cells. Its I-V and P-V curve characteristic can describe the electrical characteristic of the solar cell. Figure 2.4, shows the behavior of the output current, voltage, and power for constant solar irradiance and temperature.
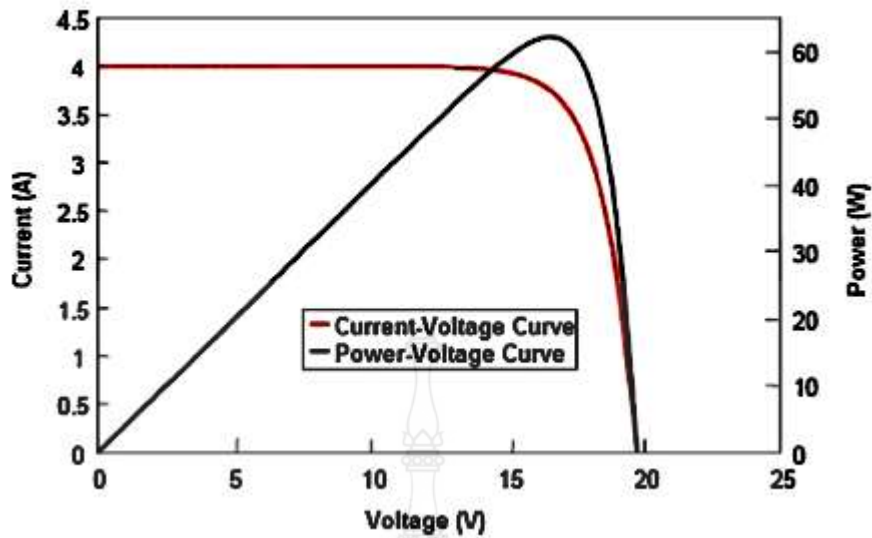
Figure 2.4 I–V curve of solar cell with the variation of power [14].

2.2.5 A Photovoltaic Array (PV Array)

A perfect PV system uses a PV array as the main voltage source for the generated electricity. The amount of output power produced by a single solar panel or module is not enough for use. The PV array can produce the required power output by connecting many single solar panels in series (for a higher voltage demand) and in parallel (for a higher current demand). The structure of PV array is shown in Figure 2.5.
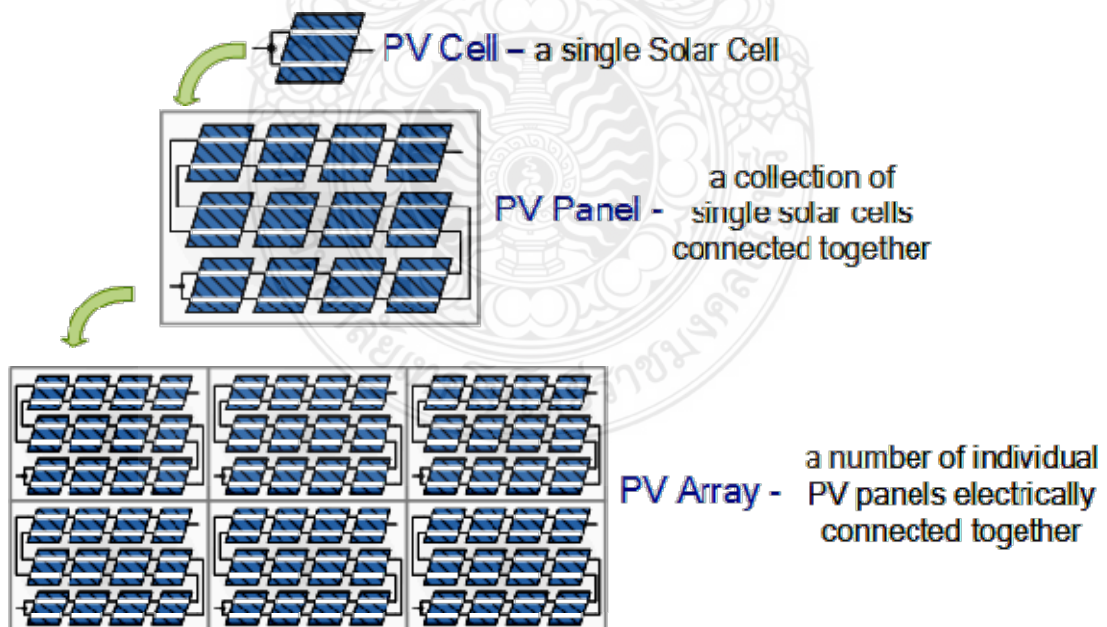
Figure 2.5 The structure of PV array [11].

2.2.6 The PV Inverter for Grid Connected

The PV Inverter is a major power electronic device that are AC converters used to convert the DC input into a sinusoidal AC output with variable frequency and amplitude for feeding directly into the distribution grid. In addition, the PV inverter is one of important PV system that requires attention in harmonic analysis. Because it is considered as contributor to network harmonic distortion of voltage. Due to its substitution mechanism causing harmonics in line current.

The PV inverter from any manufacture must be in accordance with IEC 61727 and IEC 62116. The PV inverter's electrical specification in Thailand must be in accordance with the regulations of the Provincial Electricity Authority of Thailand or other with the results of test are reported.

2.2.7 Filters

The major normal types of filters were found to be the LC and the LCL filters, in studying the available filters implemented within PV inverter [15], [16], [17] as shown in Figure 2.6. the filters are necessary to implement by standards [18], [19], [20] specially where the harmonic in line currents are important.

Figure 2.6 (a) A LC filter and (b) a LCL filter, as required for PV inverter harmonic filtering in line currents. [21]

2.3 The distribution network or grid

In the power system, the electrical energy is generated in power plant and then it is transferred through the transmission line. In the final stage, the distribution network is designed to deliver the electrical energy to the end users or the customers. The electrical energy can be transmitted by overhead lines or underground cables. A distribution line is designed by a 3×3 series impedance matrix which is shown in per unit based on the nominal line-to-ground voltages [22]. In most of the cases in Thailand, distribution lines are placed overhead line due to maintenance take to easy. Depending on the feeder performance, a distribution system can be divided into two basic ways: radial and loop systems [23].

2.4 Power quality issue relate to PV Rooftop system

Power quality is the characteristic of the current, voltage and frequency of the power supply in normal conditions, not to cause electrical equipment to malfunction or to damage [24] – [28]. The abnormal effect on PVRS is caused by dependence of PVRS on some of power supply model, which are also categorized in power disruptions. From the PQ disturbance in the IEC 61000 series can be classified as follows.

2.4.1 Voltage sag or Voltage dip

Voltage sag is the phenomena that cause the voltage to fall to 10% to 90% of the normal voltage [30]. The duration of this event is less than 1 minute. Under IEEE1159 standard, voltage drop is referred to as "Voltage Sag", referring to the voltage remaining in the system. According to EN50160 and IEC61000 standard, "Voltage Dip" refers to the voltage that is lost from normal operation [31]. Voltage sag or voltage dip is shown in Figure 2.7.
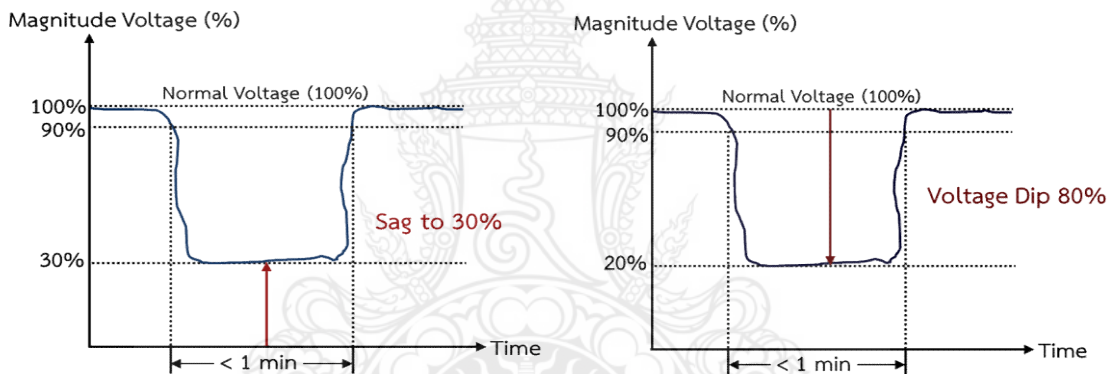
Figure 2.7 The charateristic of votage sag or voltage dip.

2.4.2 Voltage Swell

Voltage Swell, that is shown in Figure 2.8, is a phenomenon that results of voltage increase more than 110% over the normal voltage. The duration of the event is less than 1 minute [32] – [35].
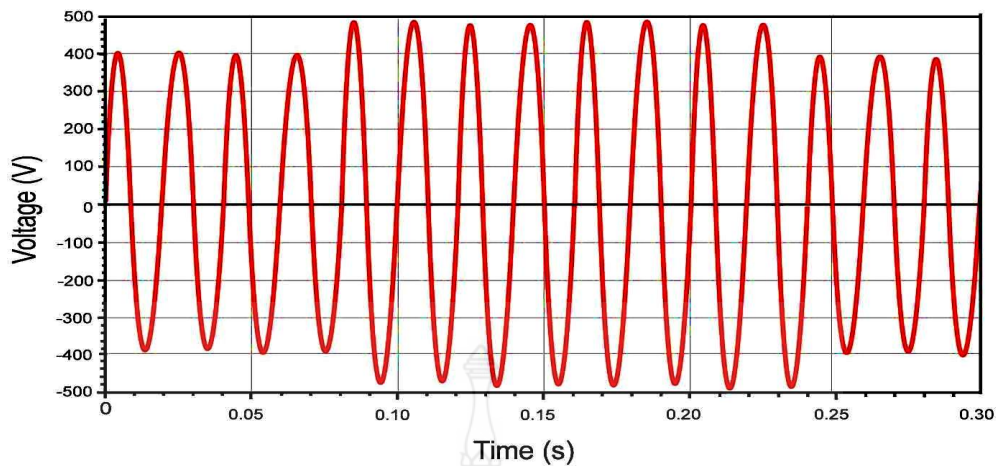
Figure 2.8 The charateristic of voltage swell.

2.4.3 Short interruption

Short Interruption, that is shown in Figure 2.9, is the phenomenon that results in a voltage drop below 10% of the normal voltage. The duration of the event is less than 1 minute [36].
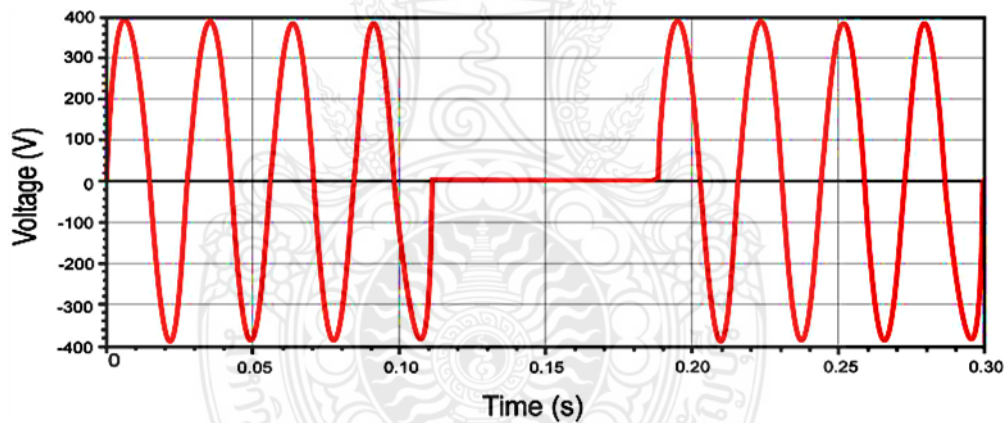
Figure 2.9 The charateristic of short interruption.

2.4.4 Under Voltage

Under voltage is the phenomenon that results in a decrease voltage to only 10% to 90% of the normal voltage. The duration of the event is more than 1 minute. The under voltage in the power system may be due to the disconnection of the power supply by clearing of a fault or intentional utility regulation [37] – [40]. The characteristic of under voltage is shown in Figure 2.10
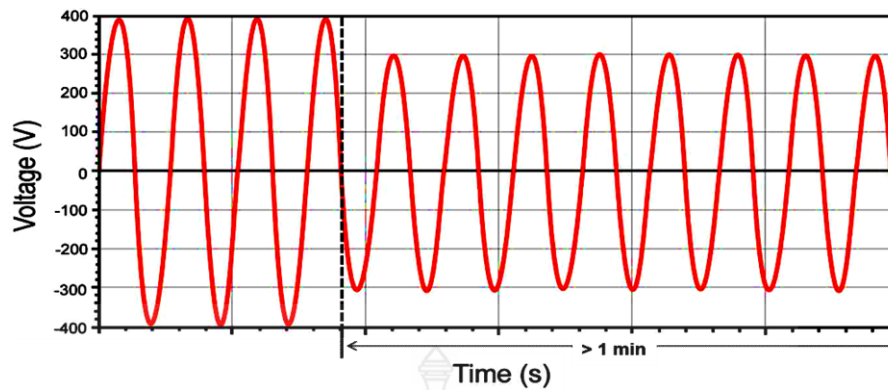
Figure 2.10 The characteristic of under voltage.

2.4.5 Over voltage

Over voltage, that is shown in Figure 2.11, is a phenomenon that results of voltage increase more than 110% over the normal voltage. The duration of the event is more than 1 minute. Often caused by disconnecting heavy load from the power system or connecting the capacitor bank to the power system [37] – [40].
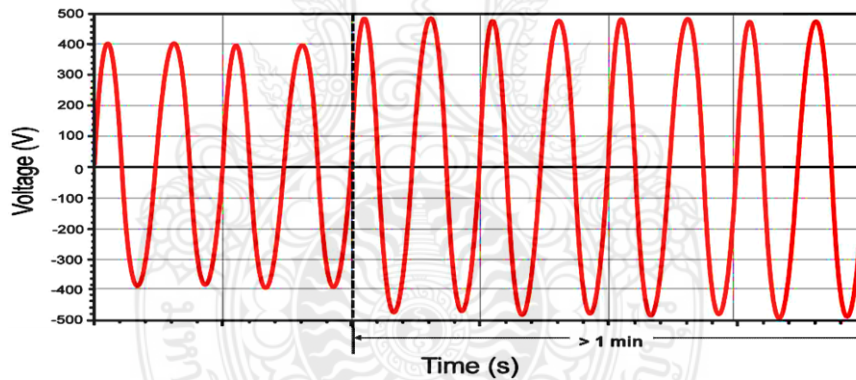
Figure 2.11 The characteristic of over voltage.

2.4.6 Long interruption

Long interruption is a complete loss of power lasting from a few milliseconds to several hours as show in Figure 2.12. Due to power system failure or due to damage to transmission lines or equipment failure [37] – [40].
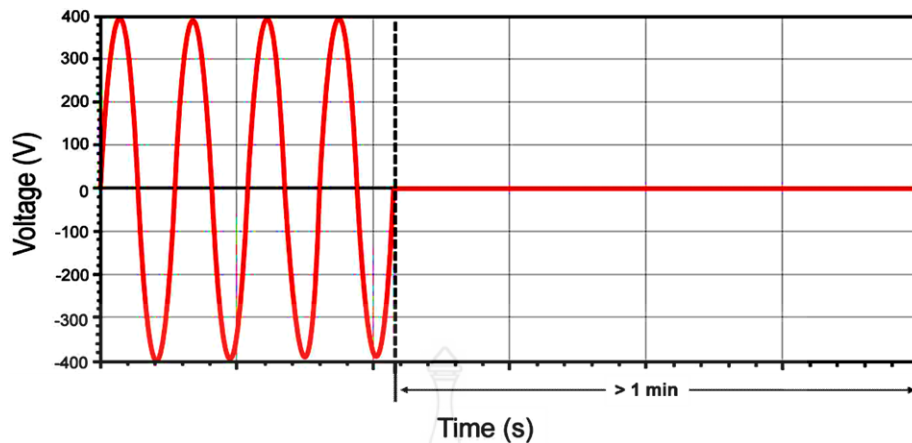
Figure 2.12 The characteristic of long interruption.

2.4.7 Voltage unbalance

Voltage unbalance is a phenomenon that the voltage of three-phase system is unequal line voltage magnitudes, or the angle of deviation is from 120 degrees, or both occur simultaneously [41]. Voltage unbalance makes negative effects on the distribution system which cause overheating of equipment. The maximum voltage unbalance in a three phase distribution system is limited to 3% [42] under IEEE/ANSI C84.1-1995 standard.

2.4.8 Harmonic

The Harmonics is a component in the sine wave of the voltage and current signals. A fundamental frequency is 50 cycles per second (Hz) in Thailand, such as harmonic second order is 100 cycles per second (Hz) and harmonic third order is 150 cycles per second (Hz) [43] – [54].

2.4.9 Harmonic distortion

Harmonic Distortion is the change of the power waveform from the sinusoidal waveform [55] – [56] by the combination of the fundamental frequency and other harmonic frequency. According to the requirements of the PEA, the total harmonic distortion of voltage (THDv) shall be controlled not exceeding 1.5% (115 kV system), which can be calculated according to equations [57] – [59]

$$\%THD_V = \frac{\sqrt{\sum_{i=2}^{n} V_i^2}}{V_1} \times 100\% \tag{2.4}$$

$$\%THD_I = \frac{\sqrt{\sum_{i=2}^{n} I_i^2}}{I_1} \times 100\% \tag{2.5}$$

where, V_i and I_i represent the individual voltage and current harmonic component.

2.4.10 Voltage fluctuation

The voltage fluctuation is a phenomenon where the voltage rises over time in the size of the scope of the normal power supply. But this voltage fluctuation will affect human vision systems, such as the illumination of light in electrical Welding. The electrical welding is a phenomenon directly related to the ever-changing load [60] – [61].

2.4.11 Frequency variation

The frequency variation is the frequency of the voltage or current varies from the standard, in Thailand frequency is to 50 Hz. Typically, the frequency variation is in the shortest time and not more than 1 Hz. The most of causes are the faults in the power system.

2.5 The standard assessment of power quality by PEA

The electrical energy is transmitted by the PV system connected to the PEA distribution system. If the PV inverter does not good perform, then it transmitted the poor power quality into the distribution system. Therefore, it is necessary to issue the criterion of power quality of the PV system.

2.5.1 Voltage RMS

Voltage regulation is to meet the power quality standards. The maximum and minimum voltage levels are determined in accordance with Table 2.1.

Table 2.1 The maximum and minimum Voltage Level Standards of Provincial Electricity Authority

Voltage Level (kV)	Steady state		Emergency	
	Max. (kV)	Min. (kV)	Max. (kV)	Min. (kV)
115	120.7	109.2	126.5	103.5
69	72.4	65.5	75.9	62.1
33	34.7	31.3	36.3	29.7
22	23.1	20.9	24.2	19.8
0.380	0.418	0.342	0.418	0.342
0.220	0.240	0.200	0.240	0.200

2.5.2 Power frequency

The frequency control of power system is 50±0.5 Hz. If the frequency is not in the range of 48.00 - 51.00 Hz more than 0.1 second, then the PV system must be disconnected from the distribution network by the small power produce.

2.5.3 Voltage Fluctuation

The voltage fluctuation is the constant change of voltage RMS that can be observed by flashing the lamp or electrical sensitive Equipment. The voltage fluctuation can be classified as follows:

1) Short-Term Severity Values, P_{st} is the assessment values intensity of the voltage fluctuation in a short time. (10 min.)

2) Long-Term Severity Values, P_{lt} is the assessment values intensity of the voltage fluctuation in the long time. (2-3 hours)

The criterion of Short-Term Severity Values and Long-Term Severity Values is shown in Table 2.2.

Table 2.2 The criterion of Short-Term Severity Values, P_{st} and Long-Term Severity Values, P_{lt}

Voltage at PCC	Pst	Plt
< 115 kV	1.0	0.8
> 115 kV	0.8	0.6

2.5.4 Harmonic

The harmonic is caused by equipment that has a relationship between current and voltage in nonlinear. The total harmonic distortion (THD) is used in measurement power quality. The limit of THD of voltage is shown in Table 2.3.

Table 2.3 The limit of total harmonic distortion of voltage

Voltage at PCC (kV)	% THDv	%THDv of each rank	
		Odd	Even
0.400	5	4	2
11, 12, 22 and 24	4	3	1.75
33	3	2	1
69	2.45	1.63	0.82
115 and above	1.5	1	0.5

2.6 The ferroresonance phenomenon

A nonlinear resonance phenomenon can affect power system that call Ferroresonance phenomenon. The impact of Ferroresonance can create the abnormal rates of harmonics and steady state or transient overvoltage and overcurrent that it causes are often malfunction or damage for electrical equipment [62] – [72].

The Ferroresonance phenomenon will occur, when the system comprises of power supply, the resonance between line capacitance and the saturated magnetizing inductance of transformer core, and one or two of the lost source phase [73].

The classification of ferroresonance phenomenon can enable into four different types, which can occur in electrical power system as shown in Figure 2.13-2.16 [74].

2.6.1 Fundamental mode

The waveform has the similar period as the power system (T). The frequency spectrums comprise of the fundamental frequency component that is pursued by the decreasing magnitude of the n-th odd harmonic, as shown in Figure 2.13

Figure 2.13 Ferroresonance in fundamental mode.

2.6.2 Subharmonic

The waveform has a period which is a multiple of the source period (nT). The frequency spectrums comprise of the fundamental frequency component that is pursued by the decreasing contents of the n-th subharmonic, as shown in Figure 2.14

29

Figure 2.14 Ferroresonance in subharmonic.
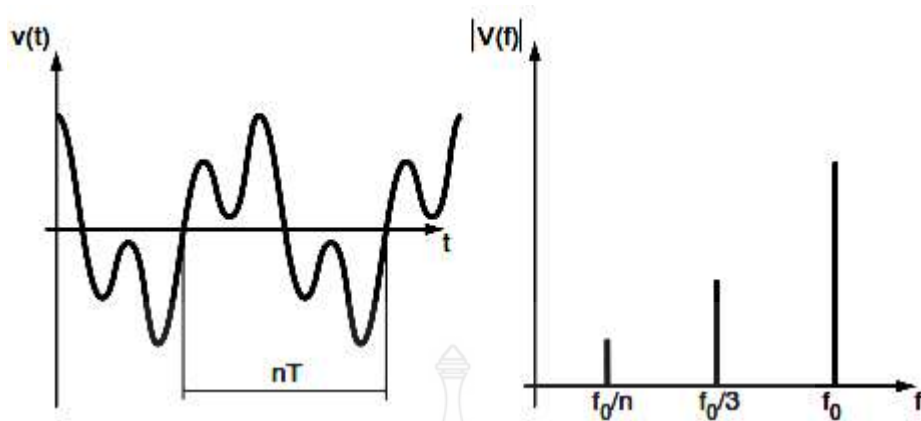
2.6.3 Quasi-periodic

The waveform is not periodic but has the duplicate platform. The frequency spectrums are intermittent and determined as nf_1+mf_2, where n and m are integers, shown in Figure 2.15
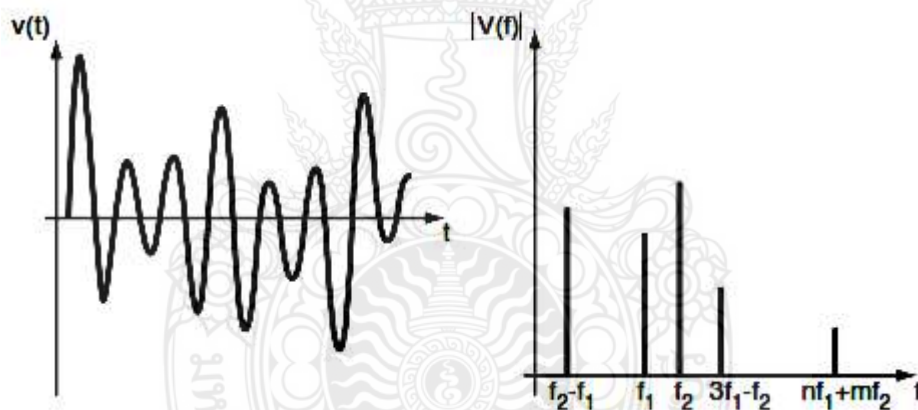
Figure 2.15 Ferroresonance in Quasi-periodic.

2.6.4 Chaotic

The waveform is not sinusoidal and the frequency spectrums are uninterrupted, shown in Figure 2.16
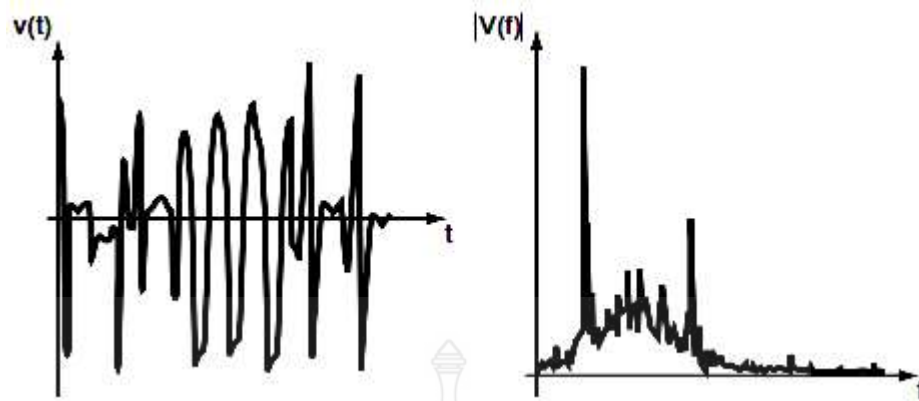
Figure 2.16 Ferroresonance in Chaotic.

2.7 PSCAD/EMTDC

Power System Computer Aided Design and Electromagnetics Transients including DC represent PSCAD/EMTDC. In this thesis, PSCAD/EMTDC is selected to use to model and analyze the PV rooftop system. A default master library of PSCAD/EMTDC covers standard circuit components of a Spice library. Moreover, goes one step further complexity by also including advanced power electronic devices and photovoltaic source. The benefit and exclusiveness of this program is the efficacy to integrate complicated power electronic circuits with large power systems and investigate the system response in the time and frequency domains [75] – [78].

2.8 Literature Review

The main aim of this research is to study impact power quality in 0.4/22 kV distribution network of PEA with a large share of PV system source. Integration of PV system source into the power system has been under extensive research and development mostly focusing on the issues like voltage, current, frequency and harmonic of the distribution network. A review was conducted into the existing literature that has been published on the inclusion of PV Systems on the distribution networks. The specific fields were considered when searching for literature relevant to this research dissertation and these were:

In 2009 Qiuye Sun, and et al. [79], in 2010 Masato Oshiro and et al. [80], and in 2012 S. A. Pourmousavi, and et al. [81] study about "Grid tied PV systems at the distribution level" and the results shown that it can have a large impact on the power systems voltage, frequency, power flow, and reliability.

Edward J Coster, and et al. [82] study about "Integration Issues of Distributed Generation in Distribution Grids," the results shown that when PV system injected power into the grid tied, the voltage profile is most impacted in the feeders.

Yun Tiam Tan and Kirschen, D.S. [83] study about "Impact on the Power System of a Large Penetration of Photovoltaic Generation". The results of analysis shown that the voltage fluctuates during periods when there is large change in solar irradiance.

Yun Seng Lim, and Jun Huat Tang [84] state that "Experimental study on flicker emissions by photovoltaic systems on highly cloudy region: A case study in Malaysia." The results reported that the passing clouds have the impact in the frequent and rapid fluctuations of PV power outputs, and created large amount of flickers to the distribution networks.

Y. Liu and et al. [85] study about "Distribution System Voltage Performance Analysis for High-Penetration PV." The results show that High-Penetration PV do not affect to the grid.

Srisaen, N. and Sangswang, A. [86] study about "Effects of PV Grid-Connected System Location on a Distribution System." The simulation results shown that the distribution system was affected by the PV system in positive impact and power quality including voltage profiles and system were being loss reduction.

Mitra, P and et al. [87] study about "The impact of distributed photovoltaic generation on residential distribution systems." The analysis results shown that the PV system can helpful and better voltage regulation and reduced line losses during both heavy load.

Shayani, R.A. and et al. [88] study about "Photovoltaic Generation Penetration Limits in Radial Distribution Systems." The results shown that the power of PV system is injected in the feeder, the voltage starting obtain place at the load bus, with a possible overload impact at the feeder.

Qiuye Sun and et al. [89] study about "Impact of Distributed Generation on Voltage Profile in Distribution System." The simulation results shown that the PQ of distribution system was affected by the DG in positive impact.

Danling Cheng and et al. [90] study about "Photovoltaic (PV) Impact Assessment for Very High Penetration Levels." The simulation results shown that the effects of solar variability can be affected the PV system. The simulation can forecast the impact of increasing levels of PV system connected to the grid.

Papaioannou, I.T and et al. [91] study about "Harmonic impact of small photovoltaic systems connected to the LV distribution network." The simulation results shown that the LV distribution network was affected by the harmonic impact from the small PV system.

Batrinu, F. and et al. [92] study about "Impacts of grid-connected photovoltaic plant operation on the harmonic distortion." The simulation and experimental results shown that the harmonic distortion from the grid-connected photovoltaic plant operation will be occurred by the consequences of the shading effect.

Menti A. and et al. [93] study about "Harmonic distortion assessment for a single-phase grid-connected photovoltaic system." The simulation results shown that the harmonic distortion is sensitive to the values of critical parameters.

Schlabbach, J. [94] study about "Harmonic current emission of photovoltaic installations under system conditions." The experimental results shown that PV-inverters without transformer produced operative lower harmonic currents than inverters with coupling transformer.

M.Kesraoui and et al. [95] study about "Grid connected solar PV system: modeling, simulation, and experimental tests." The results describe mathematical and models of PV system and then perform simulation work of the current voltage (I-V) characteristics by Matlab/Simulink.

Chen Qi and Zhu Ming [96] study about Photovoltaic Module Simulink Model for a Stand-alone PV System. The simulation results estimate behavior of PV module with respect changes on irradiance intensity, ambient temperature and parameters of the PV module.

In 2003 Miller N. [97], in 2006 V. H. M. Quezada [98], in 2007 Thomson M. [99], in 2008 S. Cobben, B. [100], and in 2009 F. Katiraei [101] study about "Impact of photovoltaic generation on power quality in Distribution system" and the results shown that there are impact on the power systems voltage, frequency, power flow, and reliability.

In the point of view of the literature review, there was very little published on the PQ impact from PV rooftop system to distribution network. Some research is simulated in Matlab/Simulink of the current voltage (I-V) characteristics. Moreover, a little research simulated Grid-Tied Photovoltaic Systems that also investigates the effect of variable atmospheric conditions in PSCAD/EMTDC.

CHAPTER 3

IMPLEMENTATION

The purpose of this chapter is to presents a measurement PQ from selected real PV rooftop power plant and investigate PQ in normal and abnormal cases base on criterion PQ assessment of PEA by simulation using PSCAD/EMTDC.

3.1 The selected real PV rooftop power plant

The selected real PV rooftop power plant is located in Samut Songkhram province, Thailand at latitude 13º 22 minutes North and 99º 58 minutes East as show in Figure 3.1-3.2. The installed capacity of this site is about 1 MW. The PV rooftop system comprise of solar panels Poly Crystalline Module Size 245 Wp, 4032 panels, and 2 inverters 500 kW per each, that are connected via Main Distribution Board (MDB) to the distribution transformer and 22 kV, 50 Hz distribution grid of PEA.
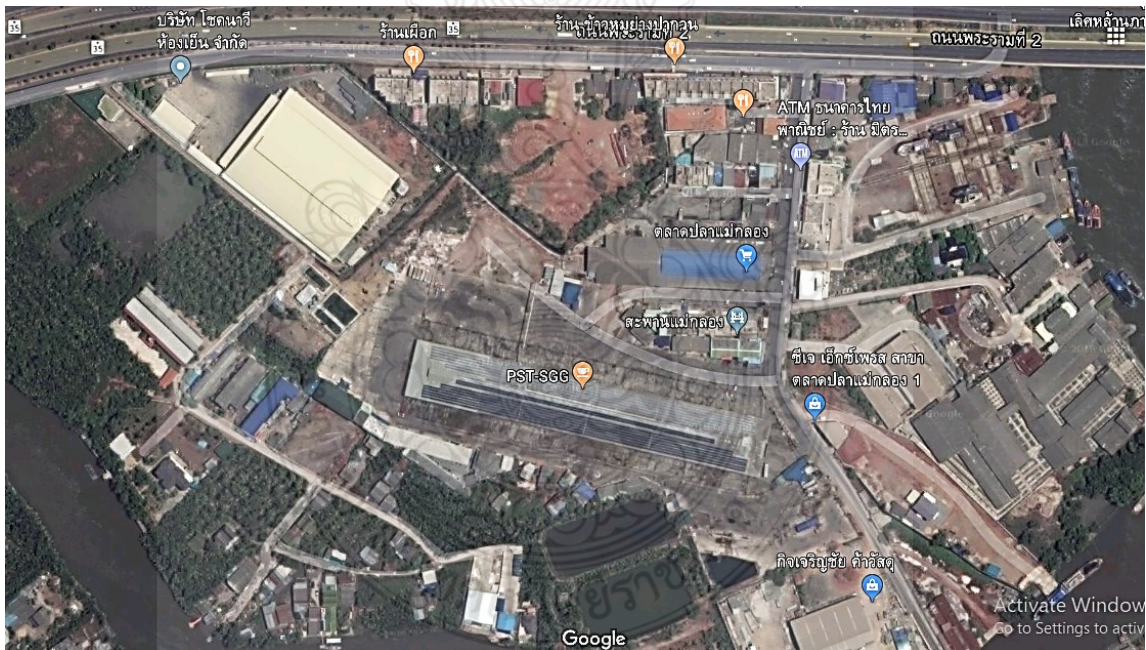
Figure 3.1 The location of selected real PV Rooftop power plant.

Figure 3.2 The location of PV rooftop system installations used in this thesis.

3.2 The Measurement and assessment power quality of PV rooftop system

The PQ data from PV rooftop system was proceeded to collect by PQ analyzer. The PQ data was measured at PCC as shown in Figure 3.3-3.5.

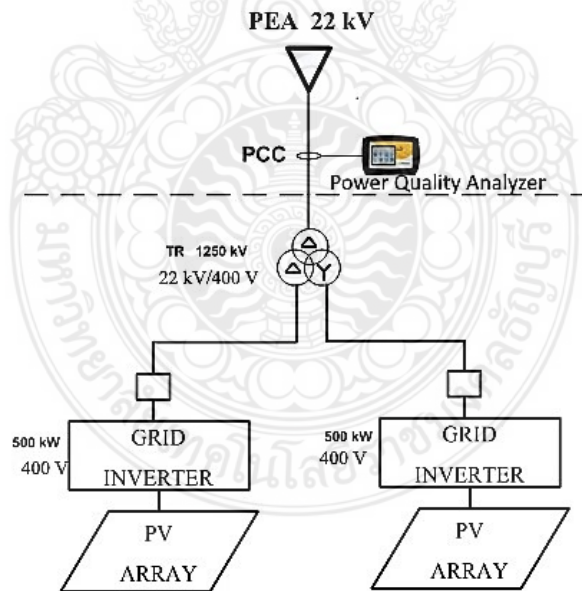**Figure 3.3** The single line diagram of the power quality analyzer installation.
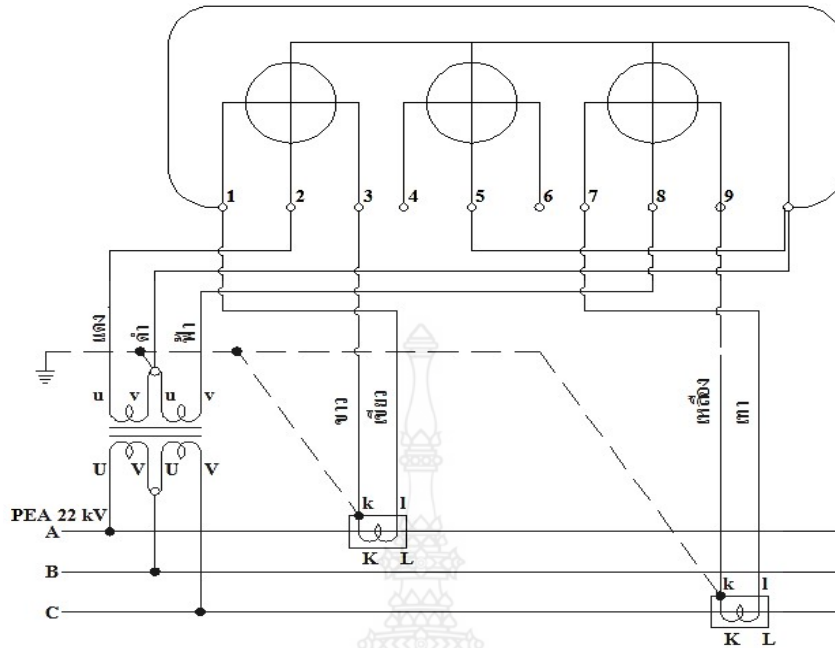
Figure 3.4 The single line diagram of the PQ analyzer connected to the grid in 3 phase 3 line.

Figure 3.5 The connecting of the power quality analyzer at PCC.

The PQ measurement is determined according to EN 50160 and PEA grid code and recorded PQ data every 10 minutes. The criterion of PQ assessment can follow:

1. Voltage RMS
2. Frequency
3. Voltage Fluctuation
4. Total Harmonic Distortion of voltage

3.3 PV Rooftop system modeling by PSCAD/EMTDC

The PV rooftop system modeling in this thesis base on the one located at the end of the branches of the PEA distribution network. The power output of PV rooftop system is about 1 MW. The parameter of distribution line is based on PEA' standard and the line voltage is about 22 kV, 50 Hz. The other system parameter will be estimated in system modeling. The PV rooftop system consist of PV array, Voltage source inverter, and distribution transformer.

3.3.1 PV array implementation by PSCAD

The PV module was developed by Manitoba HVDC Research Centre. The characteristic of this PV module is based on equation (1) in chapter 2 and depend on solar irradiance and temperature inputs. The PV module that illustrates in Figure 3.6 is in the library master component of PSCAD. The PV parameters are shown in Figure 3.7 that were used in this simulation. The PV array configuration is shown in Figure 3.8 that can change the number of cells in a module in parallel or series as well as possible can edit the PV array with parallel or series connect PV modules.
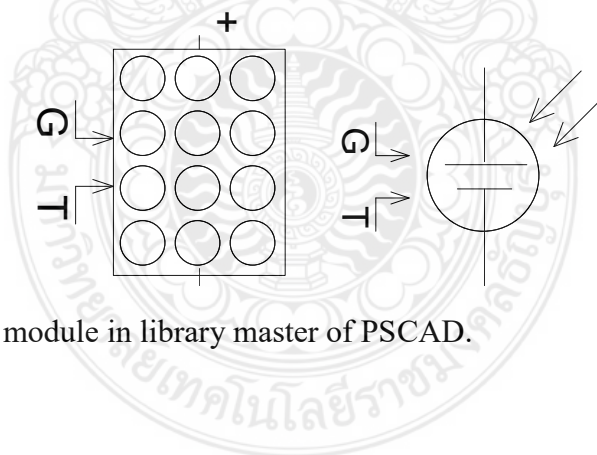

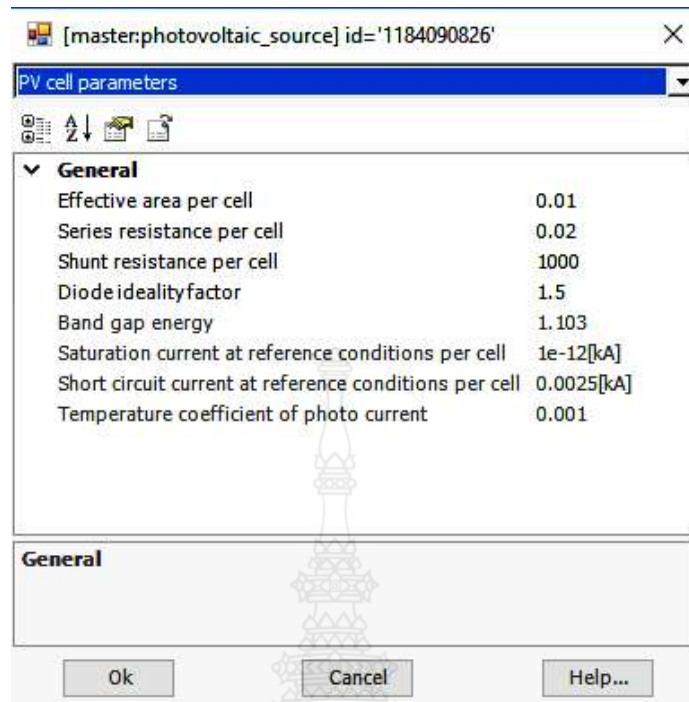**Figure 3.6** The PV module in library master of PSCAD.

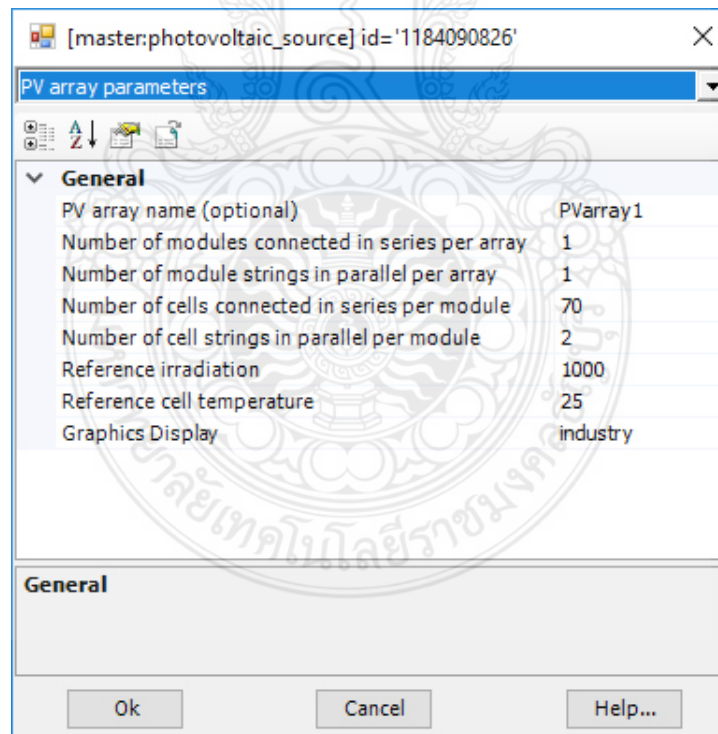**Figure 3.7** The default parameters of PV cell.

Figure 3.8 The PV array parameter in PSCAD.

3.3.2 PV inverter implementation by PSCAD

Figure 3.9 illustrates the Voltage Source Inverter (VSI) model that is used to the simulation system in this thesis. The detail of this VSI is explained in Appendix B.
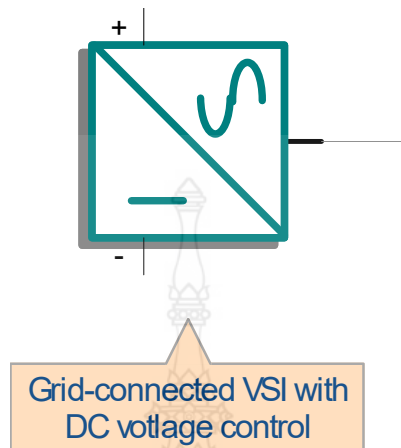
Figure 3.9 The grid connected VSI inverter.

3.3.3 The distribution transformer modeling implementation by PSCAD

Figure 3.10 illustrates the distribution transformer modeling, available in library master component of PSCAD. Due to the distribution transformer is supposed to be ideal transformer. The basic parameters required to be entered, these parameters are shown in Figure 3.11
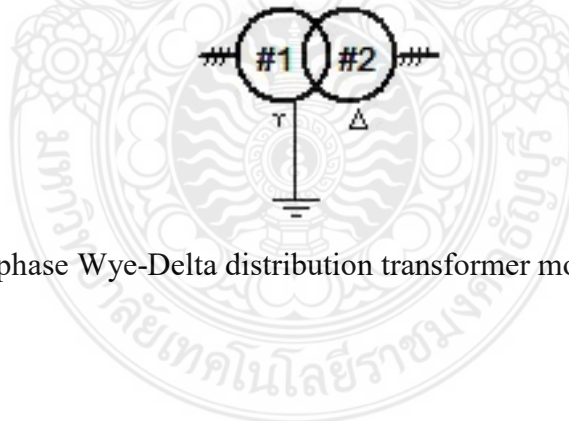
Figure 3.10 Three phase Wye-Delta distribution transformer model in PSCAD.

Figure 3.11 The configuration parameter of distribution transformer

3.4 Complete system

The approach in selecting using power system model for simulation study was based on using selected real PV rooftop power plant system in chapter 3 section 3.1. The complete system to be used in this simulation is illustrated in Figure 3.12
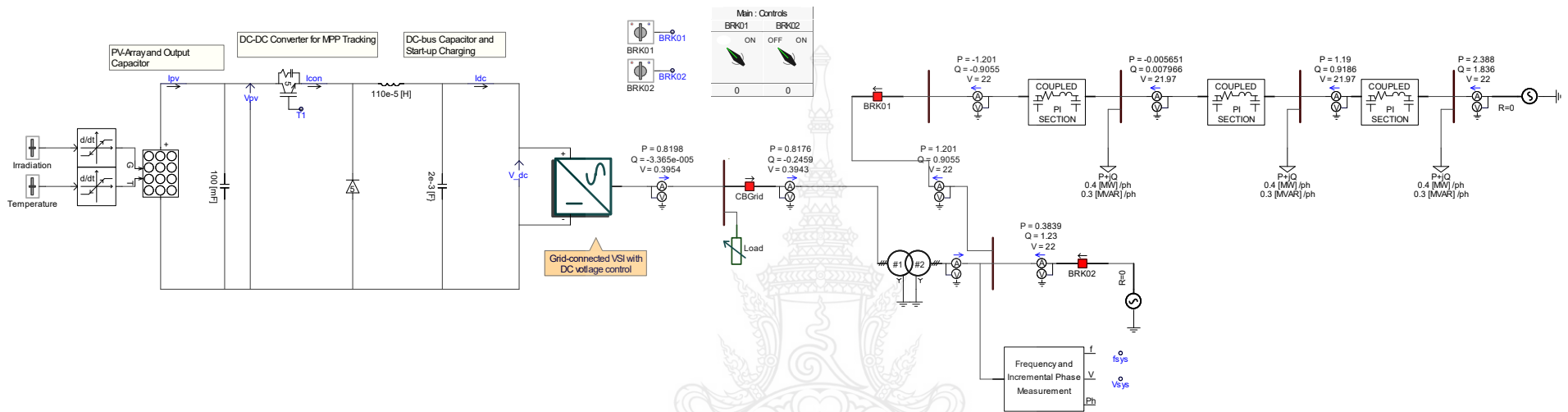
Figure 3.12 Complete PV rooftop system connected distribution network PEA modeled in PSCAD

3.5 The investigation PQ impact from PV rooftop system connected to the grid under normal and abnormal case base on criterion of PEA grid code by PSCAD/EMTDC

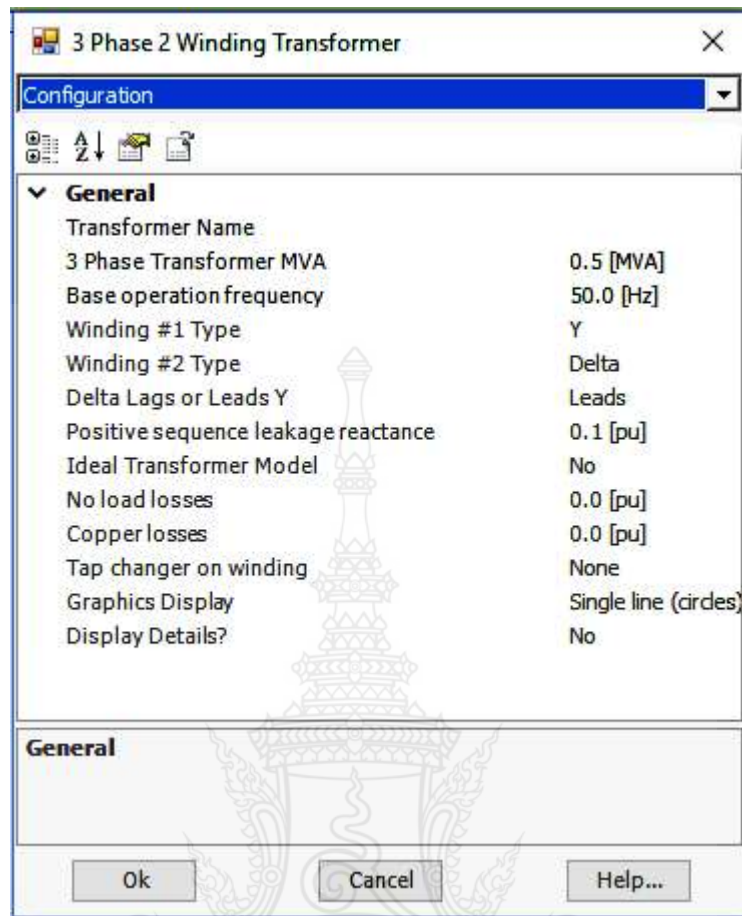The simulation of the investigation PQ impact from PV rooftop system connected to the grid under normal and abnormal case can be divided into 7 cases.

1. The investigation of I-V and P-V curve characteristic of PV module

2. The simulation under steady state operation under Standard Test Condition (STC)

3. The simulation in normal day condition

4. The simulation in raining day condition

5. The simulation in short time of solar irradiance fluctuation

6. The simulation under VSI inverter defect

7. The simulation under ferroresonance phenomenon
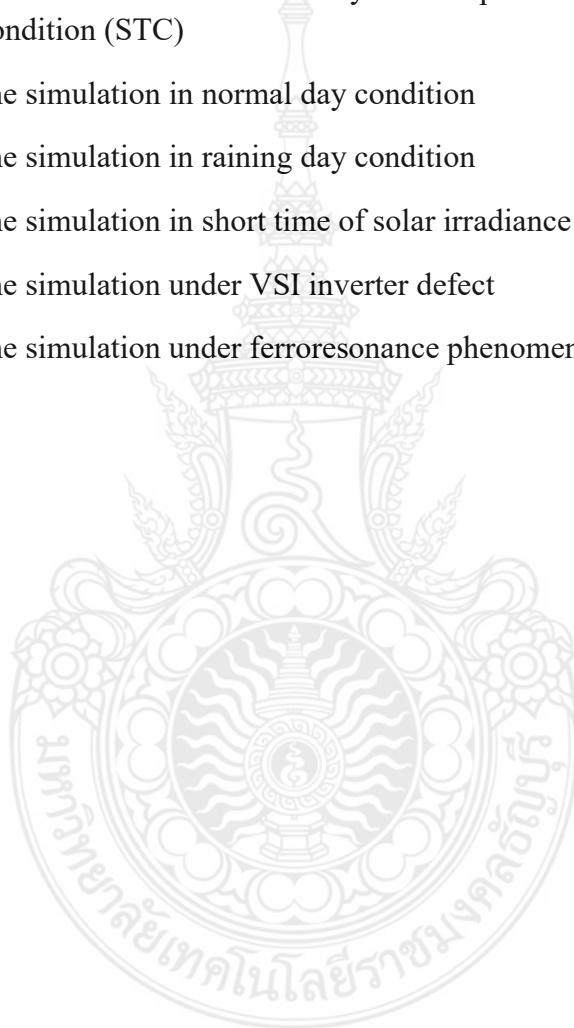
CHAPTER 4

THE MEASUREMENT AND SIMULATION RESULTS

This chapter aims to show the measurement results of PQ from the selected real PV rooftop plant and also investigates the power quality and assessment of electrical power measurement. In addition, show the simulation results of the PQ impact of PV rooftop connected to the distribution system with simulation by PSCAD/EMTDC that will be investigate under normal and abnormal case condition.

4.1 The Measurement Results

The power quality analyzer is set to record data every 10 minutes in 1 week from PV rooftop system at the Point of Common Coupling, PCC of the 22 kV PEA distribution network. All measurement data were assessed base on EN 50160. The Cumulative percentage with 95% of the data were used by the data assessment and is compared with PEA grid code. Only the frequency used the Cumulative percentage with 99% of the data. The results of the measurement and assessment of power quality are as follows.

4.1.1 RMS voltage

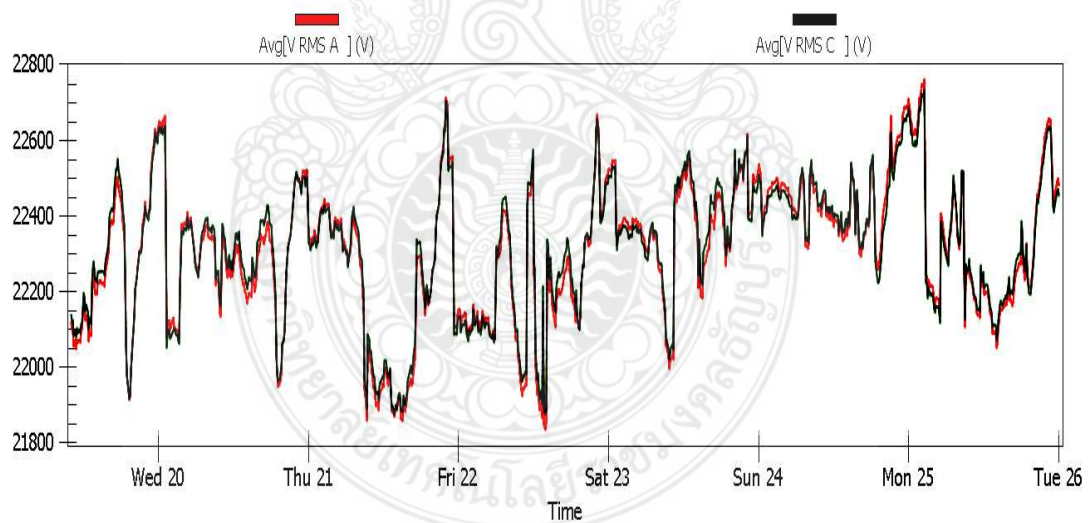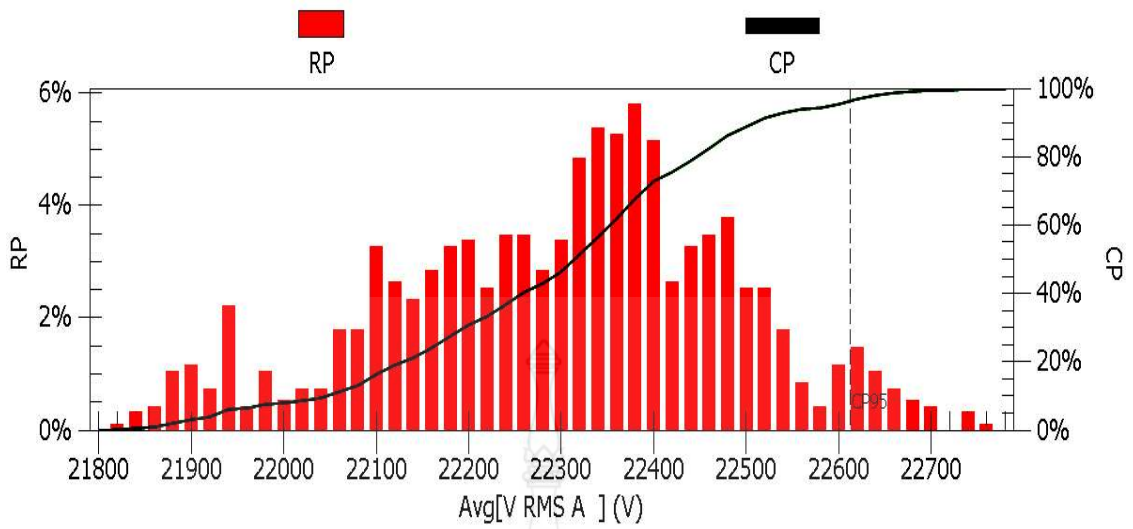**Figure 4.1** The RMS voltage measured at the PCC.

Figure 4.2 The graphic of the evaluated voltage at phase A.
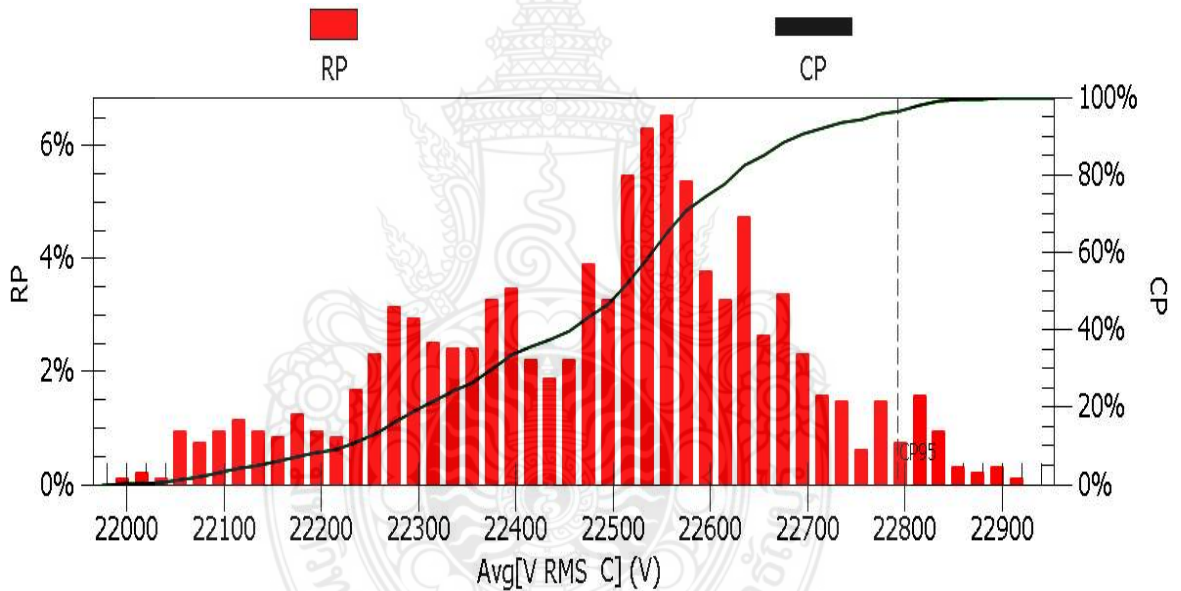
Figure 4.3 The graphic of the evaluated voltage at phase C.

Figure 4.1 shows the RMS voltage that record every 10 minutes in 1 week. Figure 4.2 and 4.3 show the evaluated voltage at phase A and C and were assessed base on EN 50160. All data of the RMS voltage were summarized in Table 4.1.

Table 4.1 The assessment of the RMS voltage from the selected real PV rooftop power plant.

Parameter		Min.	Average	Max.	CP %95
RMS Voltage (kV)	Phase A	21.84	22.31	22.76	22.613
	Phase B	-	-	-	-
	Phase C	22.01	22.5	22.93	22.793

4.1.2 The Frequency
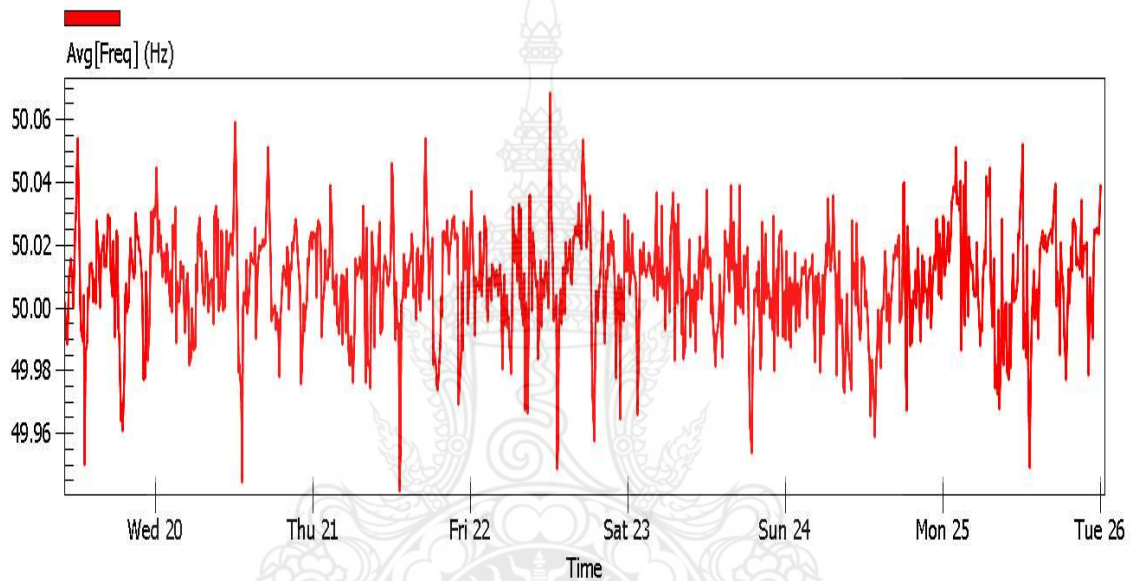
Figure 4.4 The result of measured Frequency at PCC.
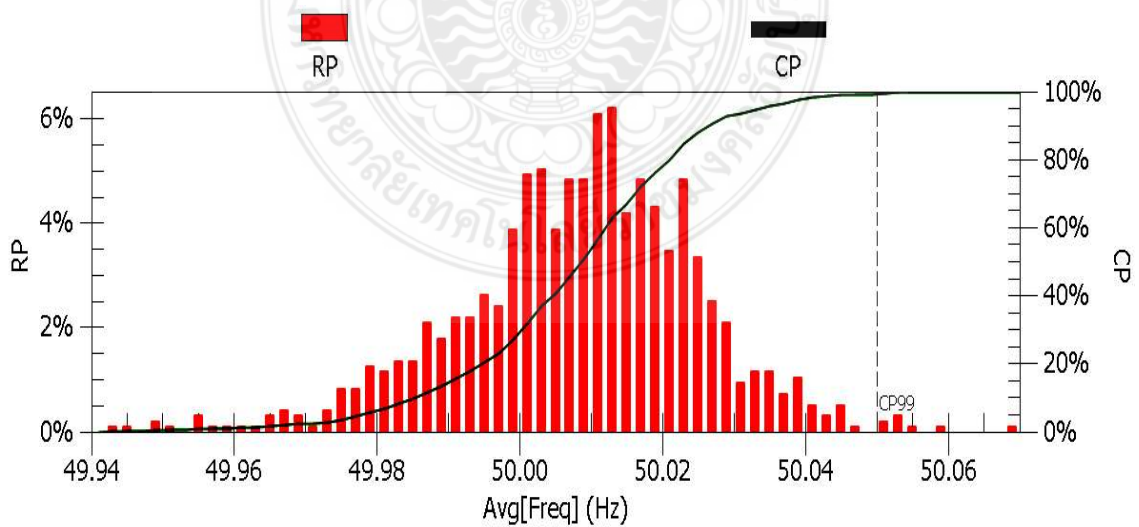
Figure 4.5 The graphic of the evaluated frequency.

Figure 4.4 shows the frequency at PCC that record every 10 minutes in 1 week. 4.5 show the evaluated frequency of the system and were assessed base on EN 50160. The data of the frequency were summarized in Table 4.2.

Table 4.2 The assessment Frequency on PEA distribution 22 kV at PCC.

Parameter	Min.	Average	Max.	CP %99
Power frequency (Hz)	49.94	50.01	50.07	50.05

4.1.3 Voltage fluctuation in Short Term Flicker: P_{st}

Figure 4.6 Short Term Flicker: P_{st} at PCC

Figure 4.7 The graphic of the evaluated voltage fluctuation in Short Term Flicker: P_{st} at phase A.

Figure 4.8 The graphic of the evaluated voltage fluctuation in Short Term Flicker: P_{st} at phase C.

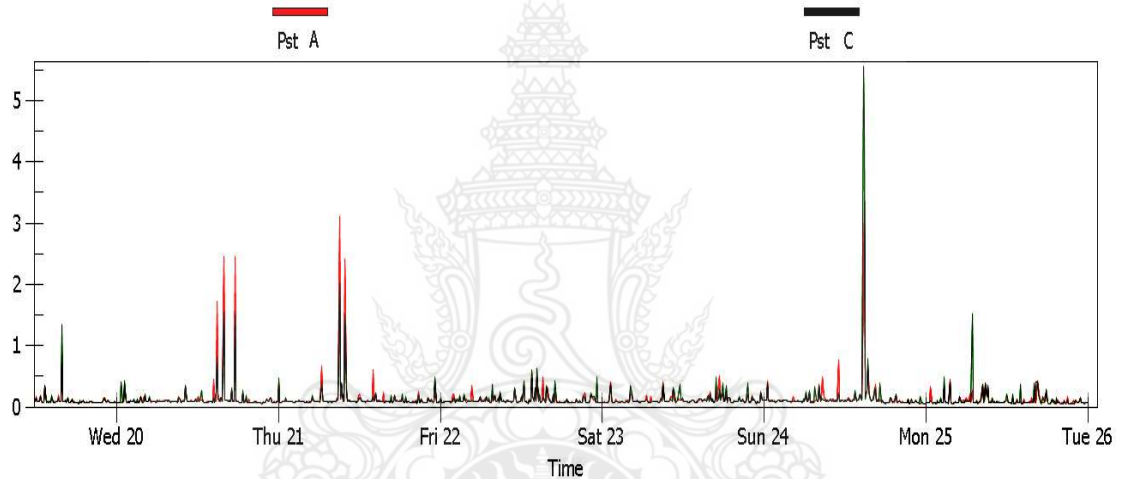Figure 4.6 shows the voltage fluctuation in Short Term Flicker: P_{st} that record every 10 minutes in 1 week. Figure 4.7 and 4.8 show the evaluated voltage fluctuation in Short Term Flicker at phase A and C and were assessed base on EN 50160. All data of the voltage fluctuation in Short Term Flicker were summarized in Table 4.3.

Table 4.3 The assessment voltage fluctuation in Short Term Flicker on PEA distribution 22 kV at PCC.

Parameter		Min.	Average	Max.	CP %95
Voltage fluctuation in Short Term Flicker: (P_{st})	Phase A	0.053	0.129	3.339	0.266
	Phase B	-	-	-	-
	Phase C	0.05	0.13	5.557	0.310

4.1.4 Voltage fluctuation in Long Term Flicker: P_{lt}

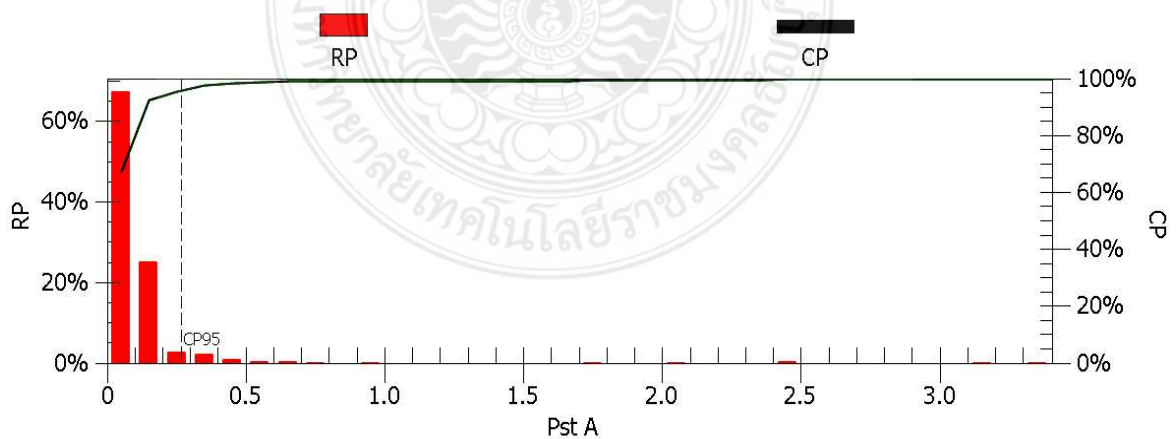**Figure 4.9** Long Term Flicker: P_{lt} at PCC.
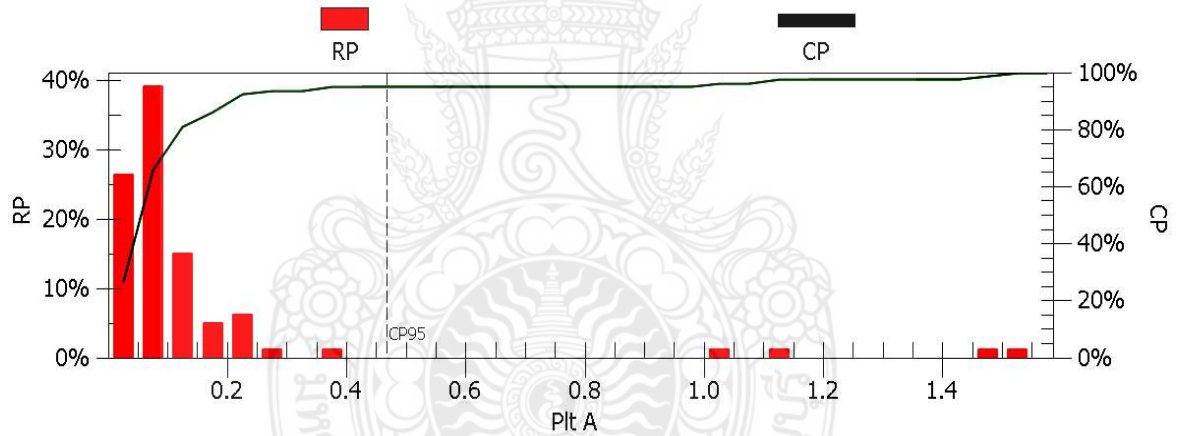
Figure 4.10 The graphic of the evaluated voltage fluctuation in Long Term Flicker: P_{lt} at phase A.
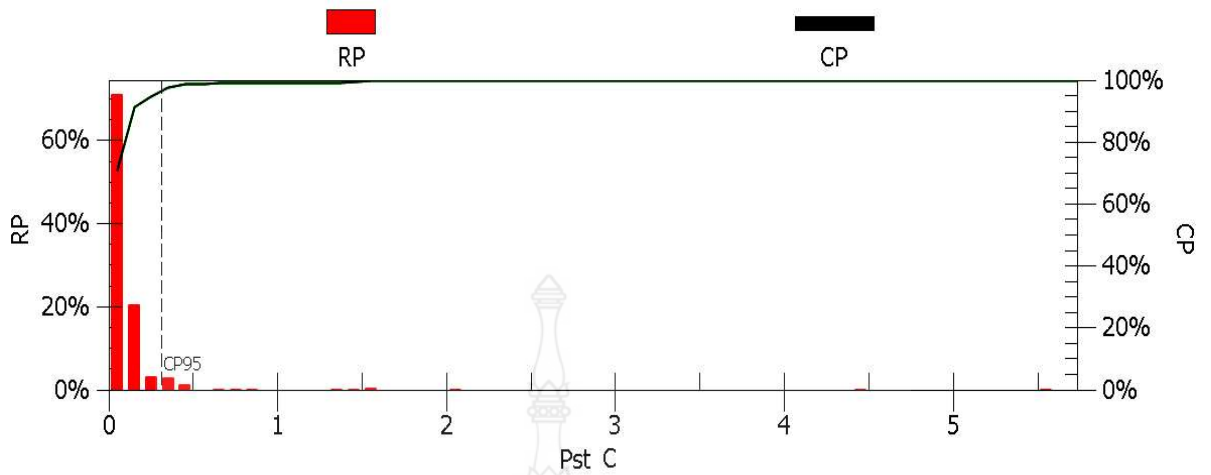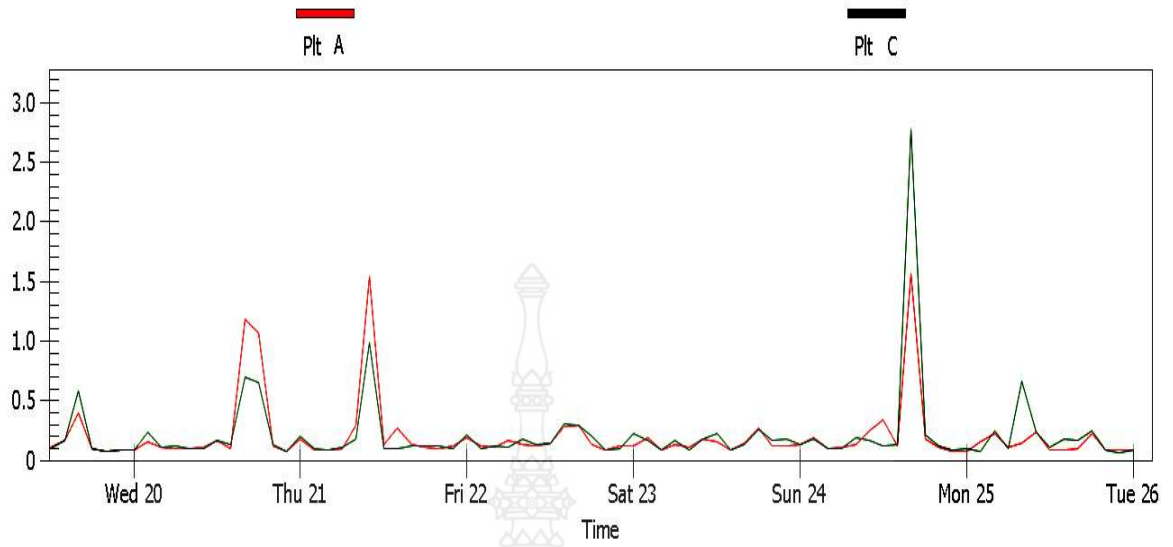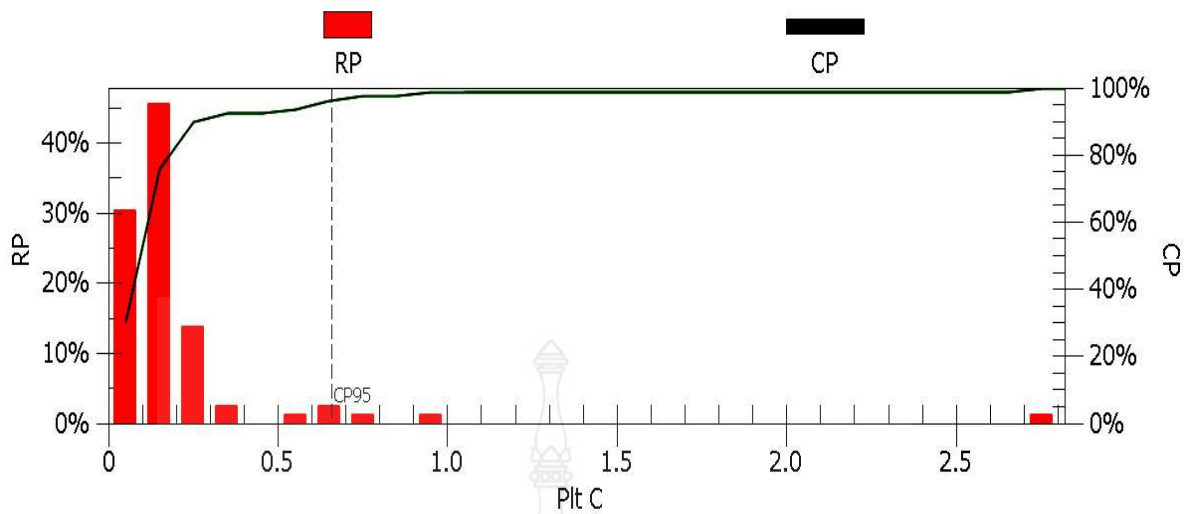
Figure 4.11 The graphic of the evaluated voltage fluctuation in Long Term Flicker: P_{lt} at phase C.

Figure 4.9 shows the voltage fluctuation in Long Term Flicker: P_{lt} that record every 10 minutes in 1 week. Figure 4.10 and 4.11 show the evaluated voltage fluctuation in Long Term Flicker at phase A and C and were assessed base on EN 50160. All data of the voltage fluctuation in Long Term Flicker were summarized in Table 4.4.

Table 4.4 The assessment voltage fluctuation in Long Term Flicker on PEA distribution 22 kV at PCC.

Parameter		Min.	Average	Max.	CP %95
Voltage fluctuation in Long Term Flicker: (P_{st})	Phase A	0.074	0.204	1.561	0.467
	Phase B	-	-	-	-
	Phase C	0.068	0.211	2.783	0.657

4.1.5 Total Harmonic Distortion of Voltage (THDv)
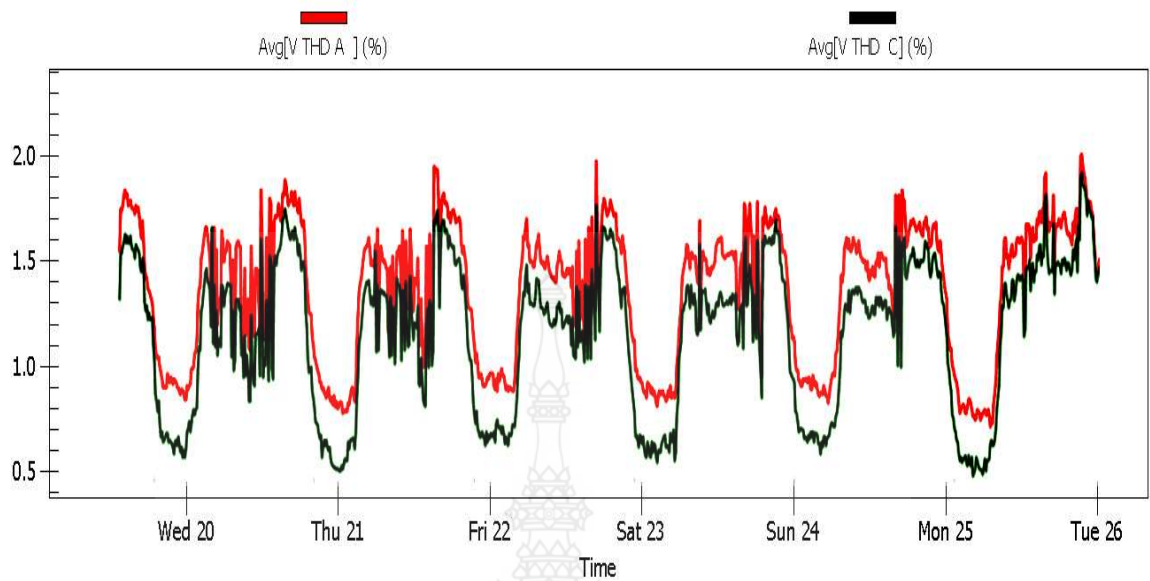
Figure 4.12 Total Harmonic Distortion of Voltage at PCC.
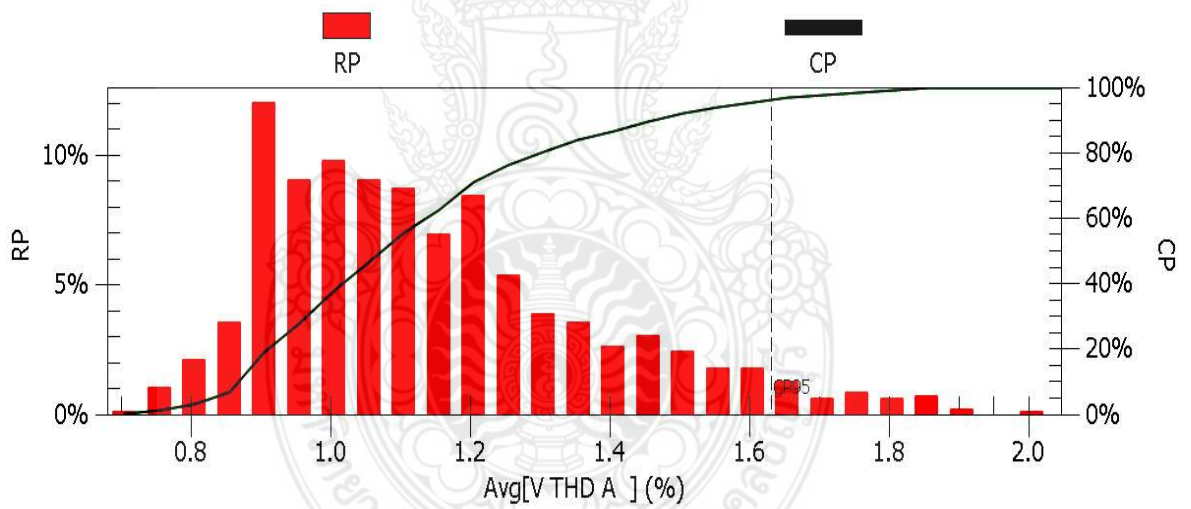
Figure 4.13 The graphic of the evaluated Total Harmonic Distortion of Voltage at phase A.
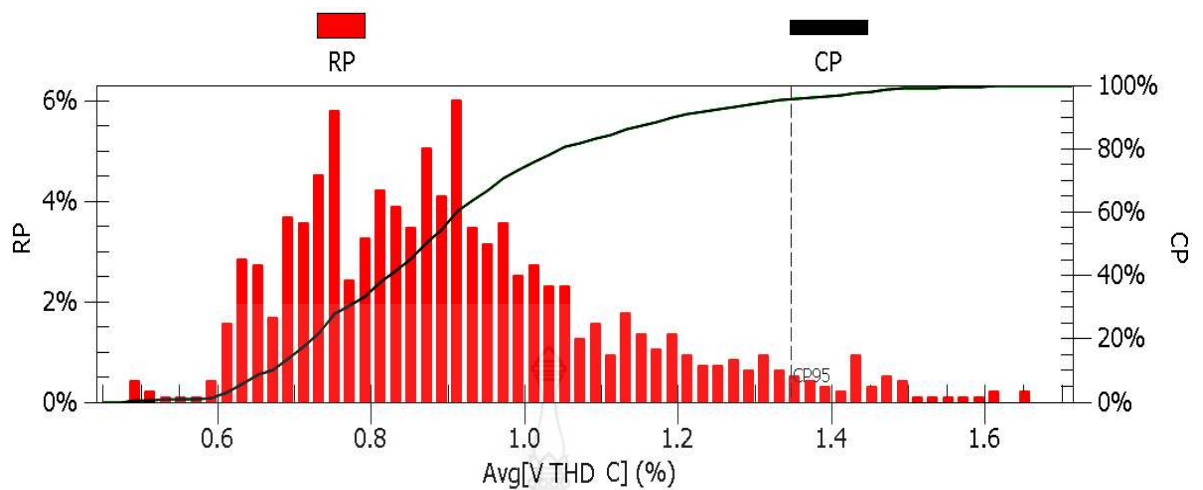
Figure 4.14 The graphic of the evaluated Total Harmonic Distortion of Voltage at phase C.

Figure 4.12 shows the Total Harmonic Distortion of Voltage that record every 10 minutes in 1 week. Figure 4.13 and 4.14 show the evaluated Total Harmonic Distortion of Voltage at phase A and C and were assessed base on EN 50160. All data of the Total Harmonic Distortion of Voltage were summarized in Table 4.5.

Table 4.5 The assessment Total Harmonic Distortion of Voltage on PEA distribution 22 kV at PCC.

Parameter		Min.	Average	Max.	CP %95
Total Harmonic Distortion of Voltage (THD_v)	Phase A	0.743	1.165	2.032	1.631
	Phase B	-	-	-	-
	Phase C	0.47	0.929	2.231	1.347

4.1.6 Total Harmonic Distortion of Current (THD$_i$)

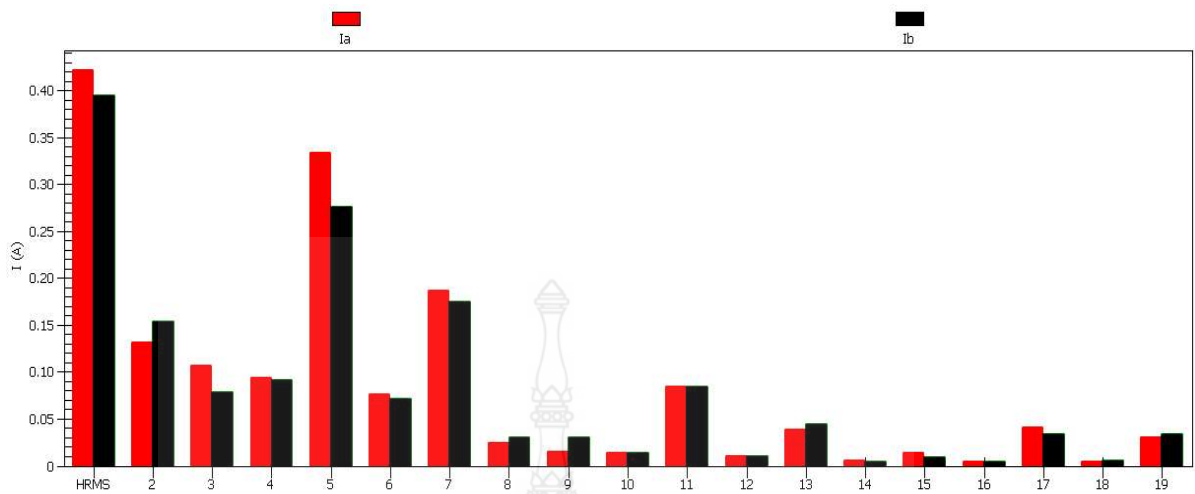**Figure 4.15** The evaluated Total Harmonic Distortion of Current at PCC.

Figure 4.15 show the evaluated Total Harmonic Distortion of Current at PCC and were assessed base on EN 50160. All data of the Total Harmonic Distortion of Current were summarized in Table 4.6.

Table 4.6 The assessment Total Harmonic Distortion of Current on PEA distribution 22 kV at PCC.

Harmonic sequence	2	3	4	5	6	7
Assessment CP 95	0.155	0.107	0.094	0.355	0.076	0.187

Harmonic sequence	8	9	10	11	12	13
Assessment CP 95	0.031	0.031	0.015	0.085	0.011	0.045

Harmonic sequence	14	15	16	17	18	19
Assessment CP 95	0.007	0.015	0.005	0.041	0.006	0.035

The measured PQ assessment results shown that RMS voltage, power frequency, voltage fluctuation and total harmonic distortion of voltage and current were also investigated to pass the criteria base on PEA grid code as shown in Table 4.7 and 4.8

Table 4.7 The evaluated PQ results of PV rooftop system at PCC.

No.	Power Quality	Benchmark	CP 95%	Assessment
1	RMS Voltage			
	- Phase A	(21.9 – 23.1) kV	22.613 kV	pass
	- Phase B	(21.9 – 23.1) kV	-	-
	- Phase C	(21.9 – 23.1) kV	22.793 kV	pass
2	Power Frequency	(49.5 - 50.5) Hz	50.05 Hz	pass
3	Voltage fluctuation (Pst)			
	- Phase A	< 1.0	0.266	pass
	- Phase B	< 1.0	-	-
	- Phase C	< 1.0	0.310	pass
4	Voltage fluctuation (Plt)			
	- Phase A	< 0.8	0.467	pass
	- Phase B	< 0.8	-	-
	- Phase C	< 0.8	0.657	pass
5	%THD$_V$			
	- Phase A	< 4%	1.631%	pass
	- Phase B	< 4%	-	-
	- Phase C	< 4%	1.347%	pass

Table 4.8 The evaluated Total Harmonic Distortion of Current results of PV rooftop
system at PCC.

Harmonic sequence	2	3	4	5	6	7
Benchmark of PEA (A)	11	7	5	9	4	6
CP 95%	0.155	0.107	0.094	0.355	0.076	0.187
Assessment	pass	pass	pass	pass	pass	pass

Harmonic sequence	8	9	10	11	12	13
Benchmark of PEA (A)	3	2	2	6	2	5
CP 95%	0.031	0.031	0.015	0.085	0.011	0.045
Assessment	pass	pass	pass	pass	pass	pass

Harmonic sequence	14	15	16	17	18	19
Benchmark of PEA (A)	2	1	1	2	1	1
CP 95%	0.007	0.015	0.005	0.041	0.006	0.035
Assessment	pass	pass	pass	pass	pass	pass

4.2 The evaluated electrical Power Measurement Result

Figure 4.16 illustrated the average power output of measurement in one-week from the selected real PV rooftop power plant. The maximum power was delivered to distribution system up to 780 kW at the noon.
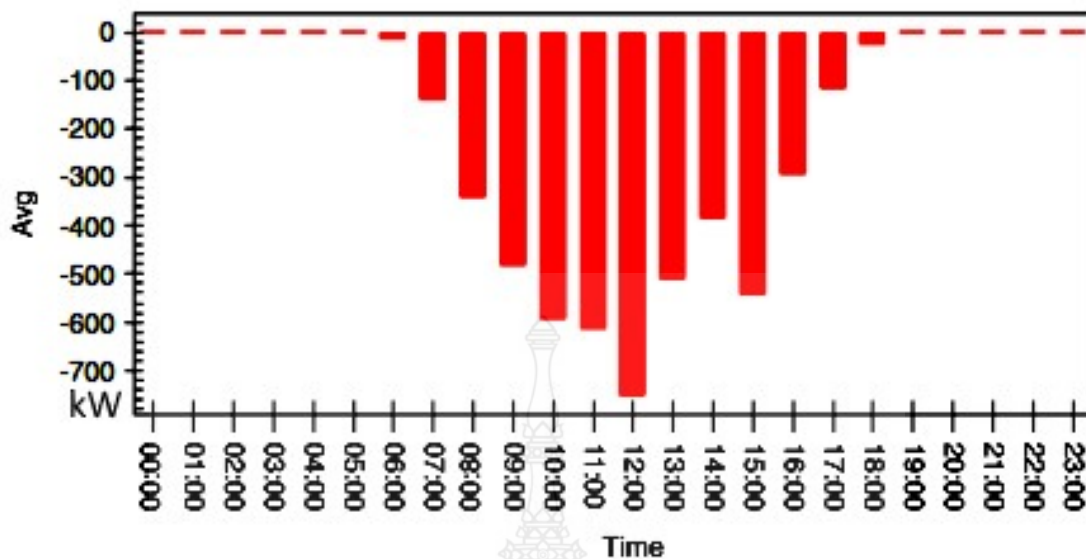
Figure 4.16 The average power output in 1 week from the selected real PV rooftop power plant.

4.3 The Simulation Results by PSCAD/EMTDC

This section aims to investigate the PQ impact of PV rooftop connected to the distribution system with simulation by PSCAD/EMTDC under normal and abnormal case condition base on criteria of PEA's grid code.

4.3.1 The investigation of I-V and P-V curve characteristic of PV module and array

This section aims to simulate I-V and P-V output characteristic curve of solar module that use in this simulation near manufacture standard. So, this simulation considers the effect under Standard Test Conditions (STC) and investigates the effect of difference solar irradiance and temperature on the performance of the components in the model.

Figure 4.17 illustrated The simulation model that simulate I-V and P-V output characteristic curve of solar module under Standard Test Conditions (STC) and difference solar irradiance and temperature. The simulation results are shown in Figure 4.18 and 4.19.
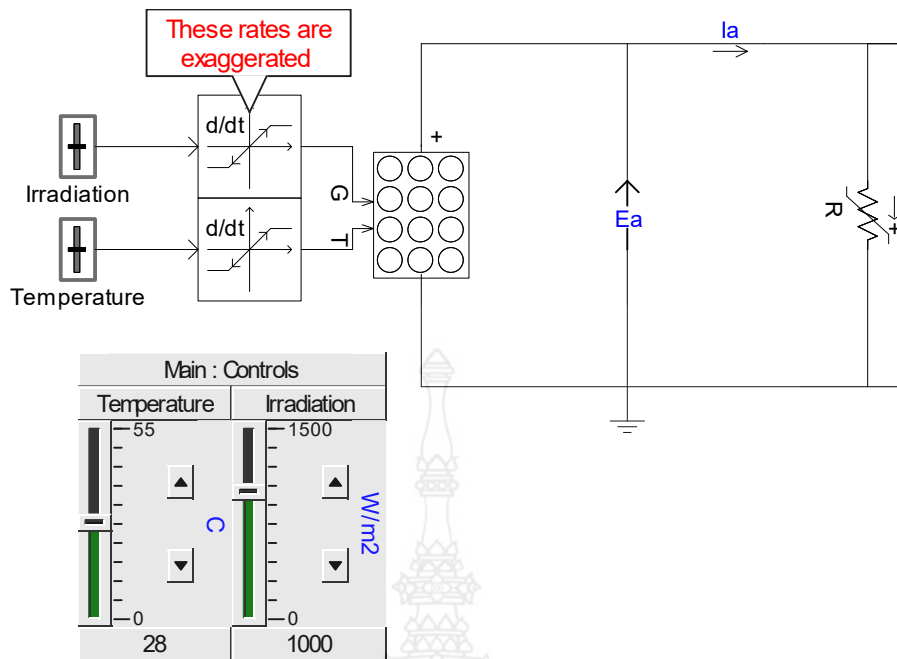
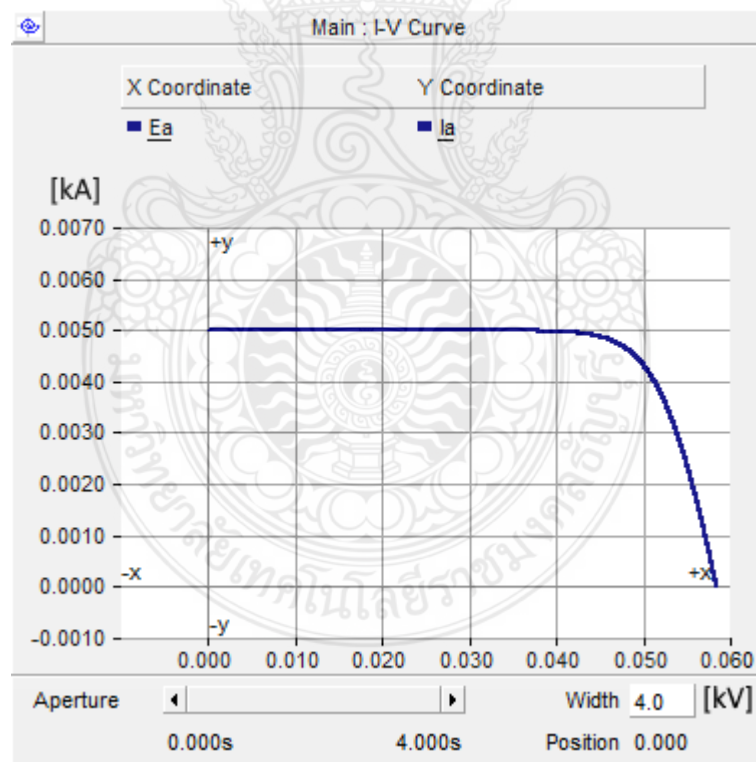**Figure 4.17** The simulation model of the studied I-V and P-V characteristic curve.

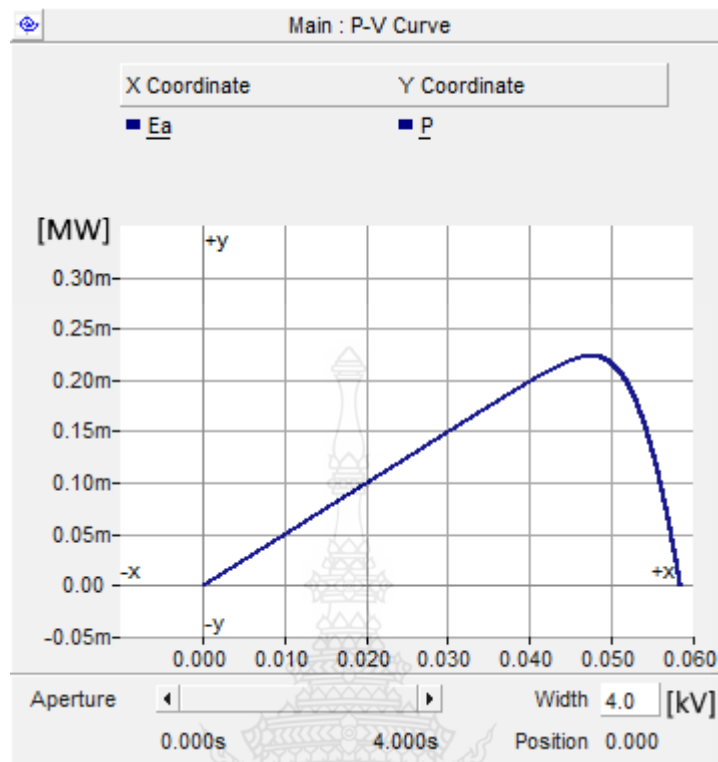**Figure 4.18** The resulting I-V curve of solar module.

Figure 4.19 The resulting P-V curve of solar module.

The output power of solar module is affected by vary the radiation and temperature. The decreasing voltage of solar module depend on the increasing temperature. The current of solar module is directly relative to illumination intensity while voltage is logarithmically proportional with light intensity. Partial shading due to passing clouds and radiation random variations are all factors that will affect photovoltaic system production, resulting in rapid fluctuations in its output power. Figure 4.20, 4.21, 4.22, 4.23 show the characteristics of PV system with 1 MW installation capacity at different temperature and sun radiation.
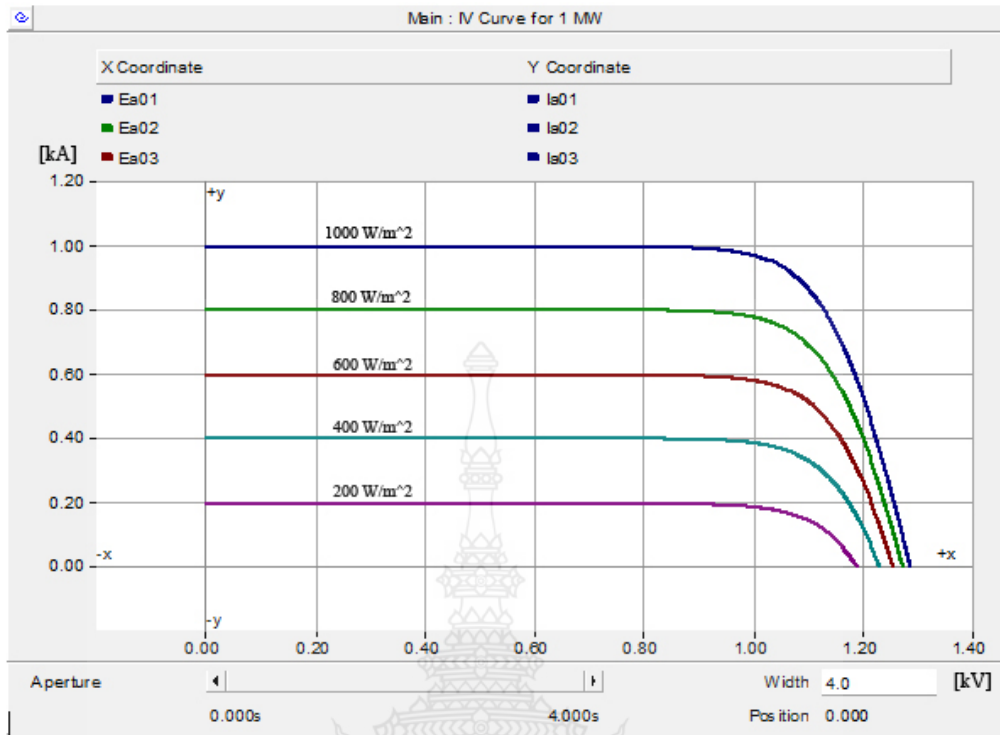
Figure 4.20 The I-V characteristic curve for PV array 1 MW with different solar irradiance.
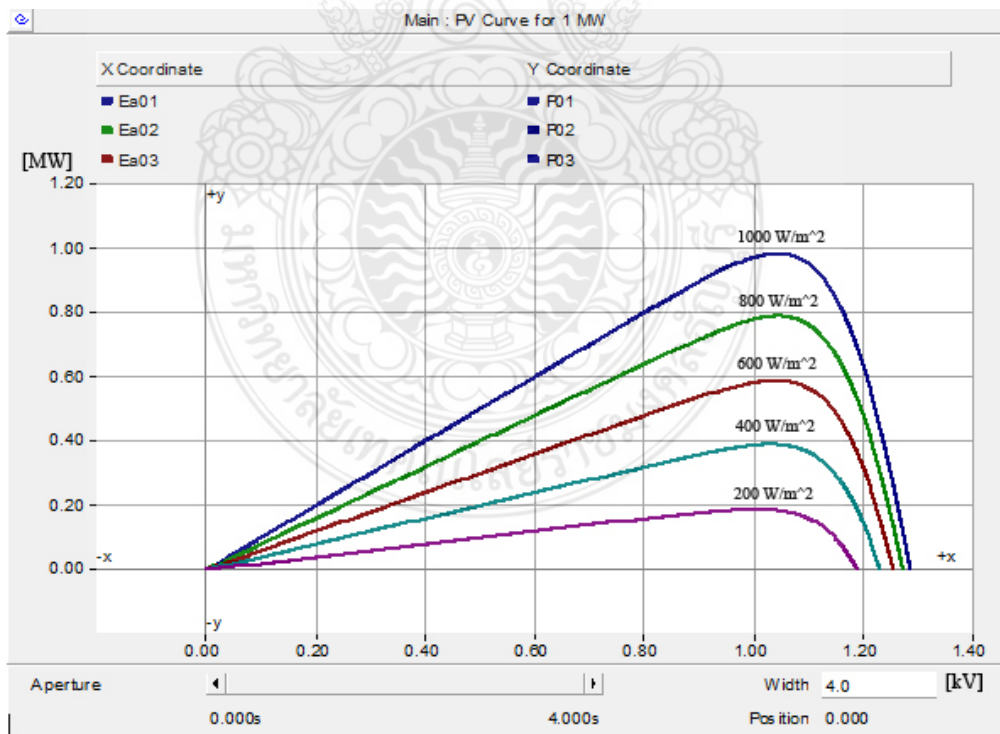
Figure 4.21 The P-V characteristic curve for PV array 1 MW with different solar irradiance.
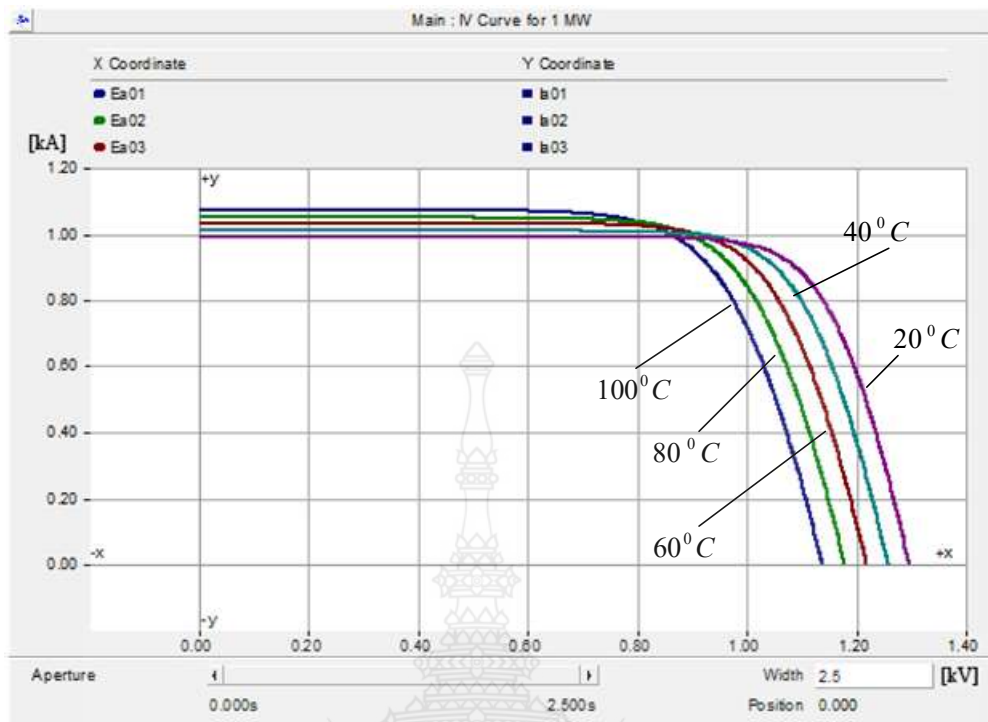
Figure 4.22 The I-V characteristic curve for PV array 1 MW with different temperature.
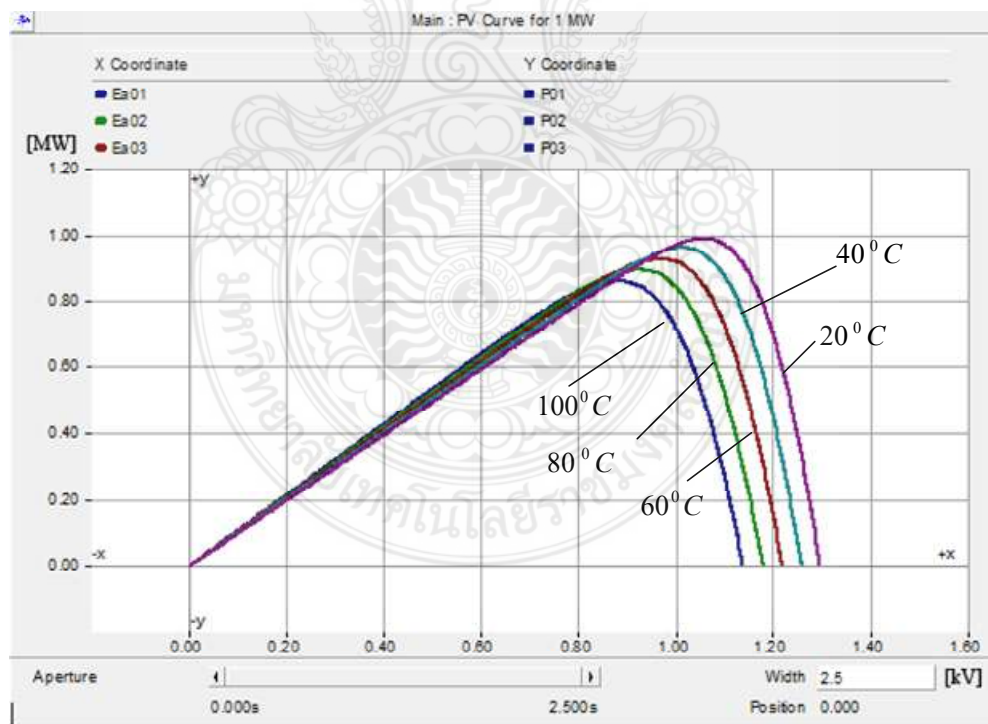

Figure 4.23 The P-V characteristic curve for PV array 1 MW with different temperature

Figure 4.17 show that The simulation model is validated and compared the data results from the manufacture in appendix A. The simulation results in Figure 4.18-4.23 show that the simulation model can simulate the I-V and P-V characteristic curve of solar module and PV array in any solar irradiance and temperature condition when the parameters were changed. This simulation model is of great importance for the study of PV system.

4.3.2 The simulation under steady state operation under Standard Test Condition (STC)

In the first time, the simulation PV rooftop system model in chapter 3 will be validated in response to normal operation. The potential for the PV rooftop system model can track the MPP, perform within THD_V and THD_i limits, and transfer electrical power to the simulated distribution system successfully. The system model will be evaluated under Standard Test Conditions (STC). The simulation results were illustrated in Figure 4.24-4.31.
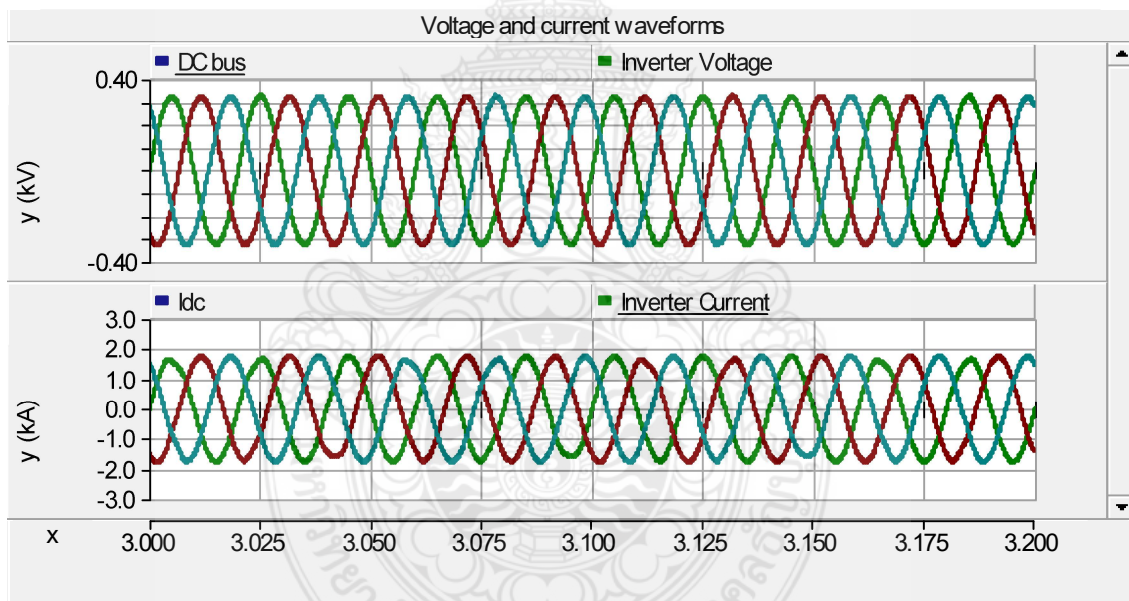

Figure 4.24 The output voltage and current waveforms from PV inverter under STC.
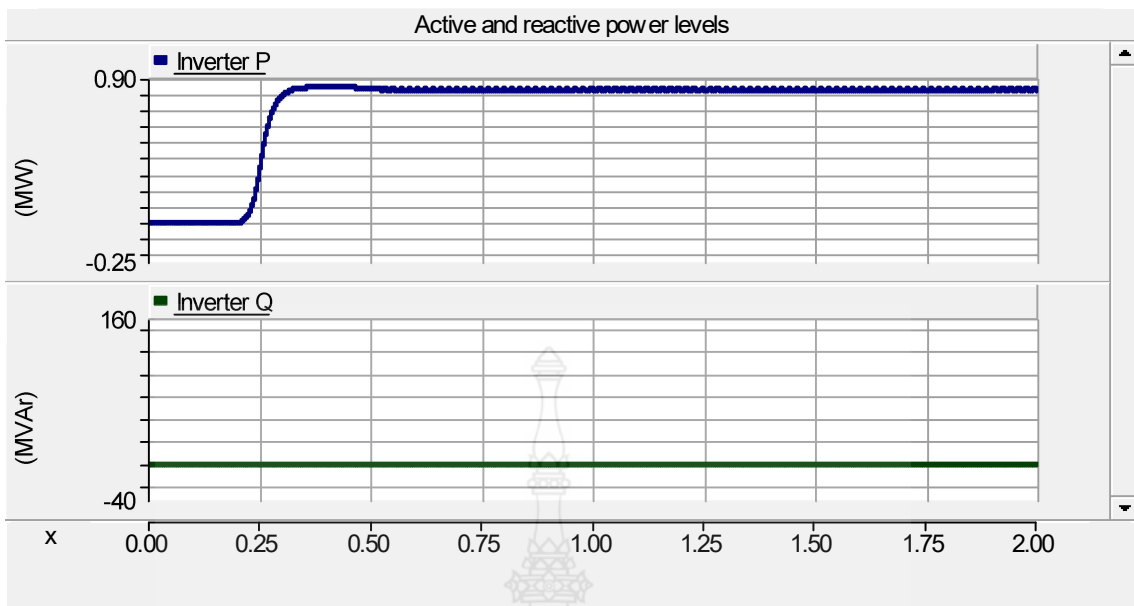
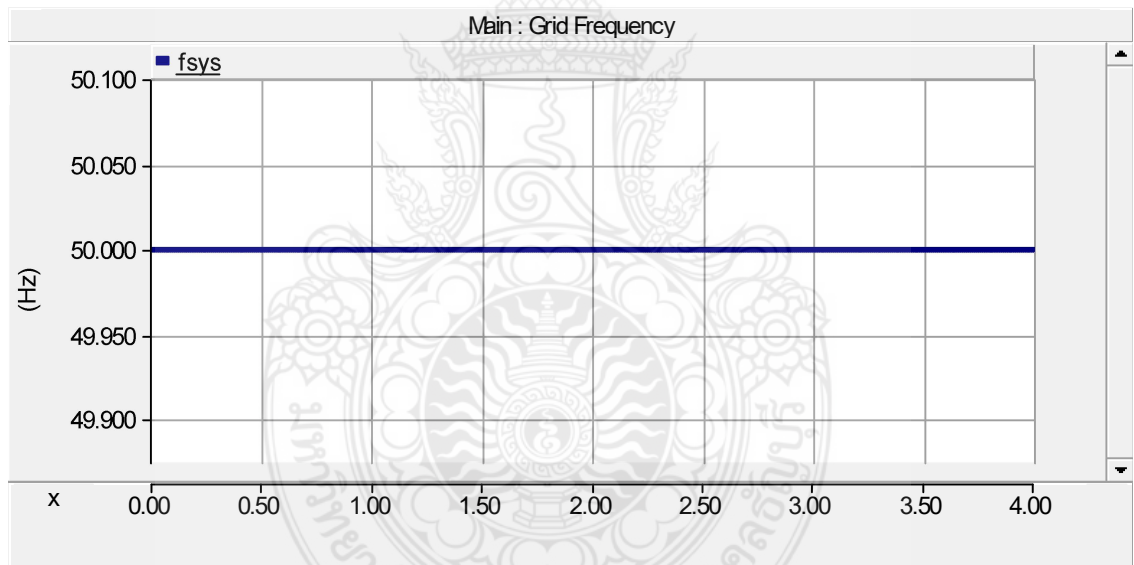**Figure 4.25** The active and reactive power from PV inverter under STC.

Figure 4.26 The inverters frequency under STC.
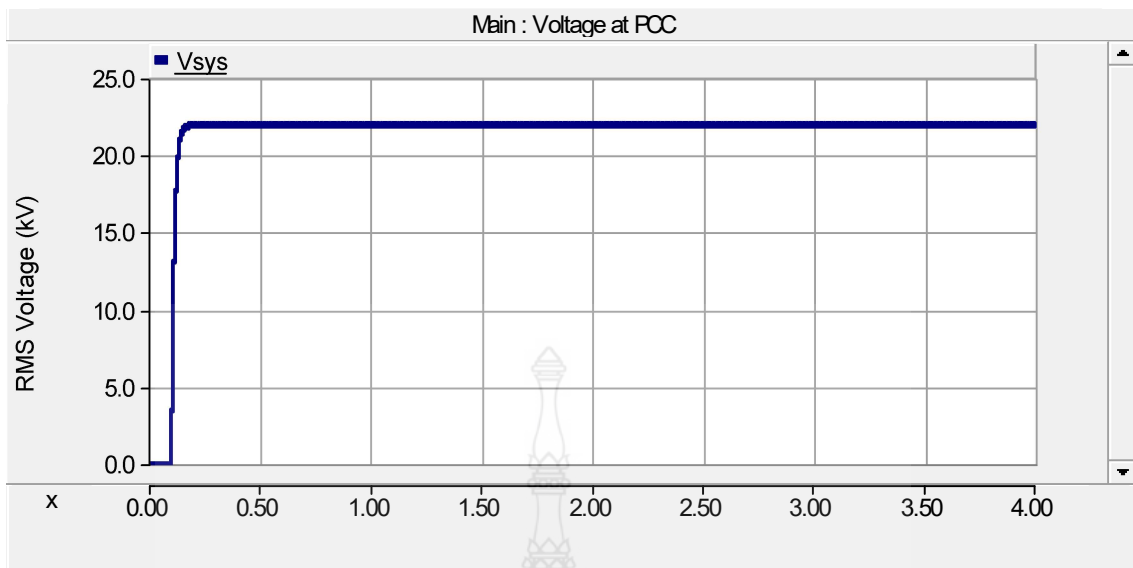
Figure 4.27 The RMS voltage at PCC under STC.

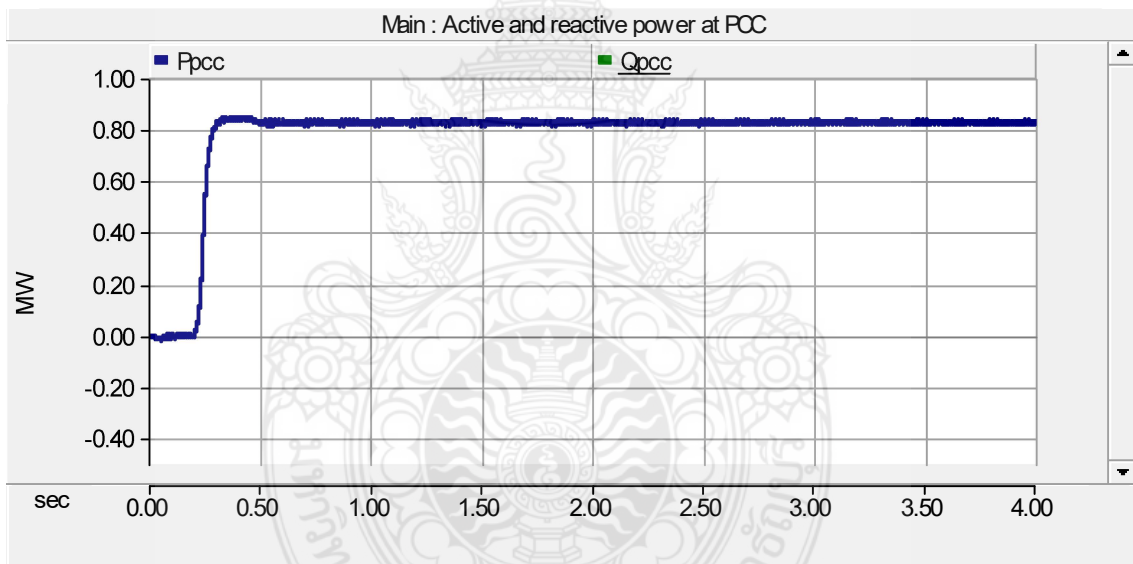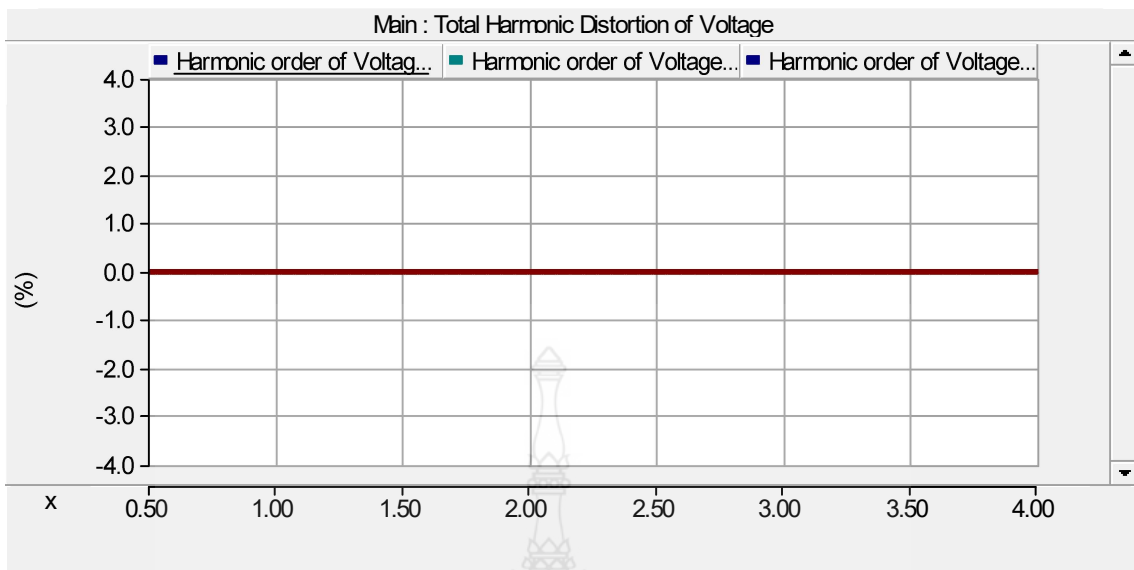**Figure 4.28** The active power of PCC under STC.

62

Figure 4.29 The total harmonic distortion of voltage under STC
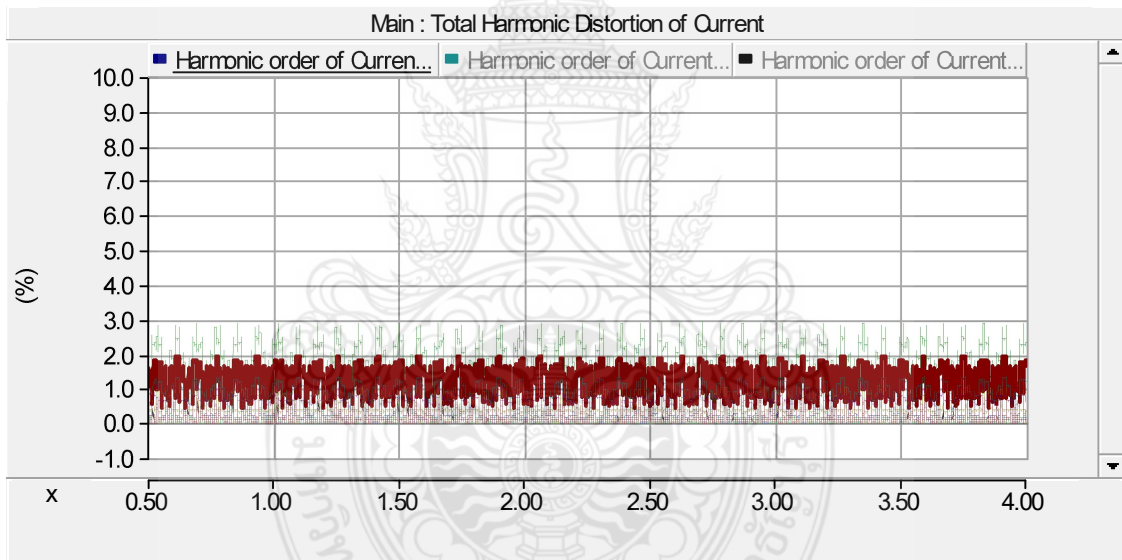

Figure 4.30 The total harmonic distortion of current under STC.

The simulated PQ assessment results shown that RMS voltage, power frequency, active power and total harmonic distortion of voltage and current were also investigated to pass the criteria base on PEA grid code.

4.3.3 The simulation in normal day condition

In this section, the operation of PV rooftop system model will be investigated under different solar irradiance and temperature that will be provided into the PV array and are used to test the effect of PV rooftop system to the distribution network. Figure 4.31 and 4.32 show the different solar irradiance and temperature in normal day. The simulation results are shown in Figure 4.33-4.37.
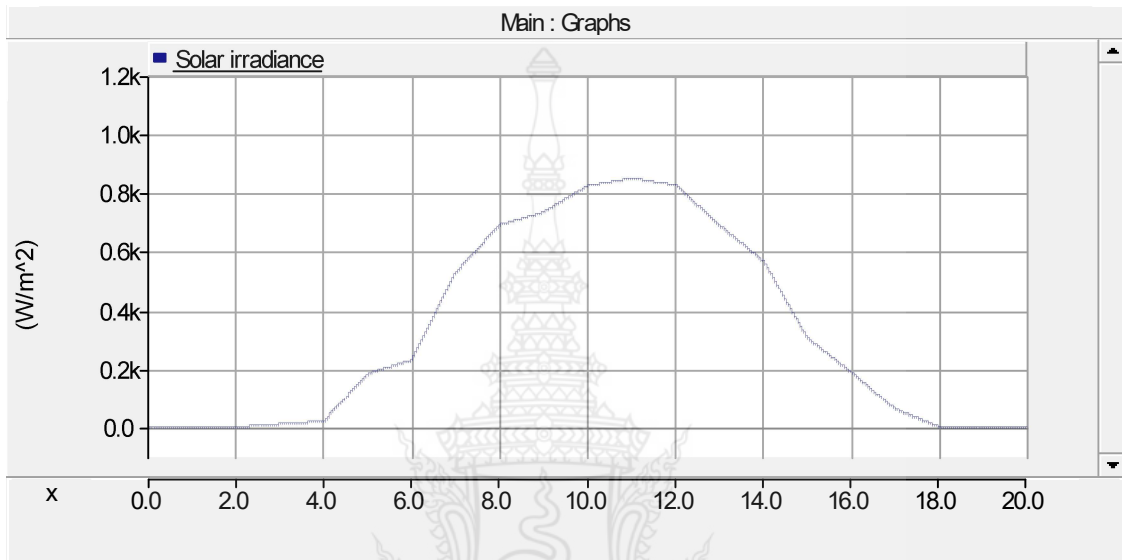

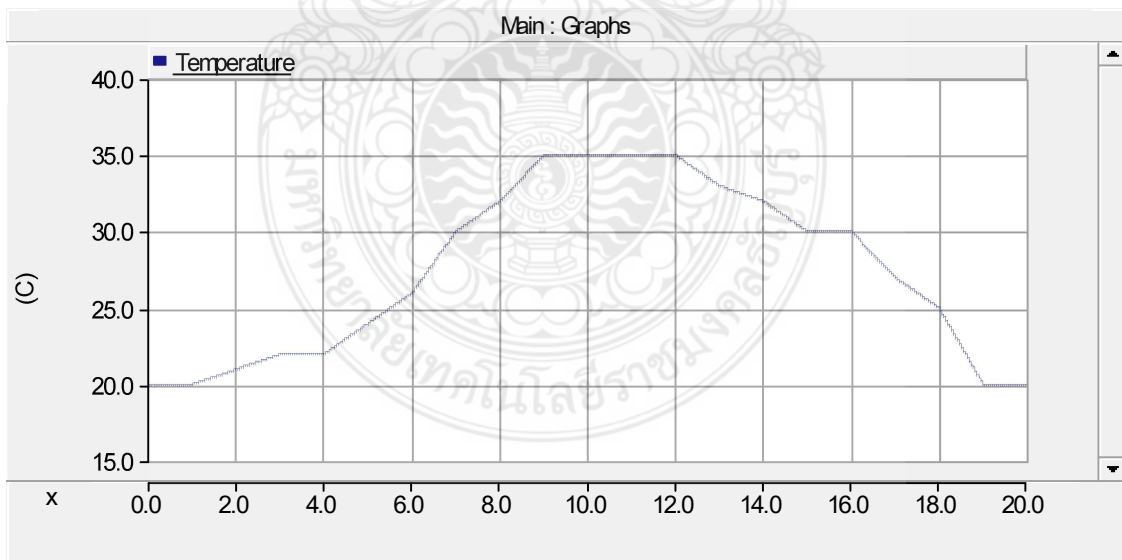**Figure 4.31** The solar irradiance in normal day.

Figure 4.32 The temperature in normal day.
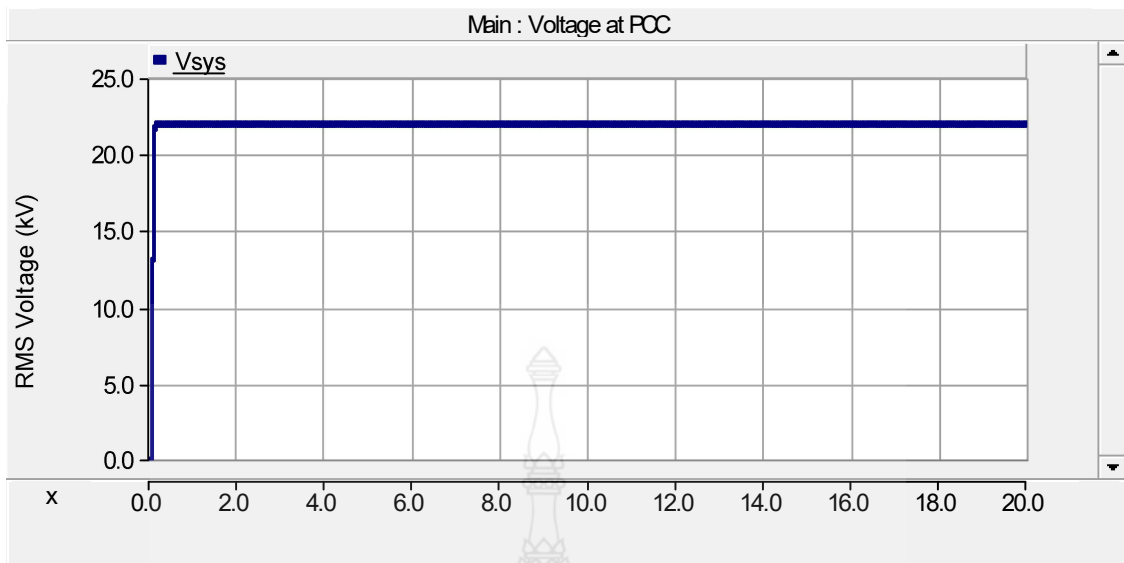
Figure 4.33 The RMS Voltage at PCC in normal day.
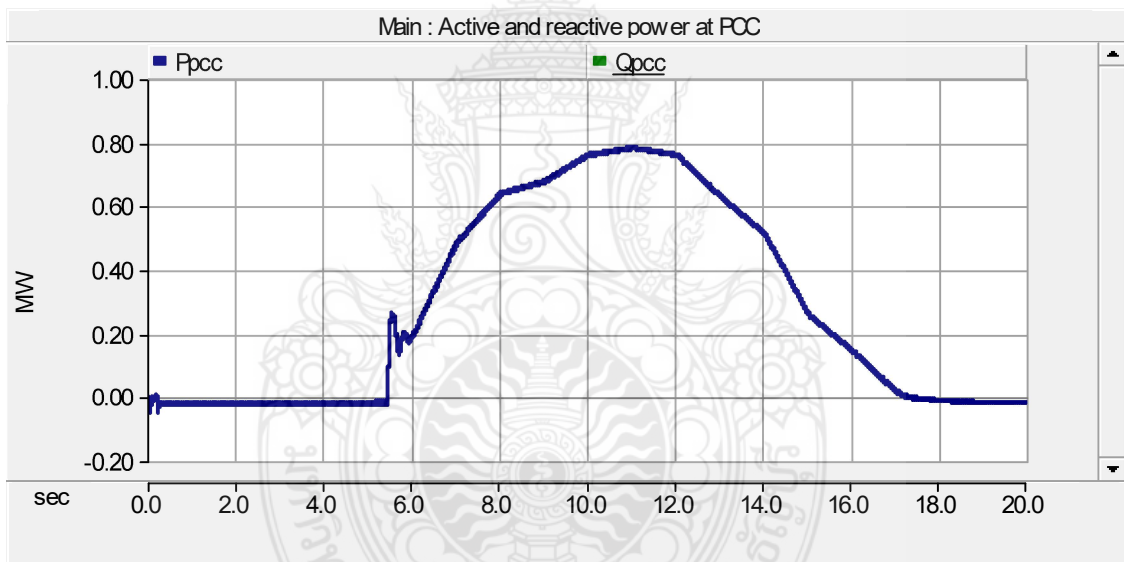
Figure 4.34 The active power at PCC in normal day.

Figure 4.35 The frequency at PCC in normal day.

Figure 4.36 The total harmonic distortion of voltage in normal day.

Figure 4.37 The total harmonic distortion of current in normal day.

The simulated PQ assessment results shown that RMS voltage, power frequency, active power and total harmonic distortion of voltage and current in normal day were also investigated to pass the criteria base on PEA grid code.

4.3.4 The simulation in raining day condition

In this section, the operation of PV rooftop system model will be investigated under immediately solar irradiance and temperature that will be provided into the PV array and are used to test the effect of PV rooftop system to the distribution network. Figure 4.38 and 4.39 show the immediately solar irradiance and temperature in raining day in the afternoon. The simulation results are shown in Figure 4.40-4.44.
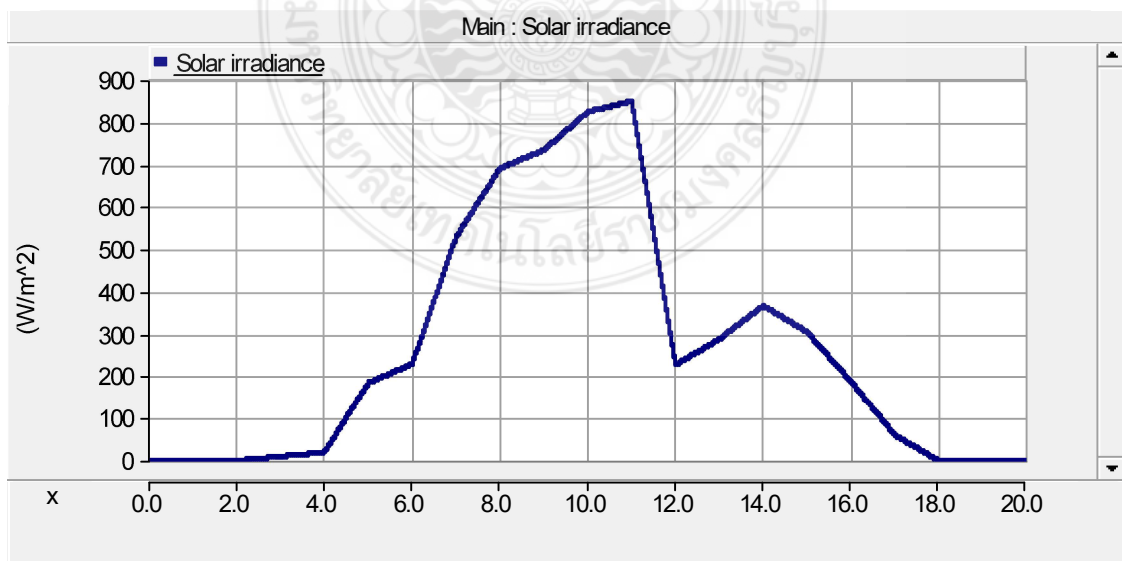
Figure 4.38 The immediately solar irradiance in raining day.
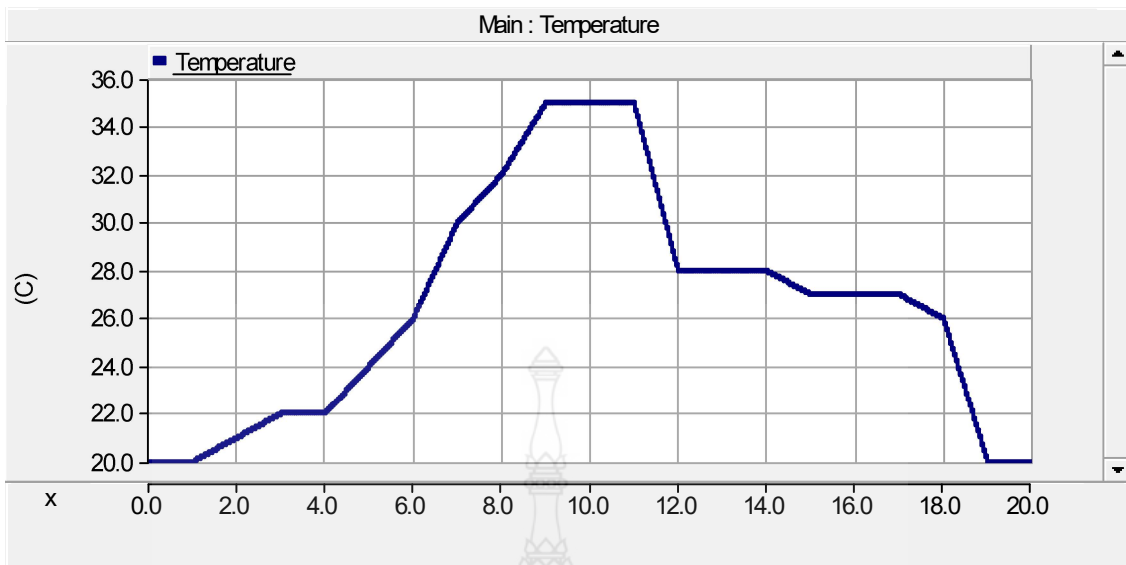
Figure 4.39 The immediately temperature in raining day.
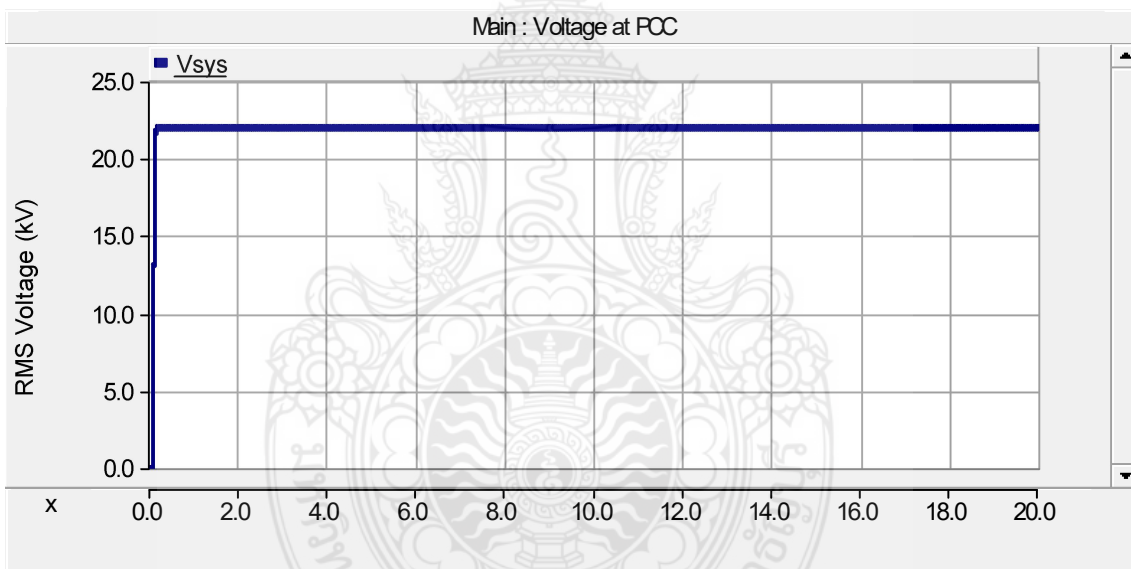
**Figure 4.40** The RMS Voltage at PCC in raining day.

68
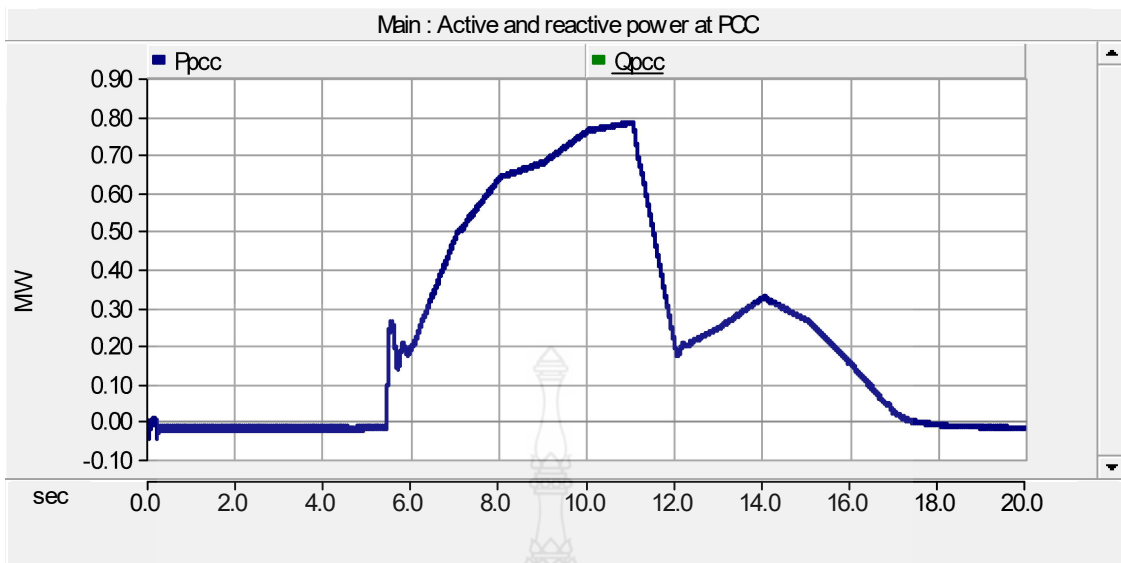
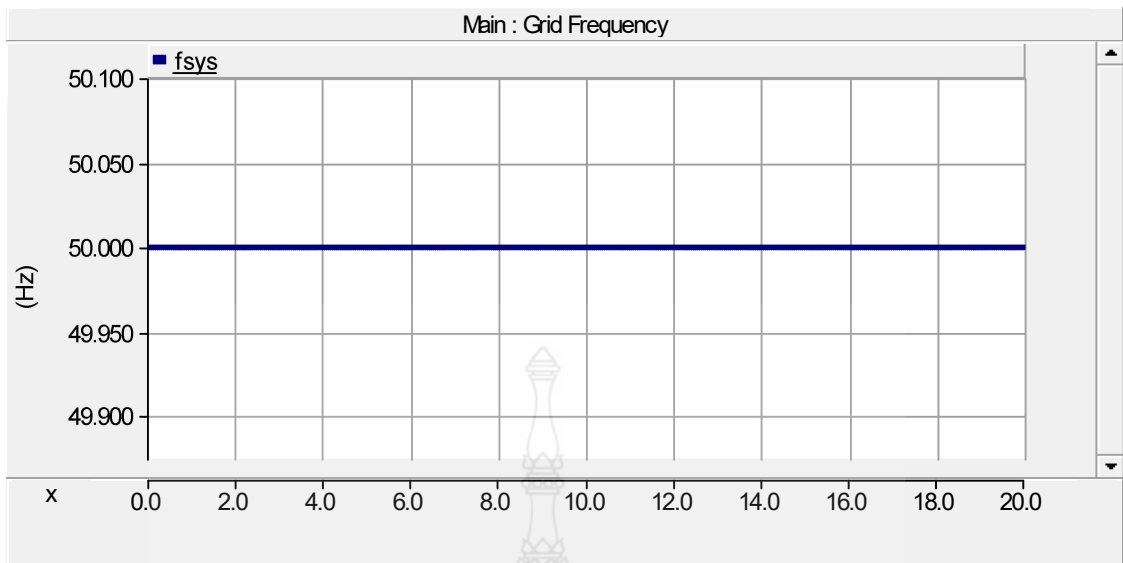**Figure 4.41** The active power at PCC in raining day.
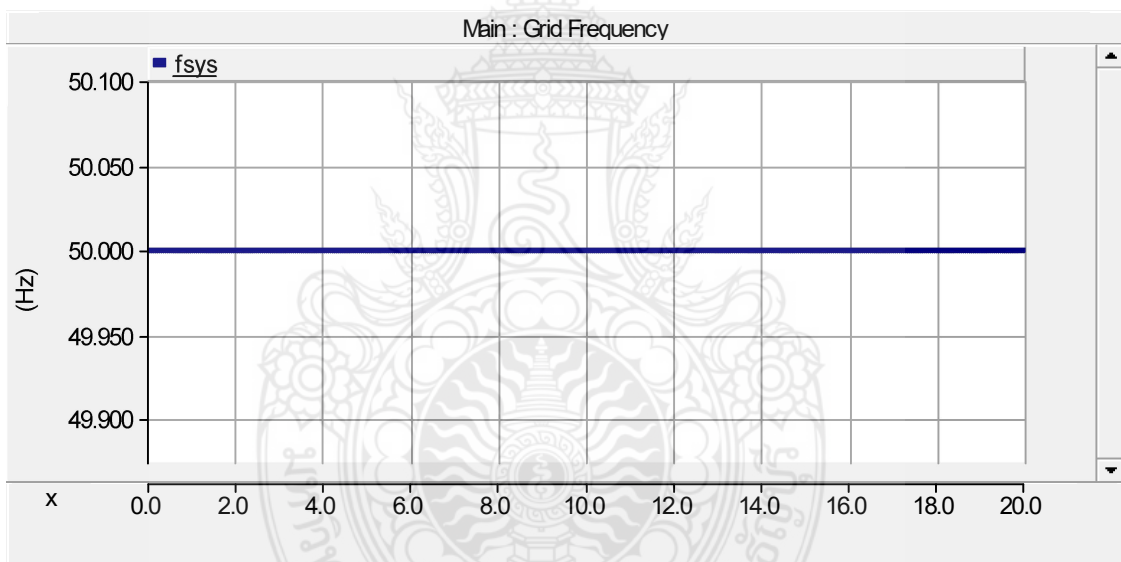
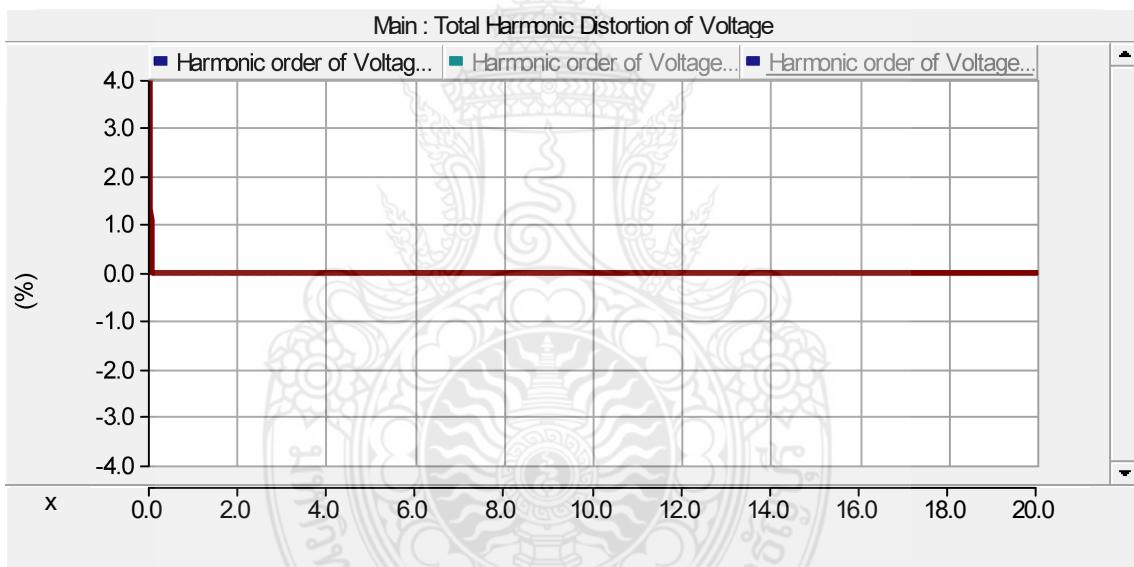**Figure 4.42** The frequency at PCC in raining day.

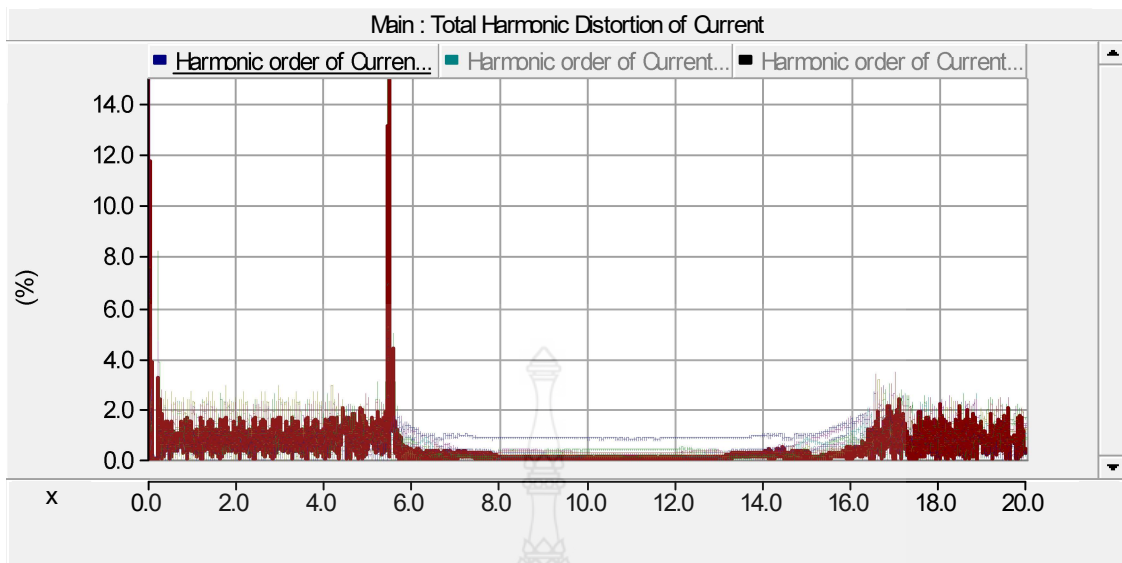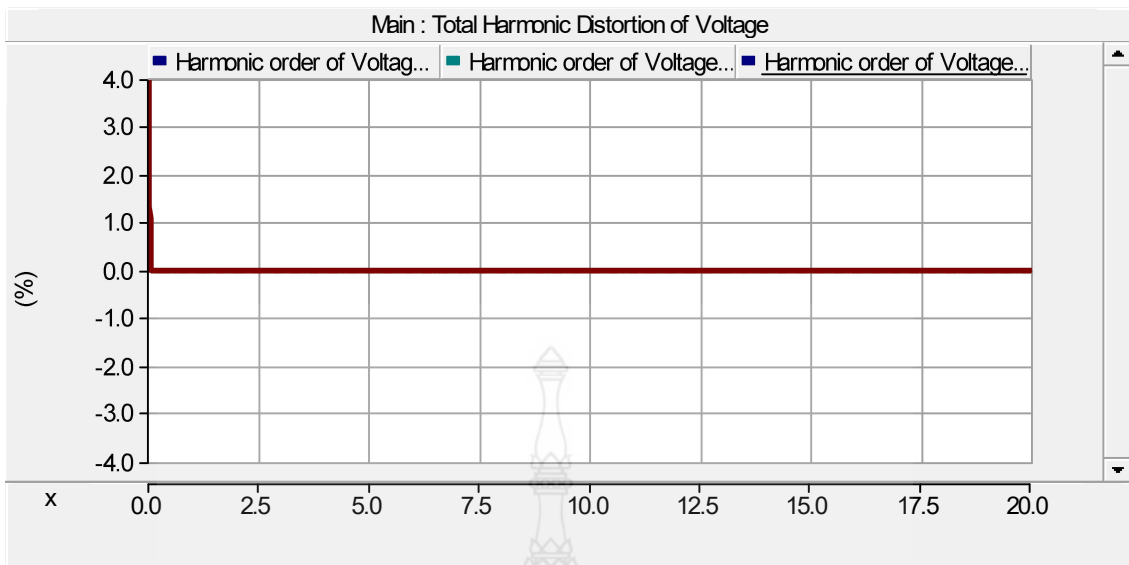**Figure 4.43** The total harmonic distortion of voltage in raining day.
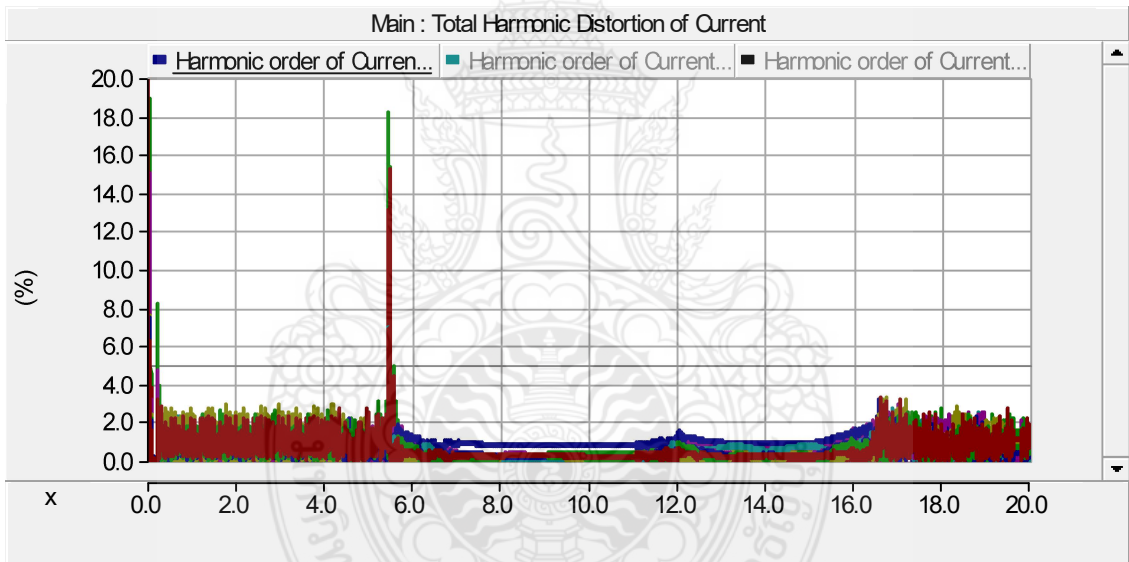
Figure 4.44 The total harmonic distortion of current in normal day.

The simulated PQ assessment results shown that RMS voltage, power frequency, active power and total harmonic distortion of voltage and current in raining day were also investigated to pass the criteria base on PEA grid code.

4.3.5 The simulation in short time of solar irradiance fluctuation

In this section, the operation of PV rooftop system model will be investigated under fluctuated solar irradiance in short time that will be provided into the PV array and are used to test the effect of PV rooftop system to the distribution network. Figure 4.45 shows the fluctuated solar irradiance in short time. The simulation results are shown in Figure 4.46-4.42.
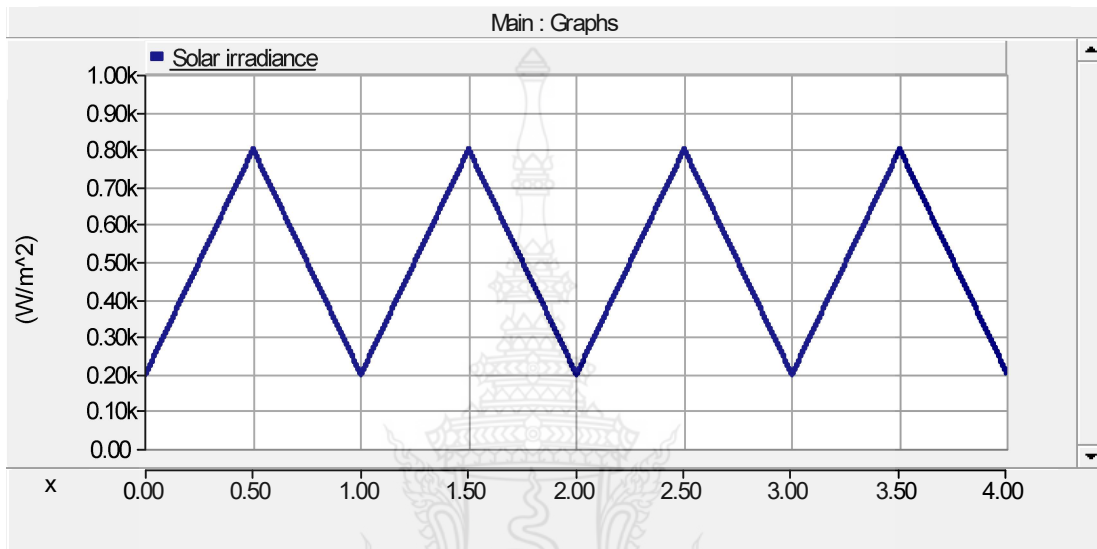
Figure 4.45 The fluctuated solar irradiance in short time.
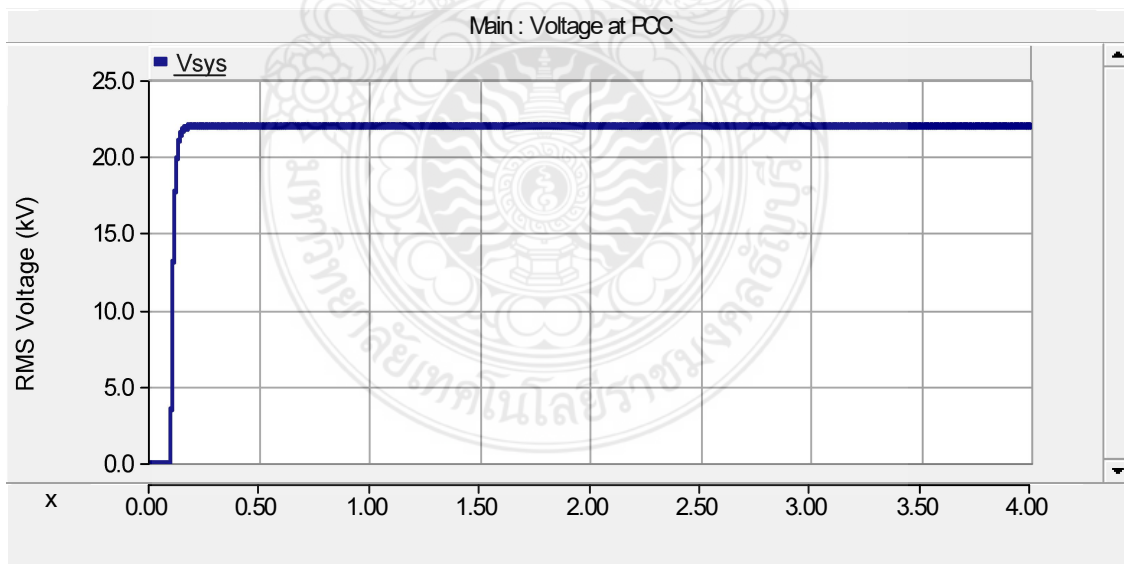
Figure 4.46 The RMS Voltage at PCC under the fluctuated solar irradiance in short time.
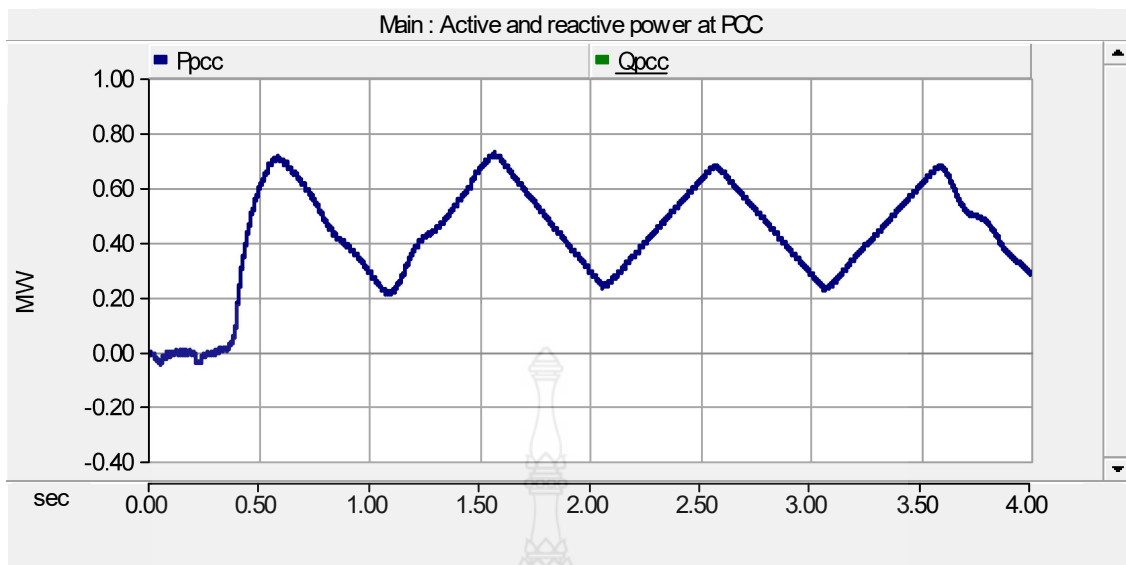
Figure 4.47 The active power at PCC under the fluctuated solar irradiance in short time.
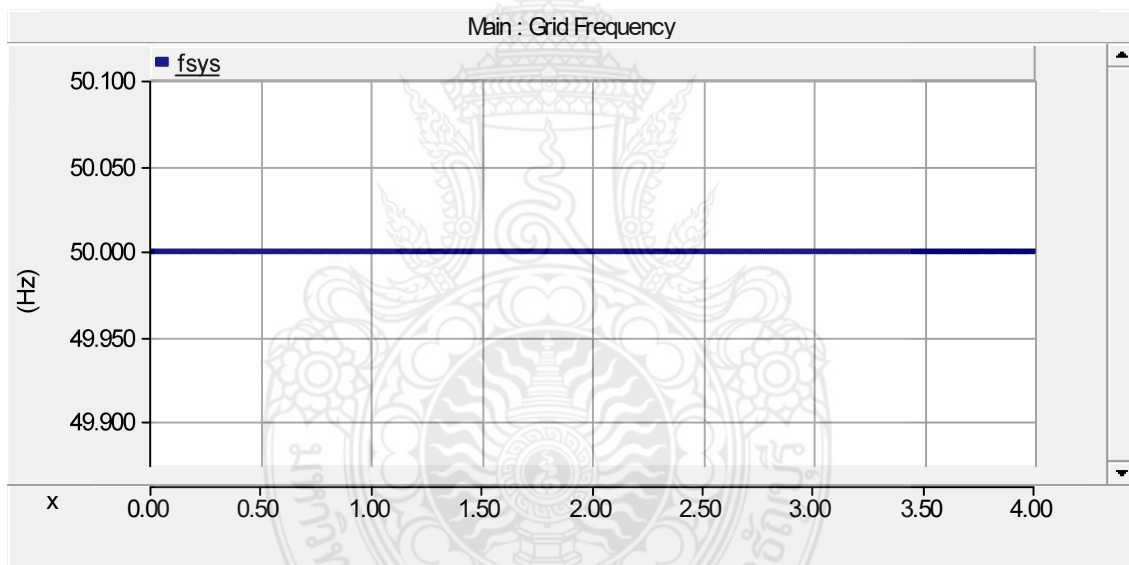
Figure 4.48 The frequency at PCC under the fluctuated solar irradiance in short time.
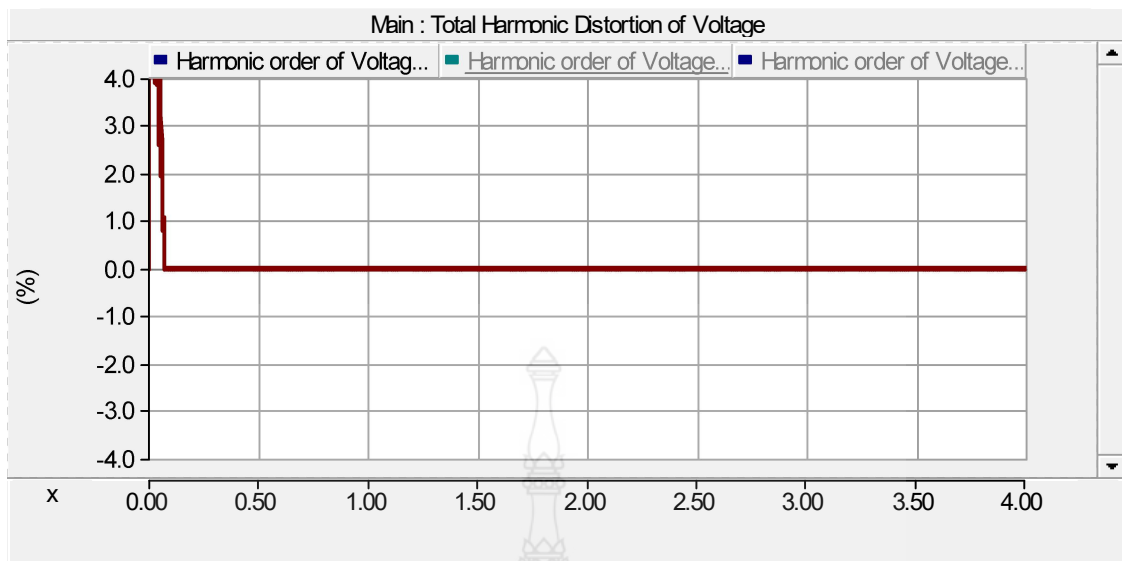
Figure 4.49 The total harmonic distortion of voltage under the fluctuated solar irradiance in short time.
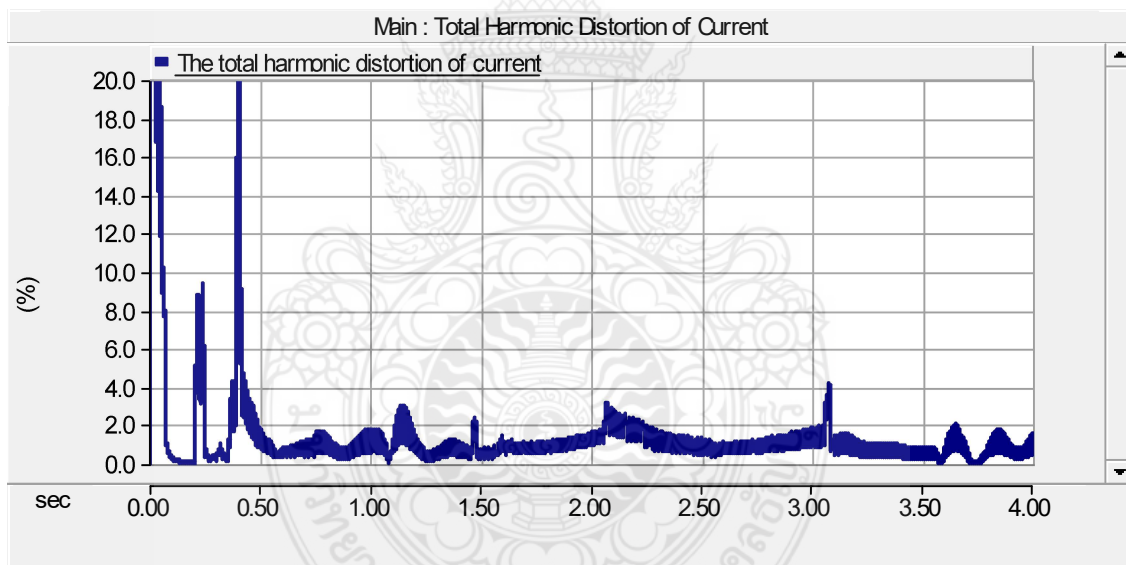
Figure 4.50 The total harmonic distortion of current under the fluctuated solar irradiance in short time.

The simulated PQ assessment results shown that RMS voltage, power frequency, active power and total harmonic distortion of voltage and current under the fluctuated solar irradiance in short time were also investigated to pass the criteria base on PEA grid code.

4.3.6 The simulation under VSI inverter defect

In this section, the operation of PV rooftop system model will be investigated under VSI inverter defect that will be provided into the PV array and are used to test the effect of PV rooftop system to the distribution network. The simulation results are shown in Figure 4.51-4.56.
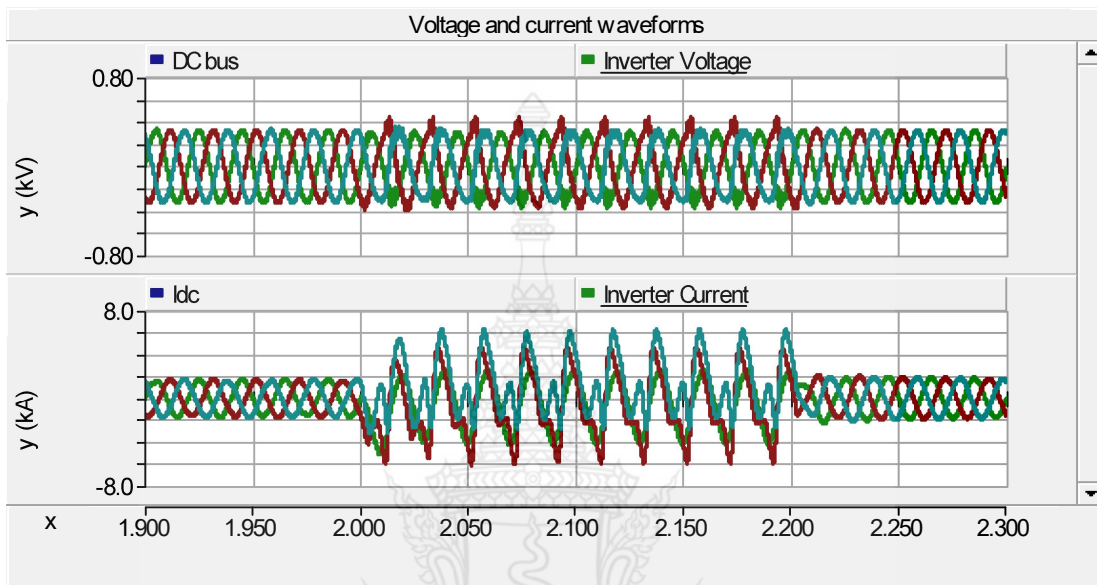
Figure 4.51 The output voltage and current waveforms from PV inverter.
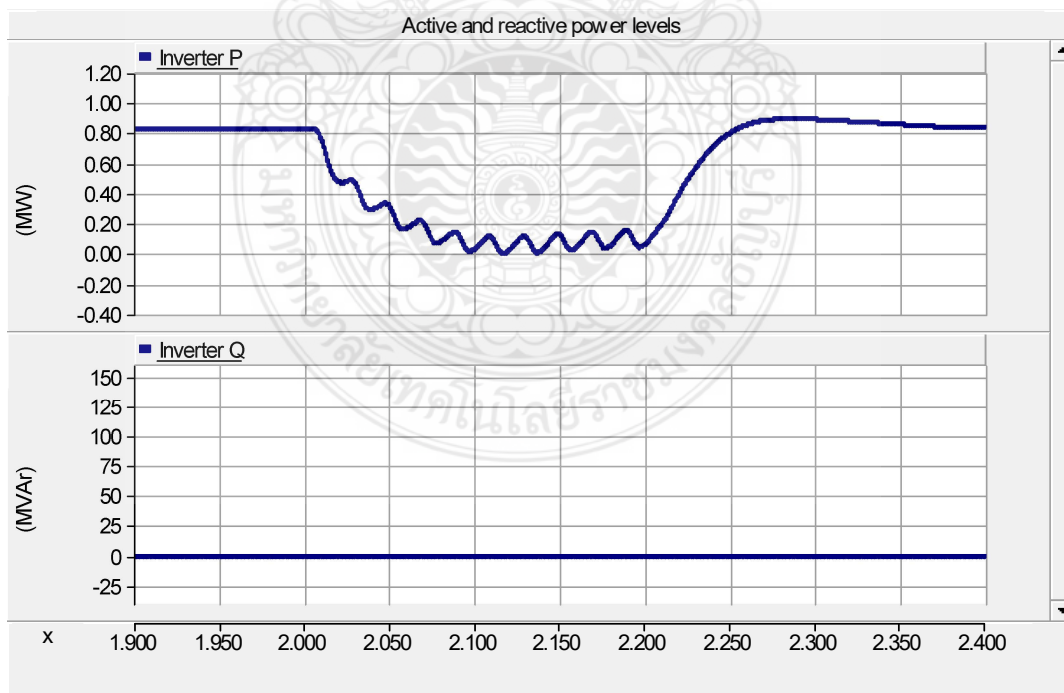
Figure 4.52 The active and reactive power from PV inverter.
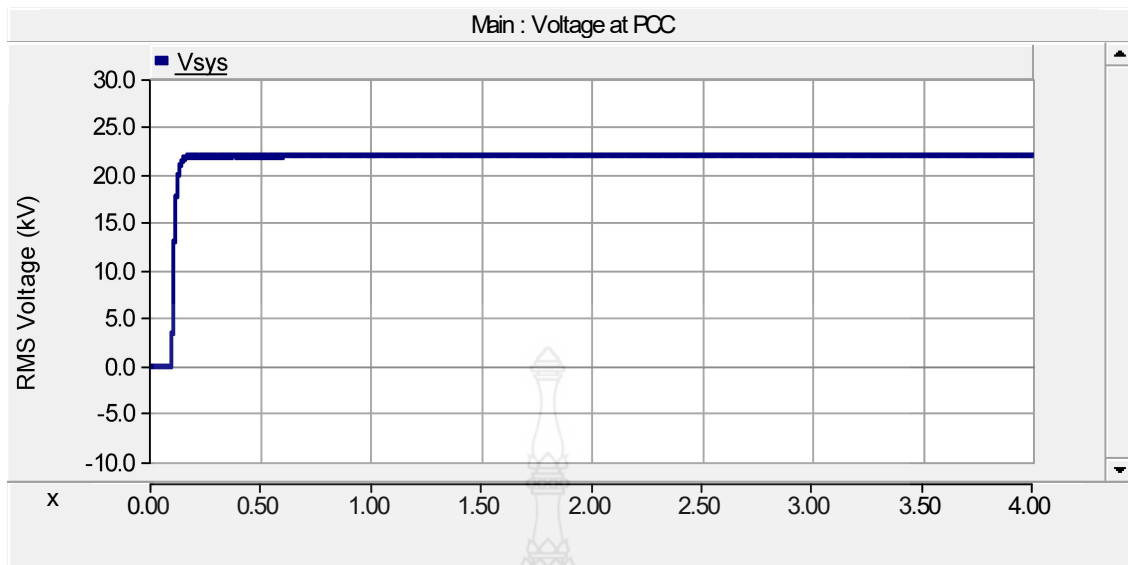
Figure 4.53 The RMS voltage at PCC.
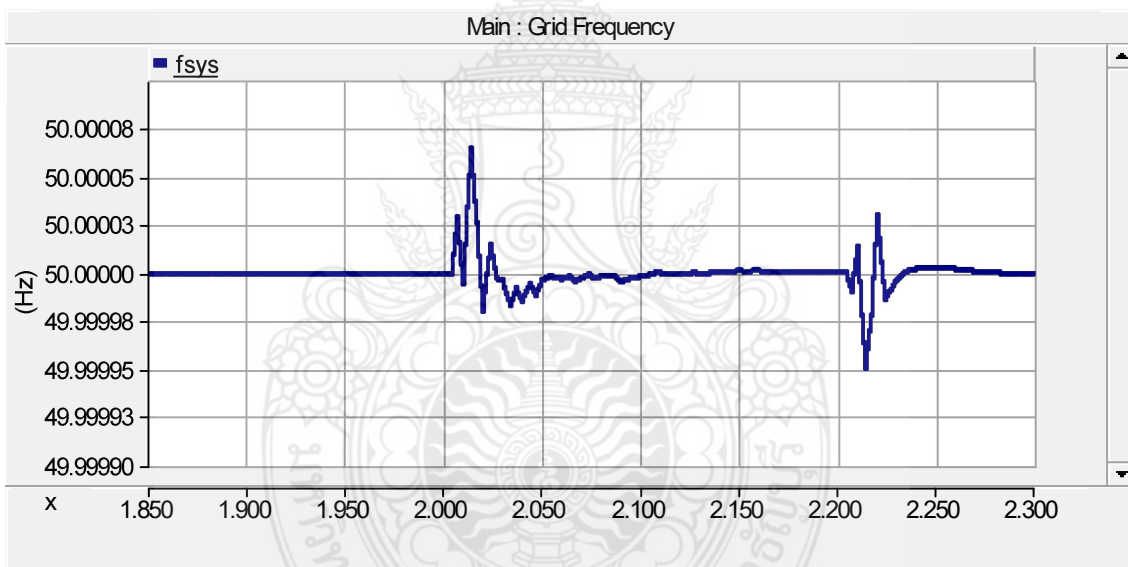
Figure 4.54 The power frequency at PCC.
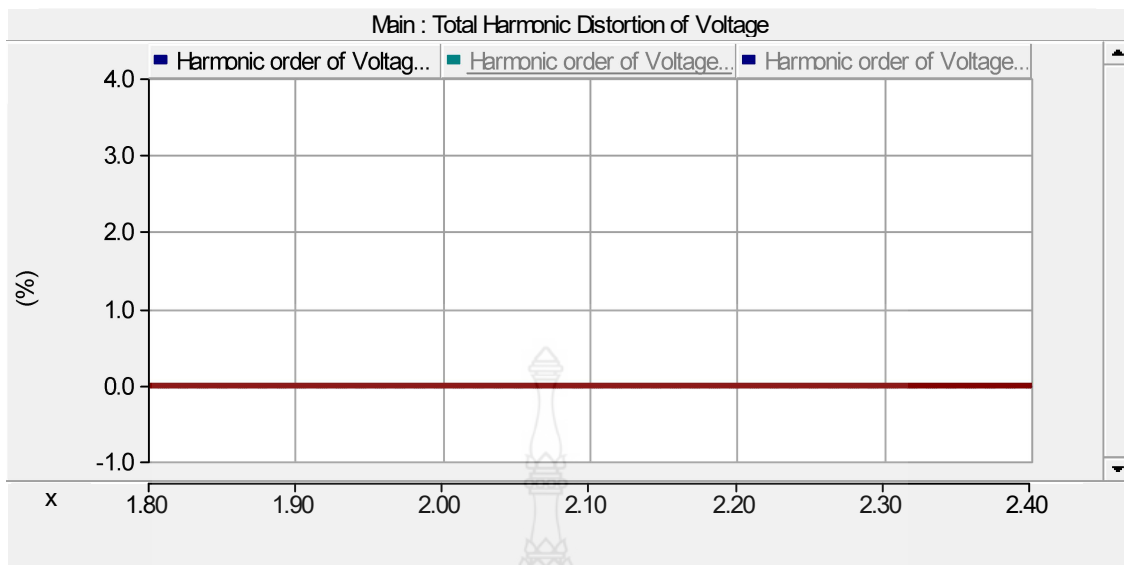
Figure 4.55 The total harmonic distortion of voltage at PCC.
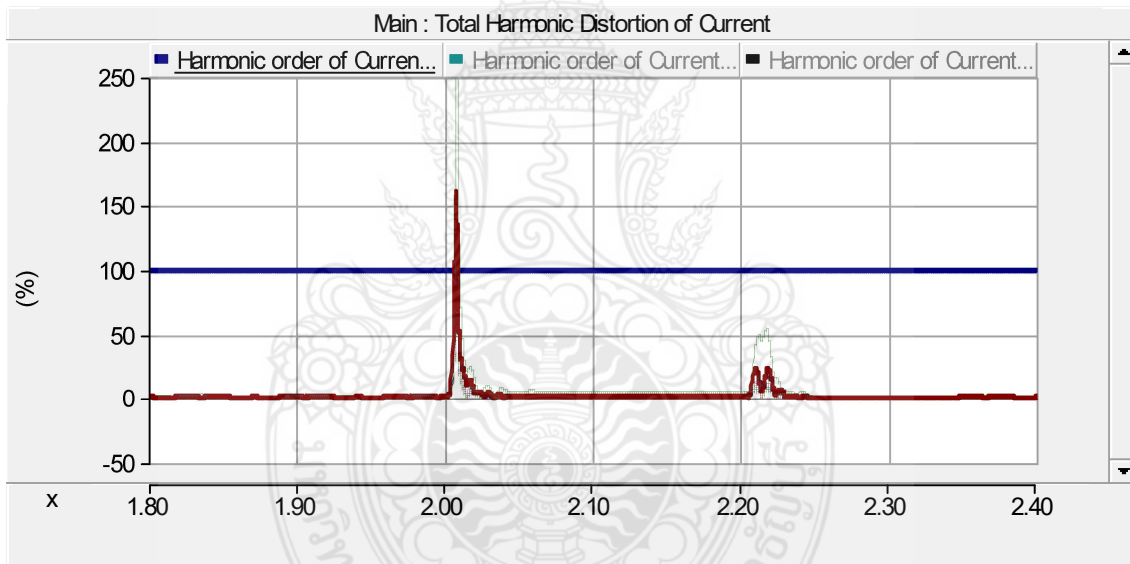
Figure 4.56 The total harmonic distortion of current at PCC.

The simulated PQ assessment results shown that The output voltage and current from PV inverter are fluctuation in short time and recovery to normality, the output power from inverter cannot inject the power into the distribution system in short time, RMS voltage at PCC is normality, power frequency is fluctuation in short time and recovery to normality, and total harmonic distortion of voltage was investigated to pass the criteria and total harmonic distortion of current is fluctuation in short time and recovery to normality. After the recovery, all parameters were also investigated to pass the criteria base on PEA grid code.

4.3.7 The simulation under ferroresonance phenomenon

The main purpose of this section is to remind the Provincial Electricity Authority of Thailand (PEA) about the possible occurrence of ferroresonance in the low voltage side of the distribution transformer that is connected to PV rooftop system. Various situations have been introduced and simulated together with the analysis the effect of the system parameters for instances, line capacitance, transformer's core inductance and PV source. It is known that testing of ferroresonance in the transformer could lead the damage to the transformer or even completely destroy it if the resonance is in the unstable region. For this reason, the PSCAD/EMTDC software for investigating this phenomenon was decided to use, which is flexible for arranging the experiment and collecting the data. The single line diagram for specific this case is shown in Figure 4.57. In addition, the parameters and data are concluded in Table 4.9.
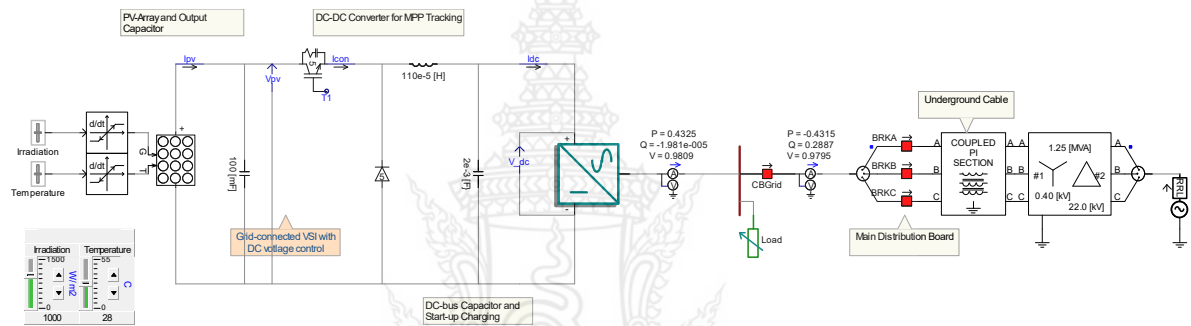
Figure 4.57 The single line diagram of PV rooftop system connected to the grid and light load through 1.25 MVA transformer.

Table 4.9 The parameter model system for ferroresonance simulation.

Name	Parameter	Value
PV module data	Ref. Solar irradiance	800 W/m^2
	Ref. Temperature	30 ºC
Coupled PI Model	Feeder Rated Frequency	50 Hz
	Feeder Length	0.2 km
Transformer	Distribution Transformer MVA	1.25 MVA
	Primary voltage	0.4 kV
	Secondary voltage	22 kV
	Type: Wye ground – Delta	

	Base operation frequency	50 Hz
Load	Customer Load	0.1 MW per phase

The three single phase circuit breaker (BRKA, BRKB, and BRKC) in main distribution board are connected to distribution transformer through underground feeder. Each circuit breakers are correspondingly switched from phase B, C and A for disconnecting and then they are correspondingly switched from phase A, C and B for connecting.

Figure 4.58 (a) and (b) illustrated the overall ferroresonance that happen in the system at low voltage side of distribution transformer connected PV rooftop system. The voltage and current waveform are fluctuation.
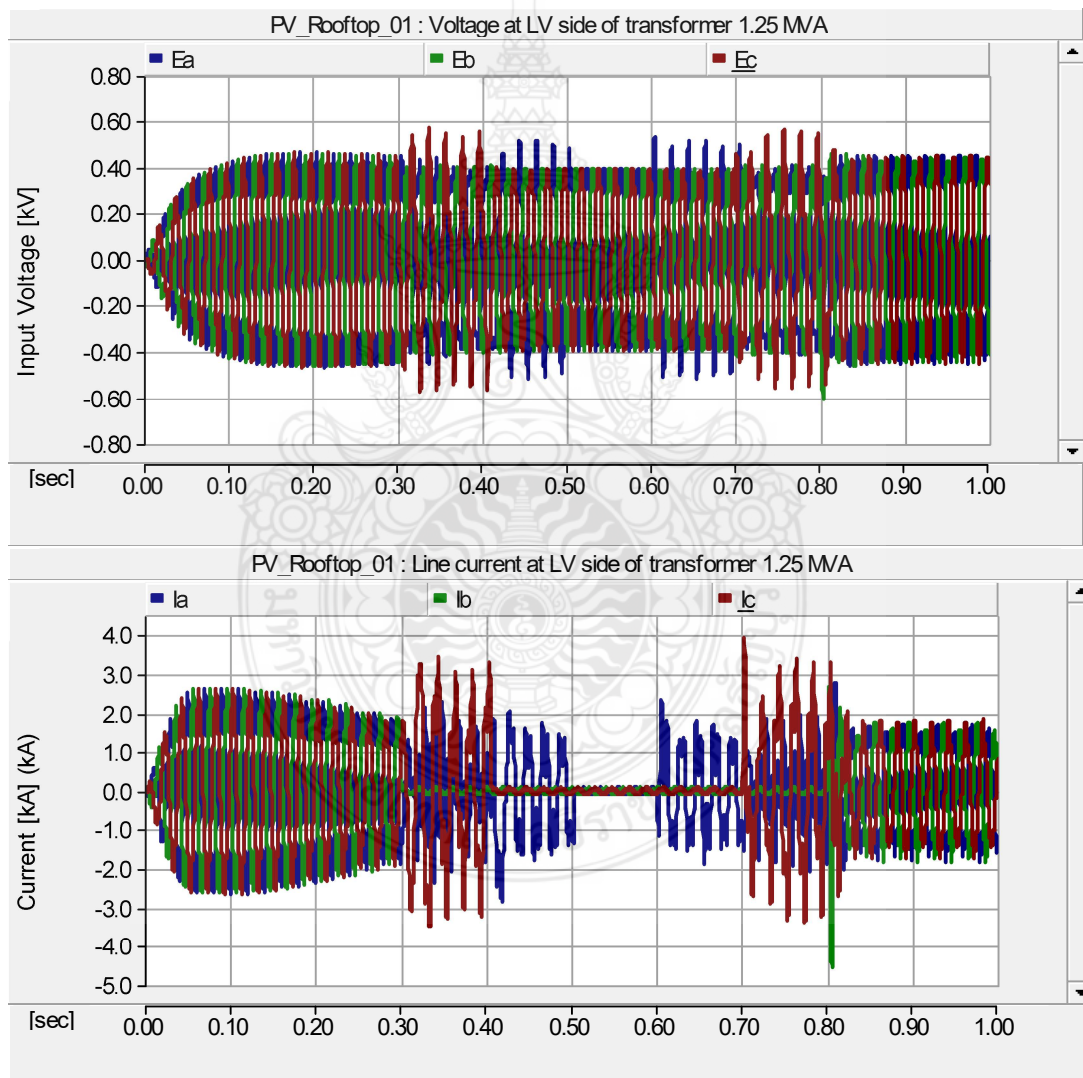
Figure 4.58 The fluctuated voltage and current waveform at the distribution transformer connected PV rooftop system.

By the way, the simulation results of the disconnecting of single circuit breaker in the step by step are illustrated. Firstly, phase B is disconnected at 0.3 sec.as shown in Figure 4.59, the voltage and current waveform are shown in Figure 4.60.

Figure 4.59 The LC ferroresonance circuit with disconnecting CB2 phase B.

(a) Phase A

(b) Phase B

(c) Phase C

Figure 4.60 The Voltage and current waveform at LV side of transformer 1.25 MVA when BRKB disconnecting at 0.3 sec.

The simulation results in Figure 4.60 are definitely sighted that the ferroresonance affected to phase A and C. The voltage comprises of the fundamental mode ferroresonance and the current comprise of the cohesion of fundamental mode and quasi-periodic mode ferroresonance.

By the way, secondly, phase C is disconnected at 0.4 sec. as shown in Figure 4.61, the voltage and current waveform are shown in Figure 4.62.
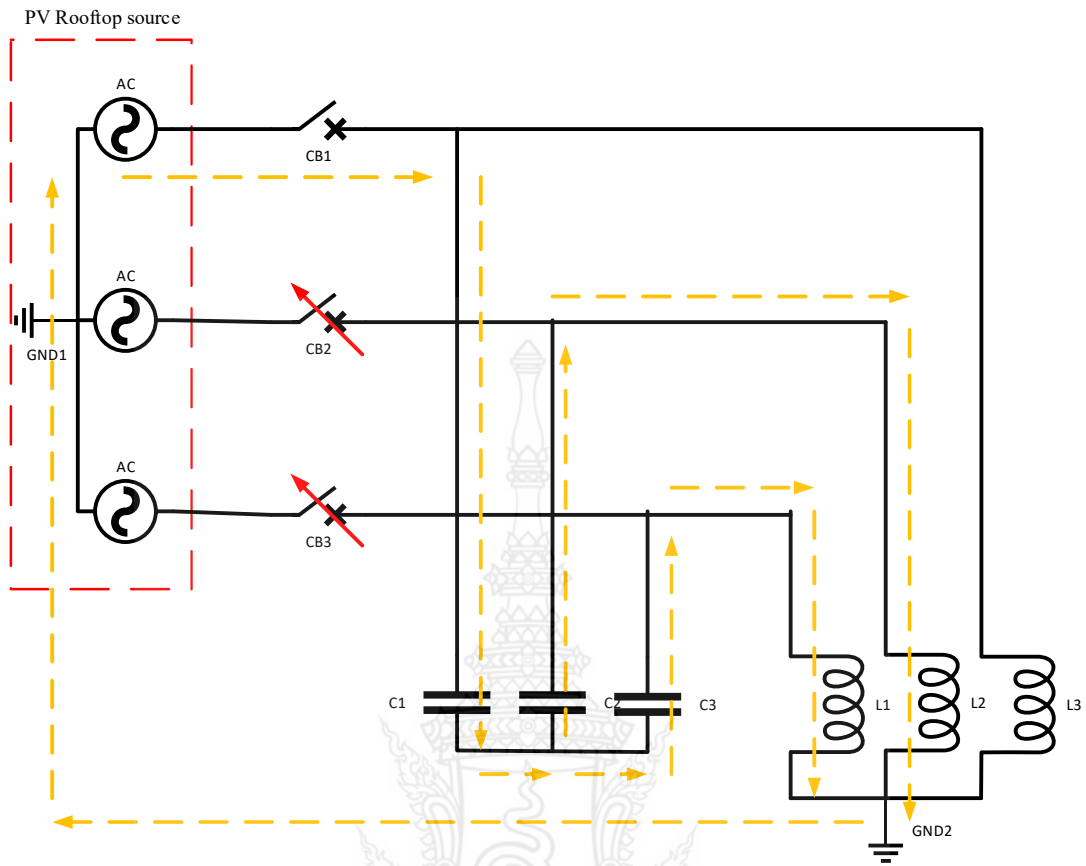
Figure 4.61 The LC ferroresonance circuit with disconnecting CB3 phase C.
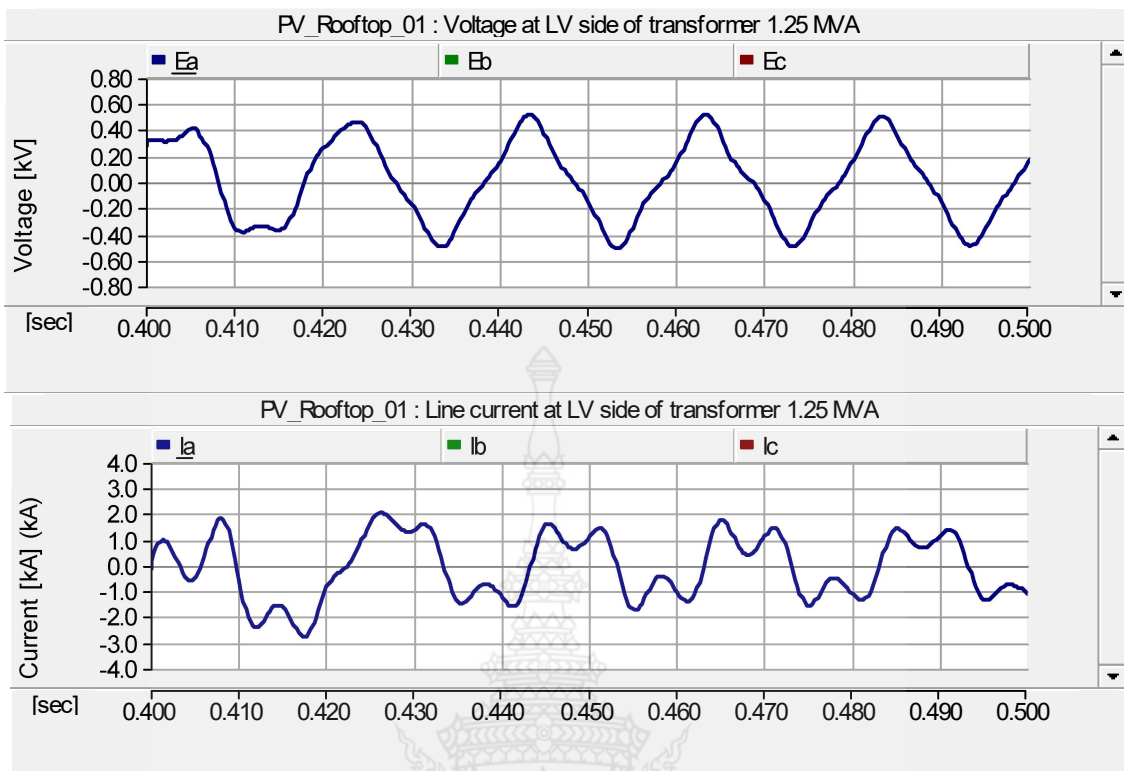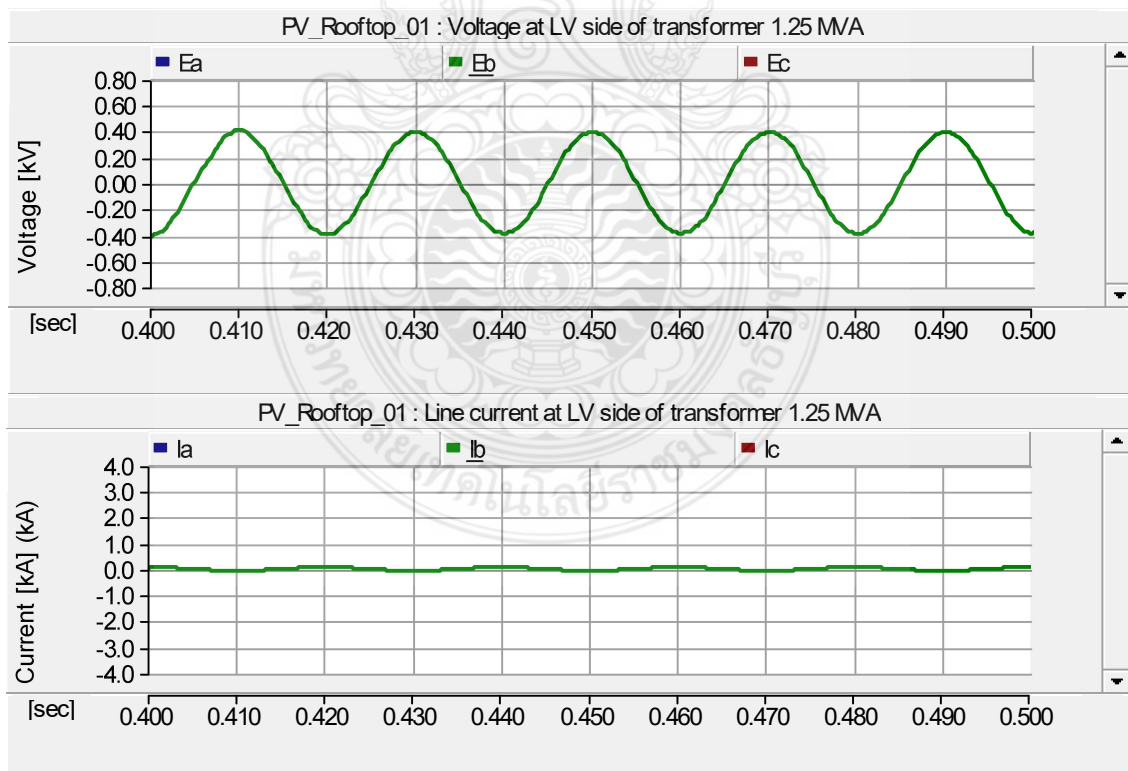
(a) Phase A

(b) Phase B
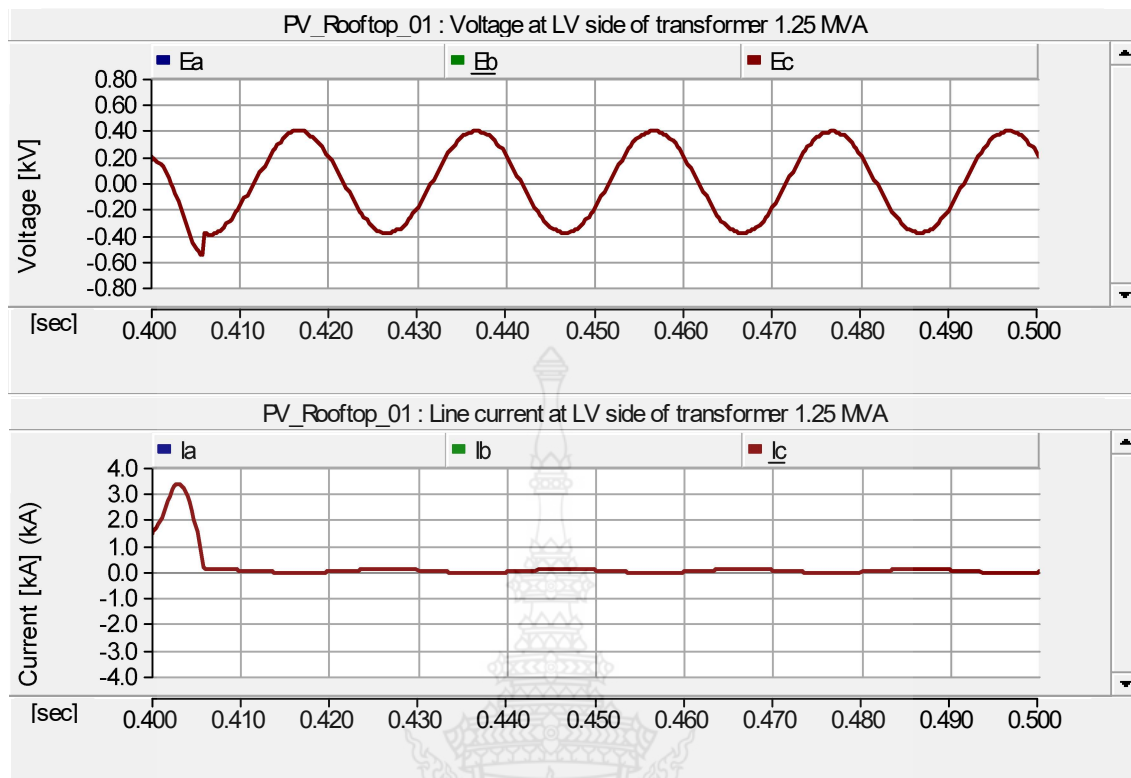
(c) Phase C

Figure 4.62 The Voltage and current waveform at LV side of transformer 1.25 MVA when BRKC disconnecting at 0.4 sec.

The simulation results in Figure 4.62 are definitely sighted that the ferroresonance affected to phase A. The voltage comprises of the fundamental mode ferroresonance and the current comprise of the cohesion of fundamental mode and quasi-periodic mode ferroresonance.

By the way, thirdly, phase A is disconnected at 0.5 sec. as a shown in Figure 4.63, the voltage and current waveform are shown in Figure 4.64.
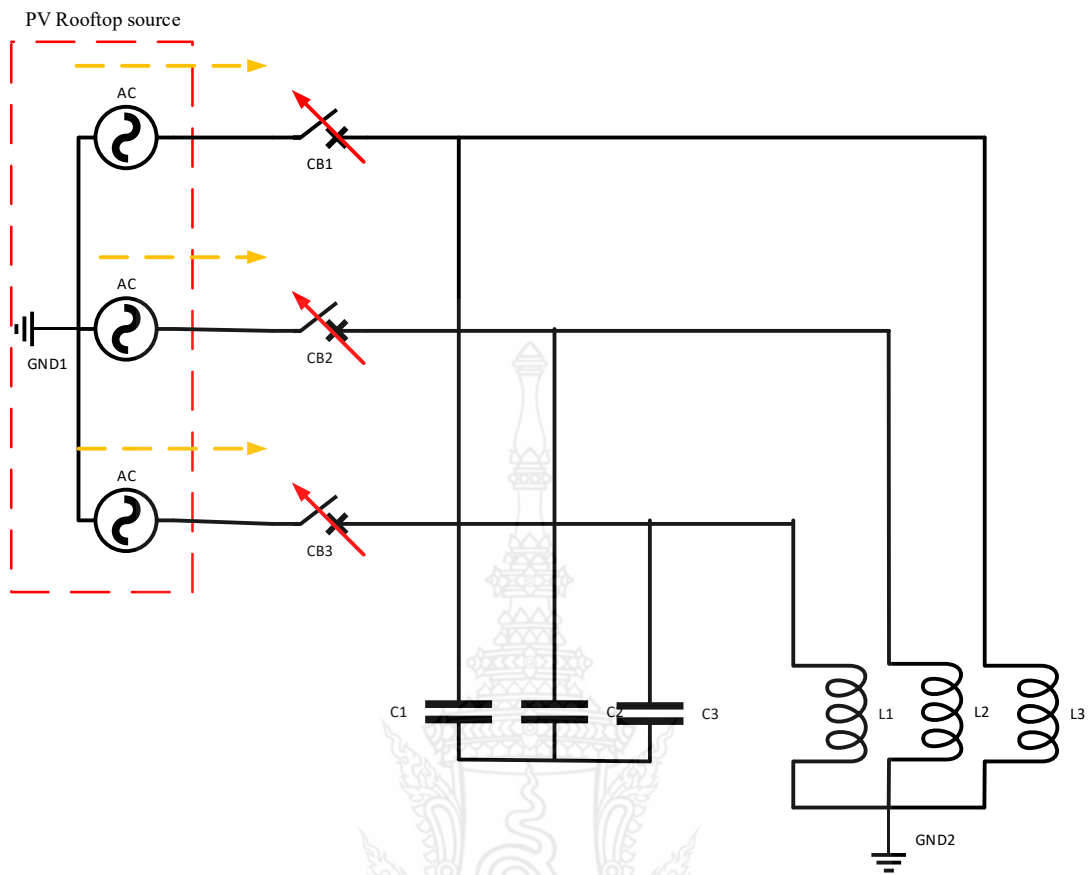
Figure 4.63 The LC ferroresonance circuit with disconnecting CB1 phase A.
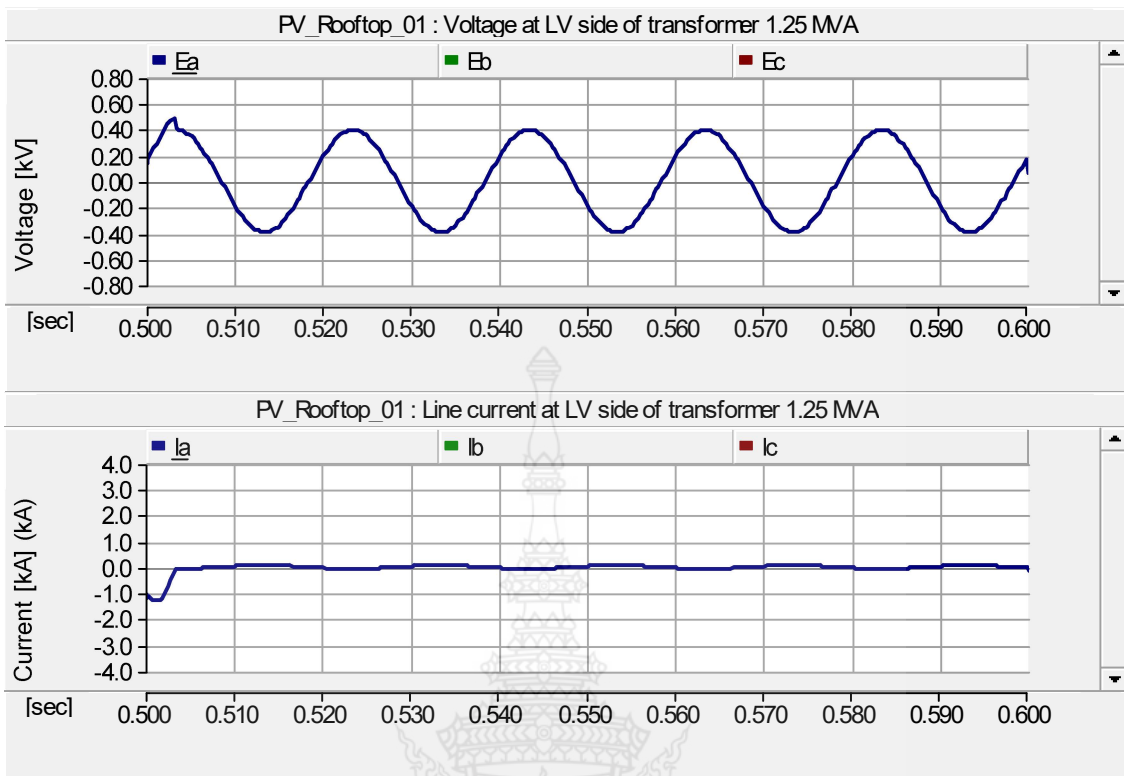
(a) Phase A
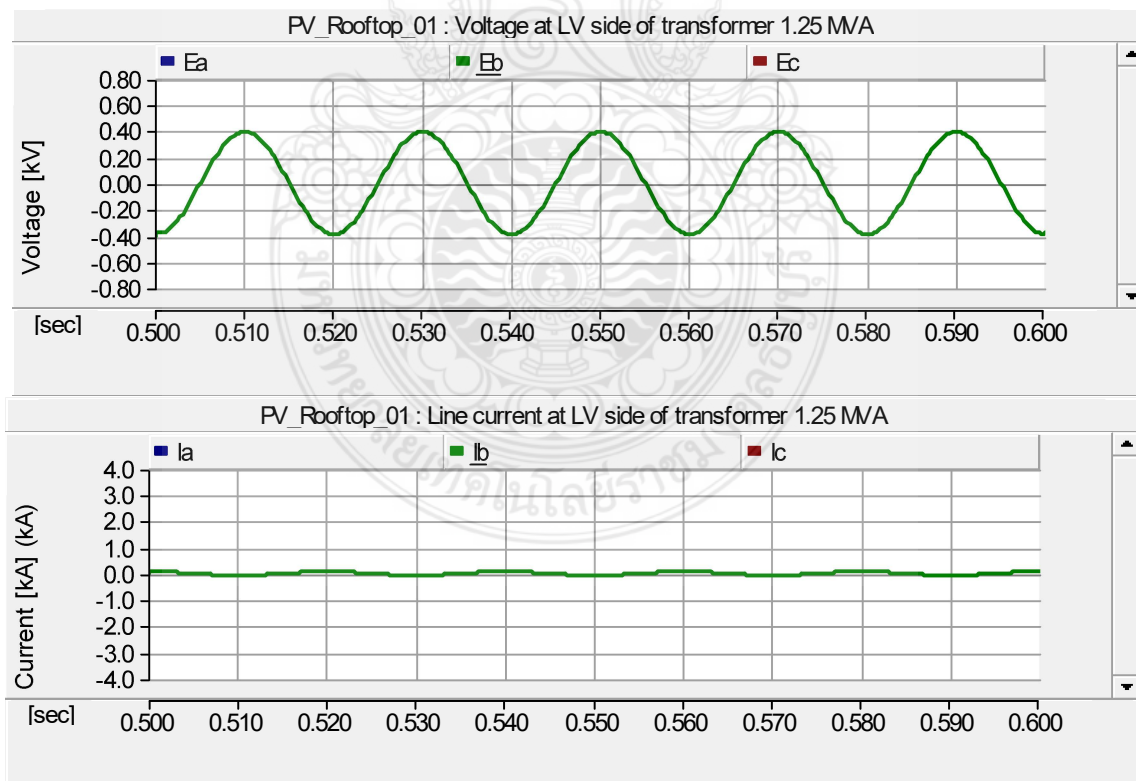
(b) Phase B
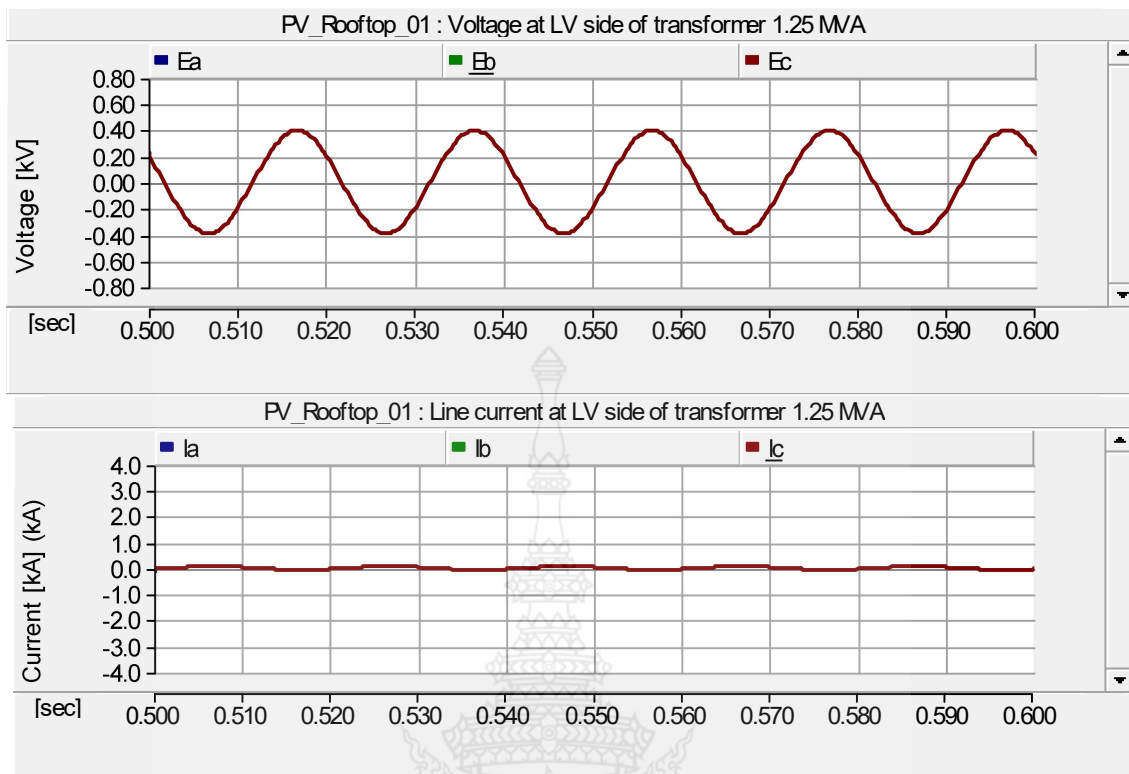
(c) Phase C

Figure 4.64 The Voltage and current waveform at LV side of transformer 1.25 MVA when BRKA disconnecting at 0.5 sec.

The simulation results in Figure 4.64 are definitely sighted that the ferroresonance has no effect all phase.

Moreover, the connecting characteristics of each single phase circuit breaker are analyzed after all are disconnected. Firstly, phase A is disconnected at 0.6 sec. as shown in Figure 4.65, the voltage and current waveform are shown in Figure 4.66.
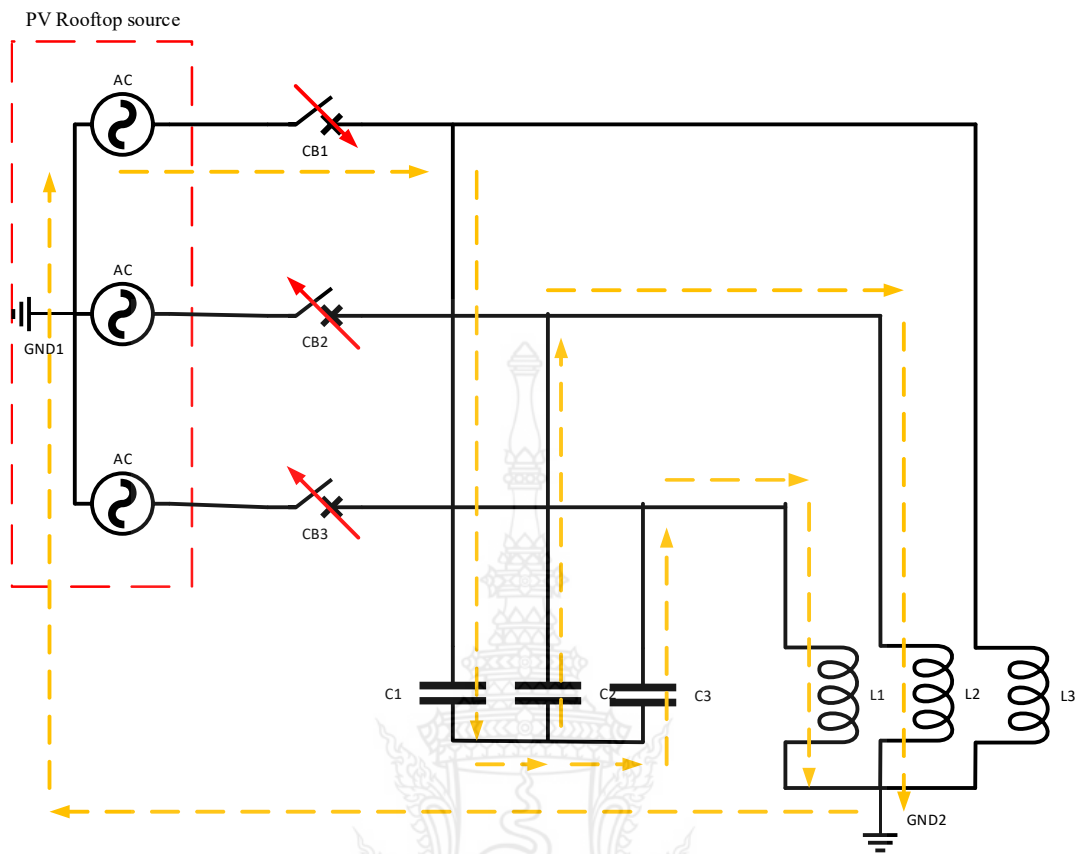
Figure 4.65 The LC ferroresonance circuit with connecting CB1 phase A.
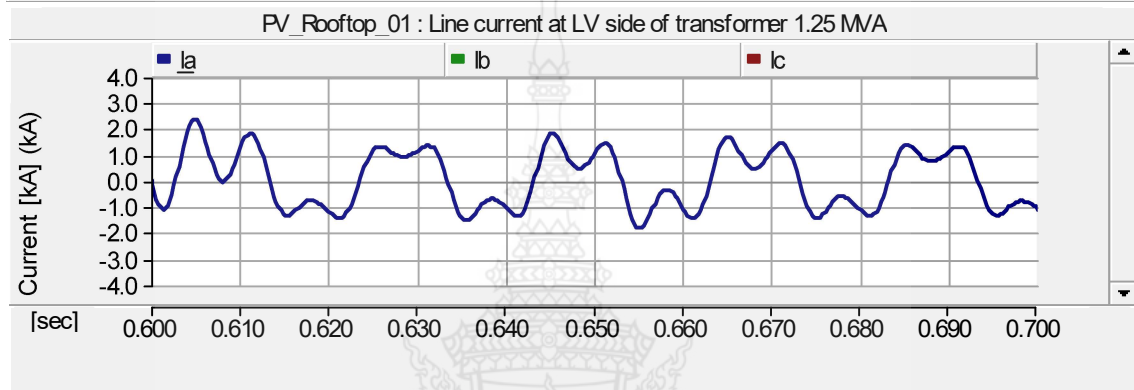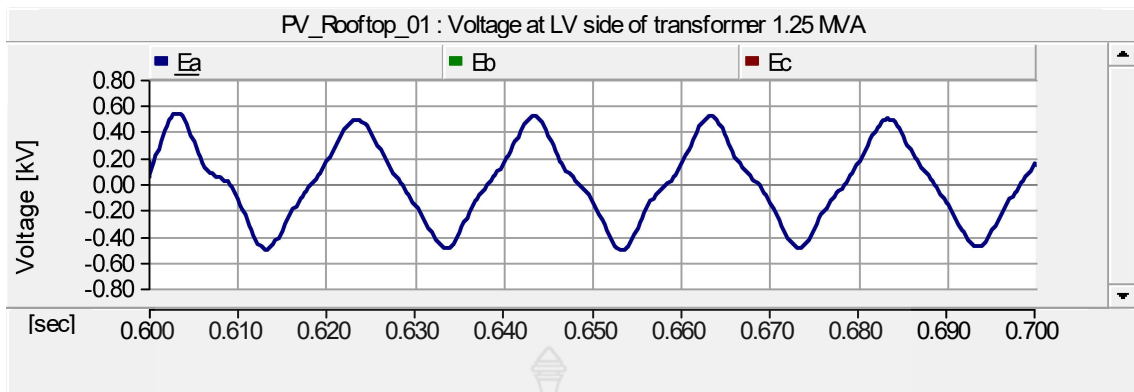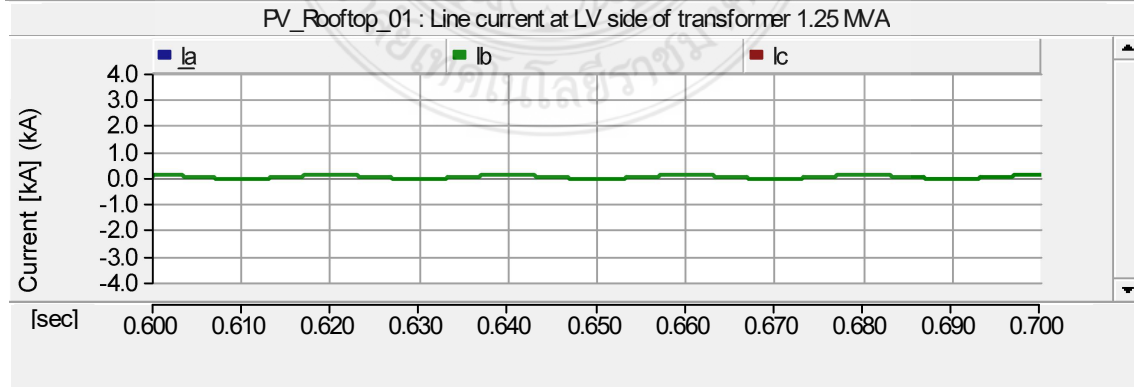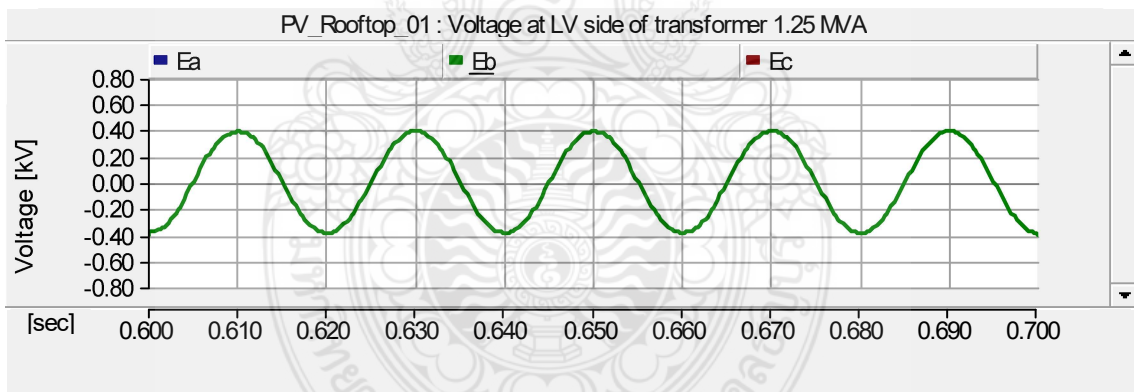
(a) Phase A

(b) Phase B
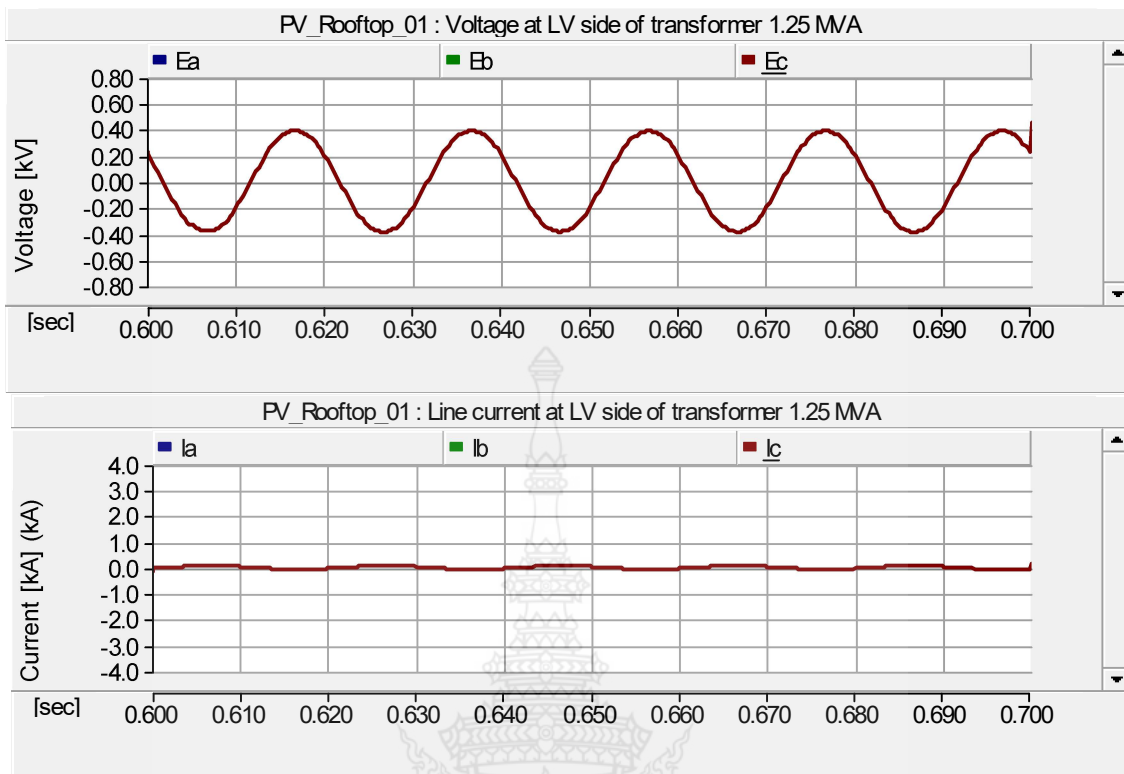
(c) Phase C

Figure 4.66 The Voltage and current waveform at LV side of transformer 1.25 MVA
when BRKA connecting at 0.6 sec.

The simulation results in Figure 4.66 are definitely sighted that the ferroresonance affected to phase A. The voltage comprises of the fundamental mode ferroresonance and the current comprise of the cohesion of fundamental mode and quasi-periodic mode ferroresonance.

By the way, secondly, phase C is connected at 0.7 sec. as shown in Figure 4.67, the voltage and current waveform are shown in Figure 4.68.
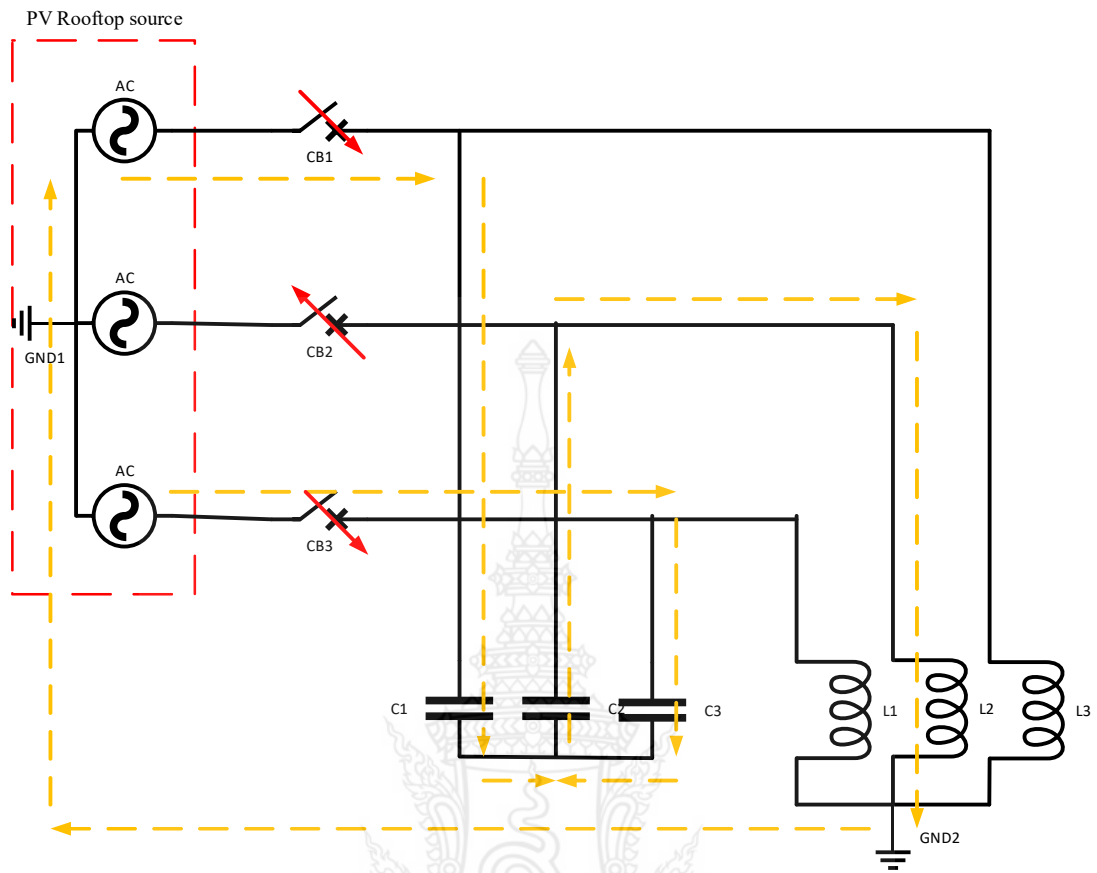
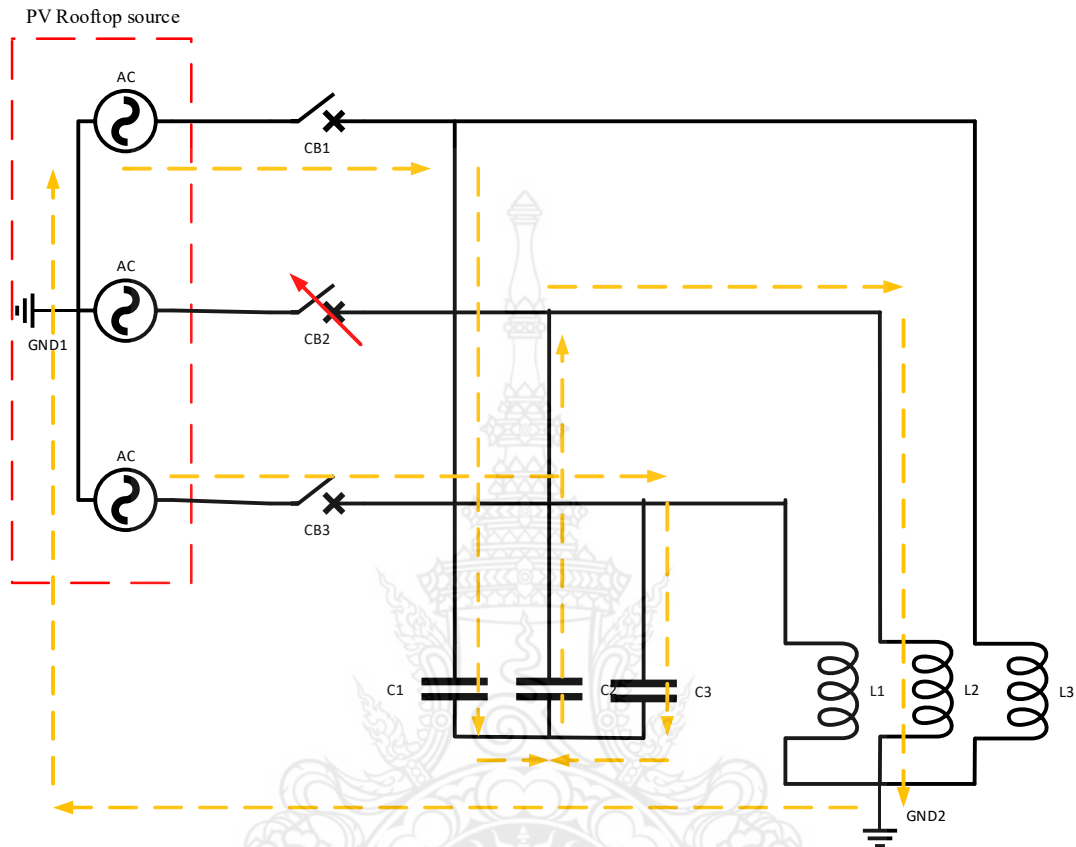**Figure 4.67** The LC ferroresonance circuit with connecting CB3 phase C.
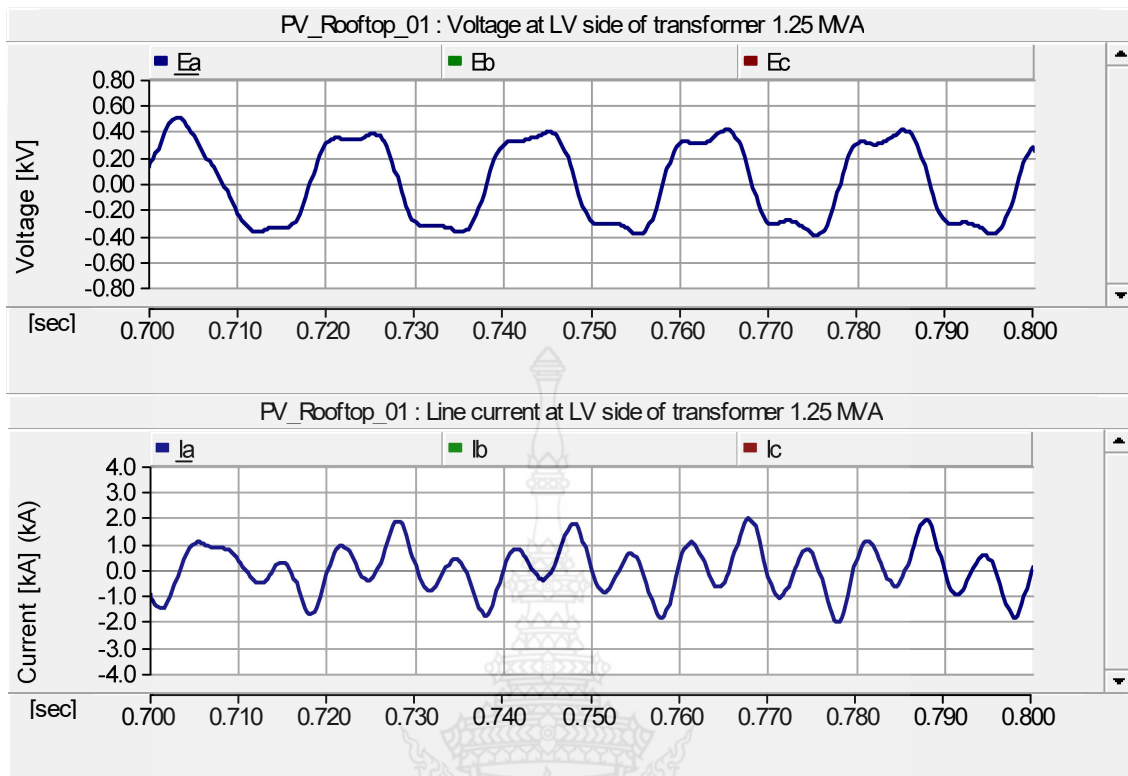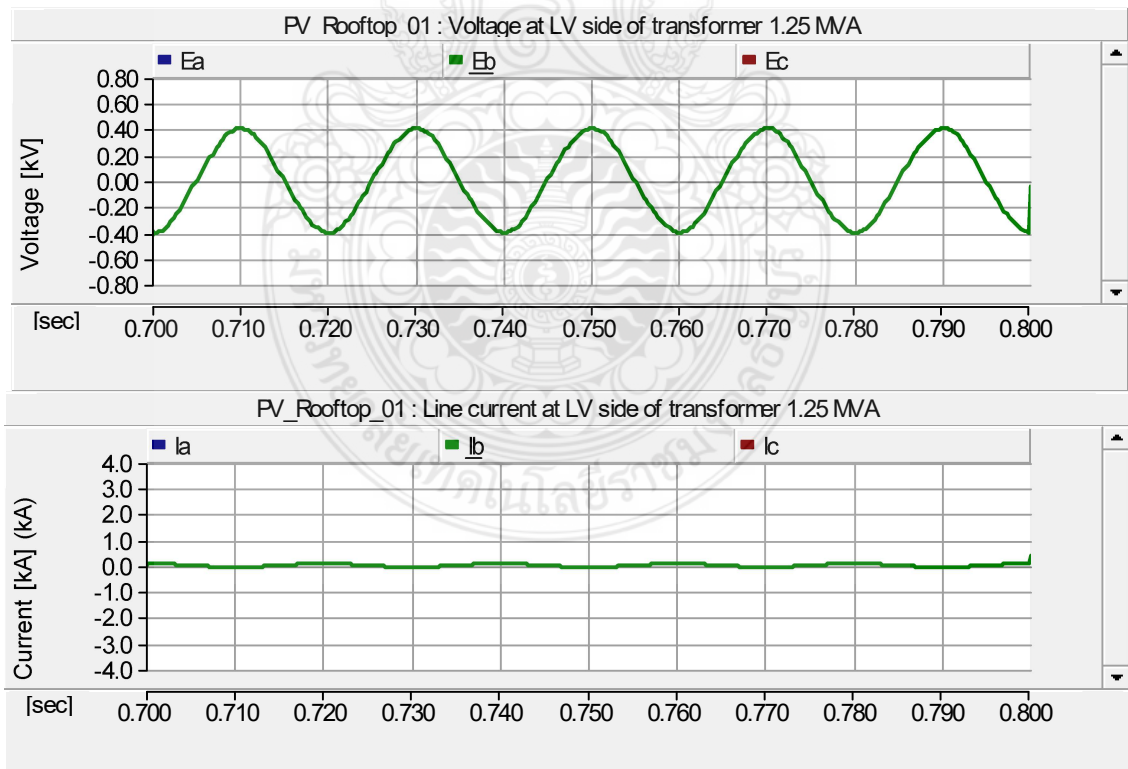
(a) Phase A

(b) Phase B
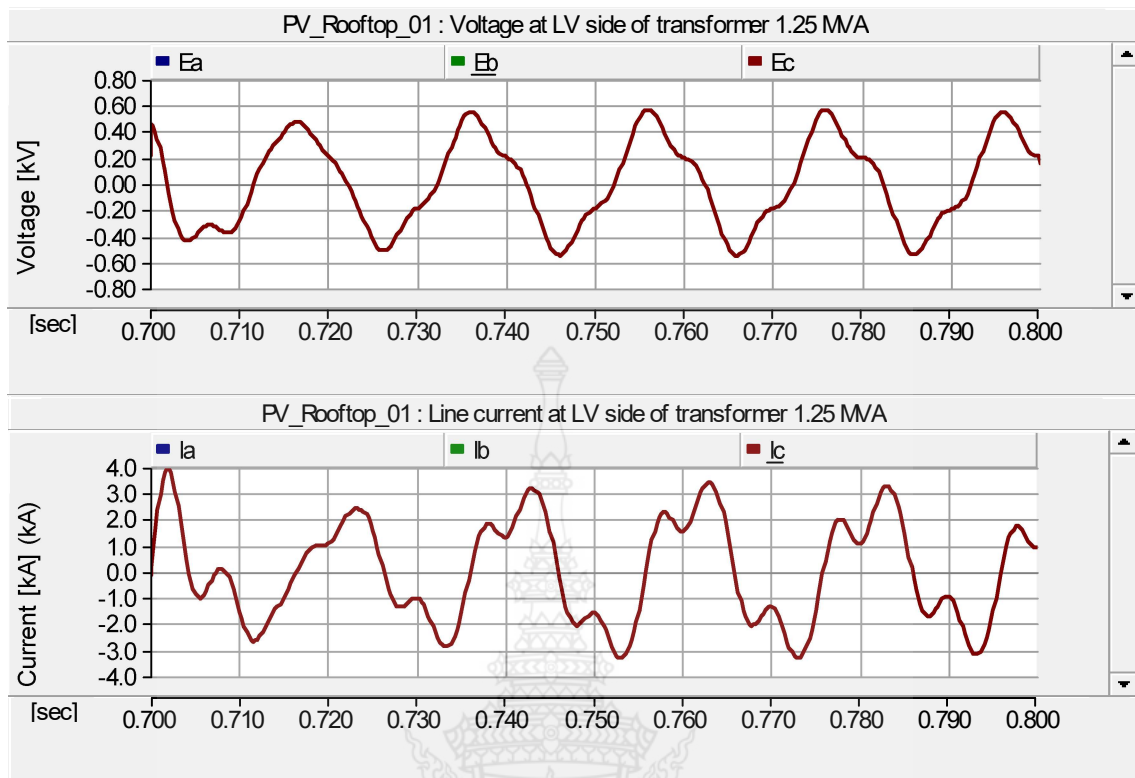
(c) Phase C

Figure 4.68 The Voltage and current waveform at LV side of transformer 1.25 MVA when BRKC connecting at 0.7 sec.

The simulation results in Figure 4.68 are definitely sighted that the ferroresonance affected to phase A and C. The voltage comprises of the fundamental mode ferroresonance and the current comprise of the cohesion of fundamental mode and quasi-periodic mode ferroresonance.

Finally, phase B is connected at 0.8 sec. as shown in Figure 4.69, the voltage and current waveform are shown in Figure 4.7.
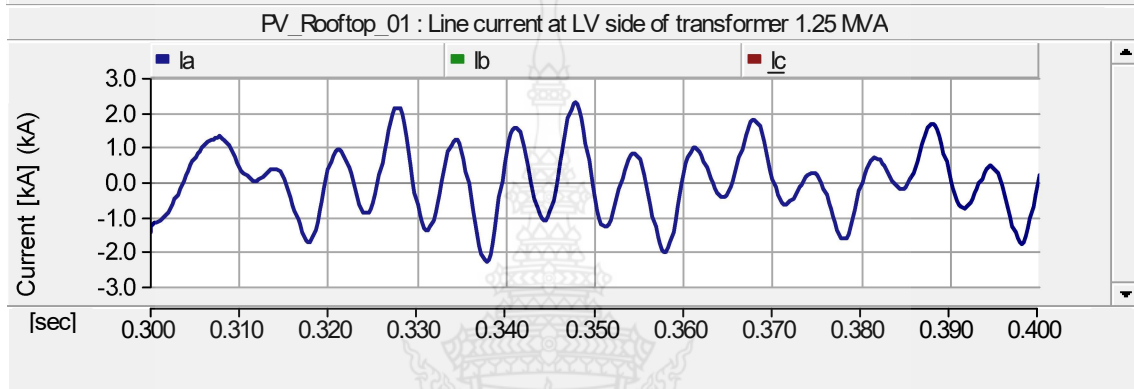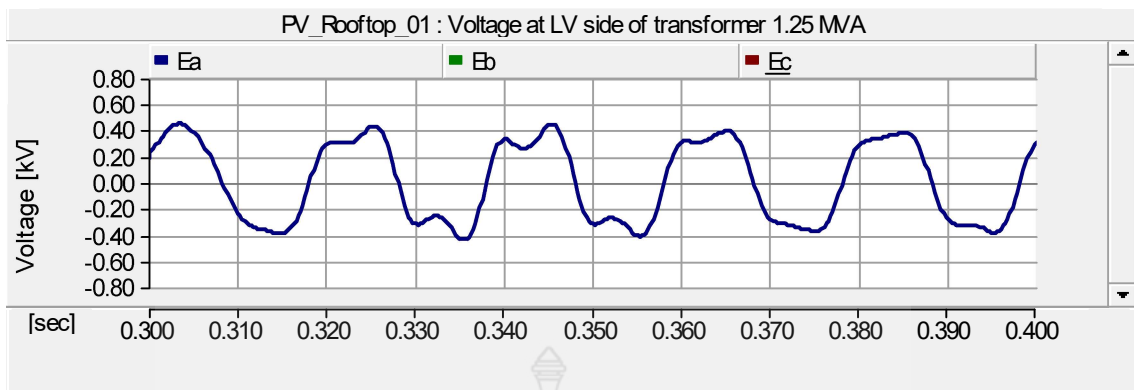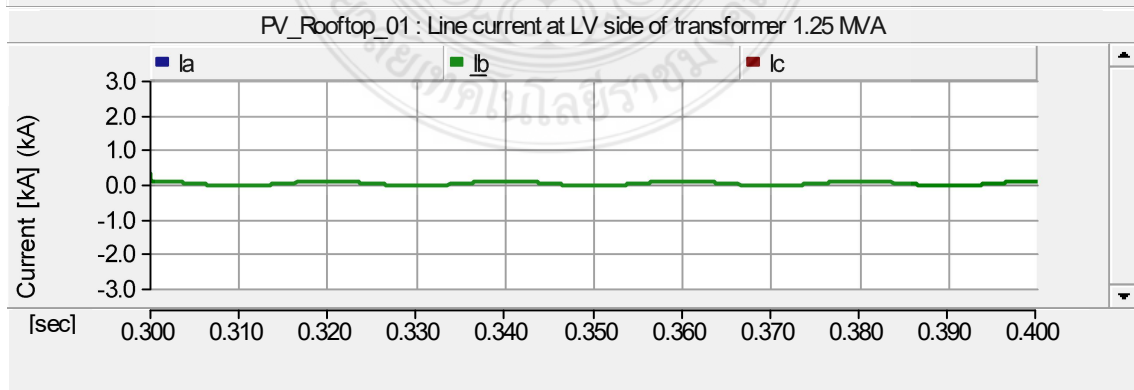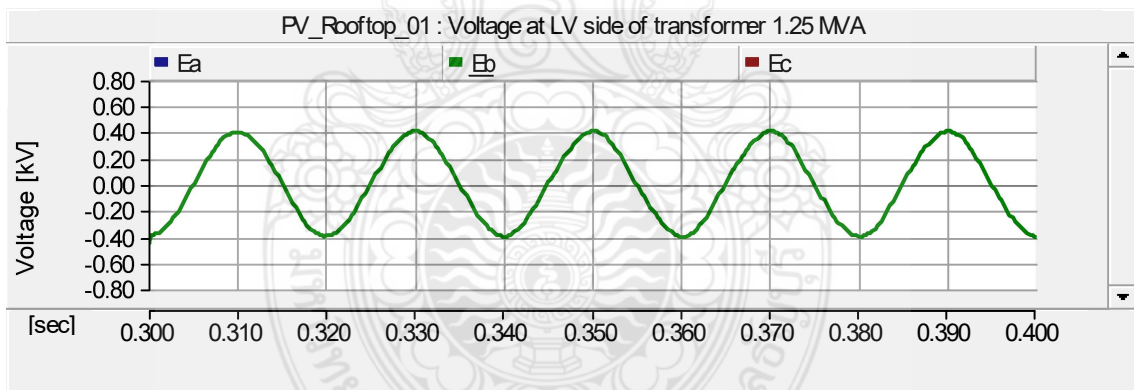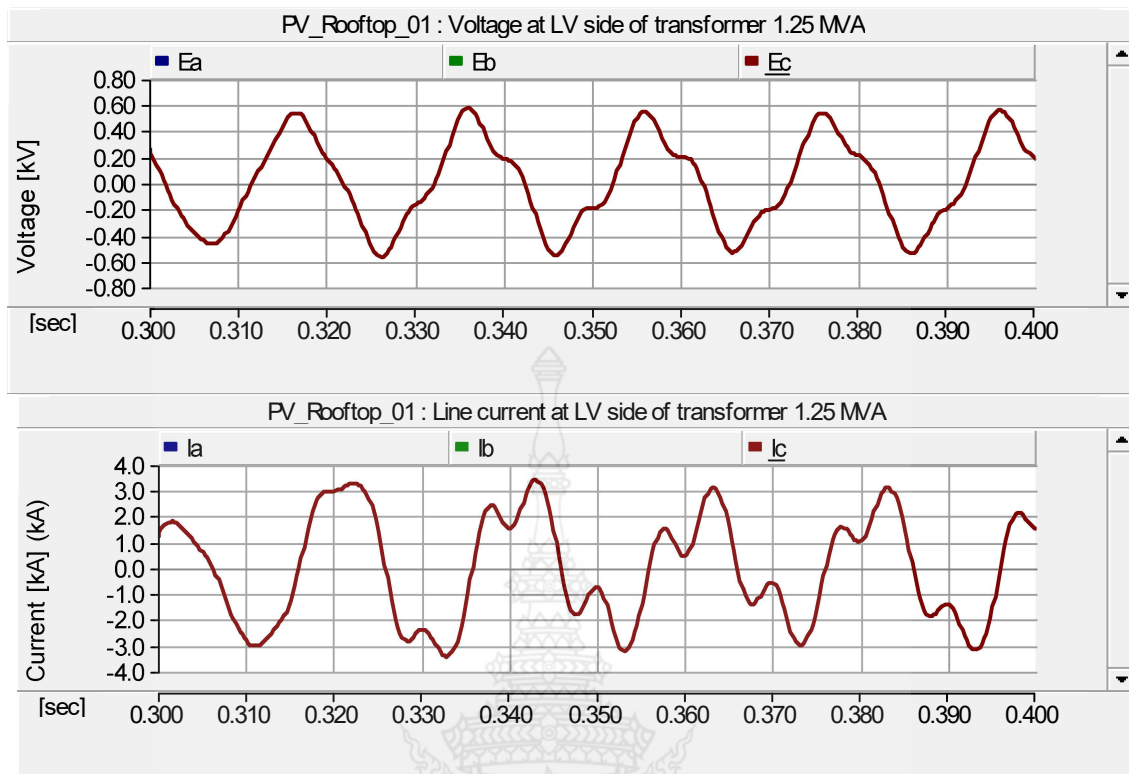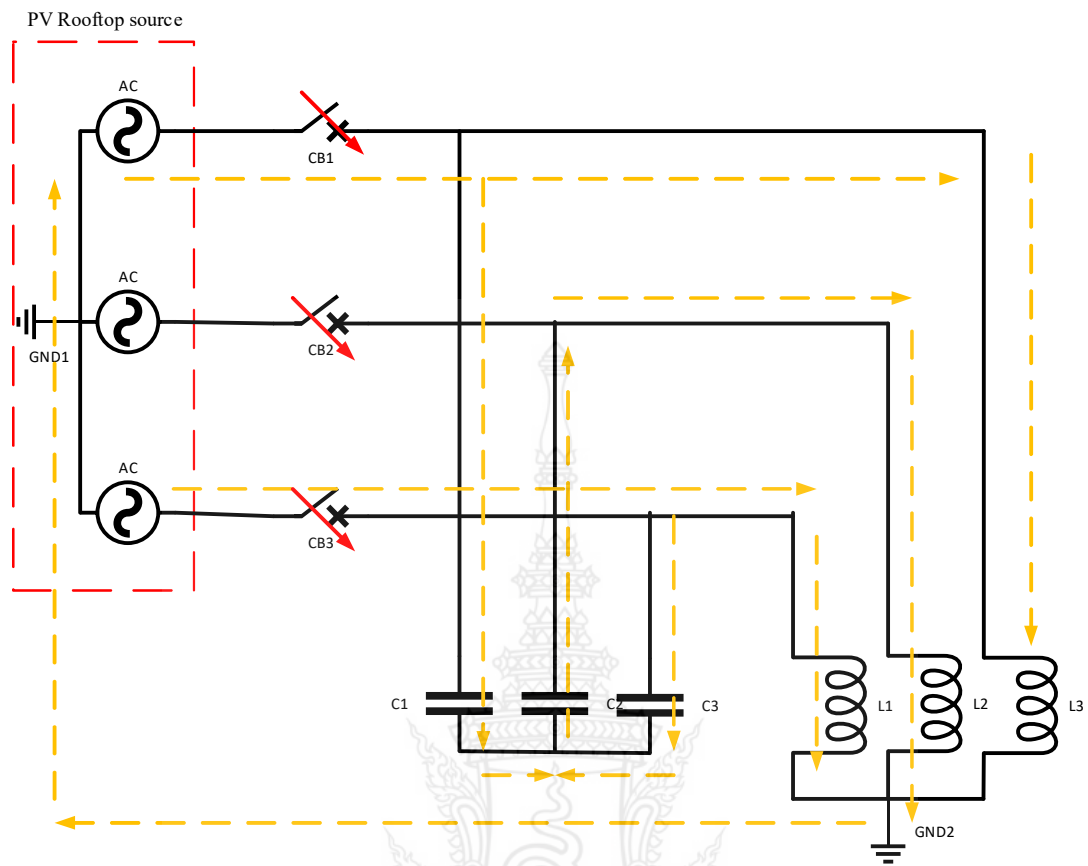
Figure 4.69 The LC ferroresonance circuit with connecting CB2 phase B.
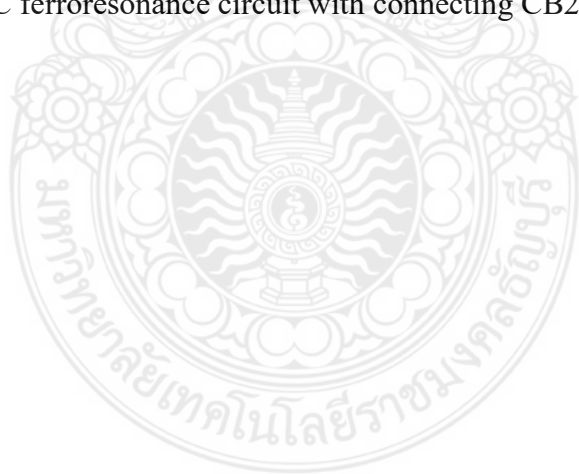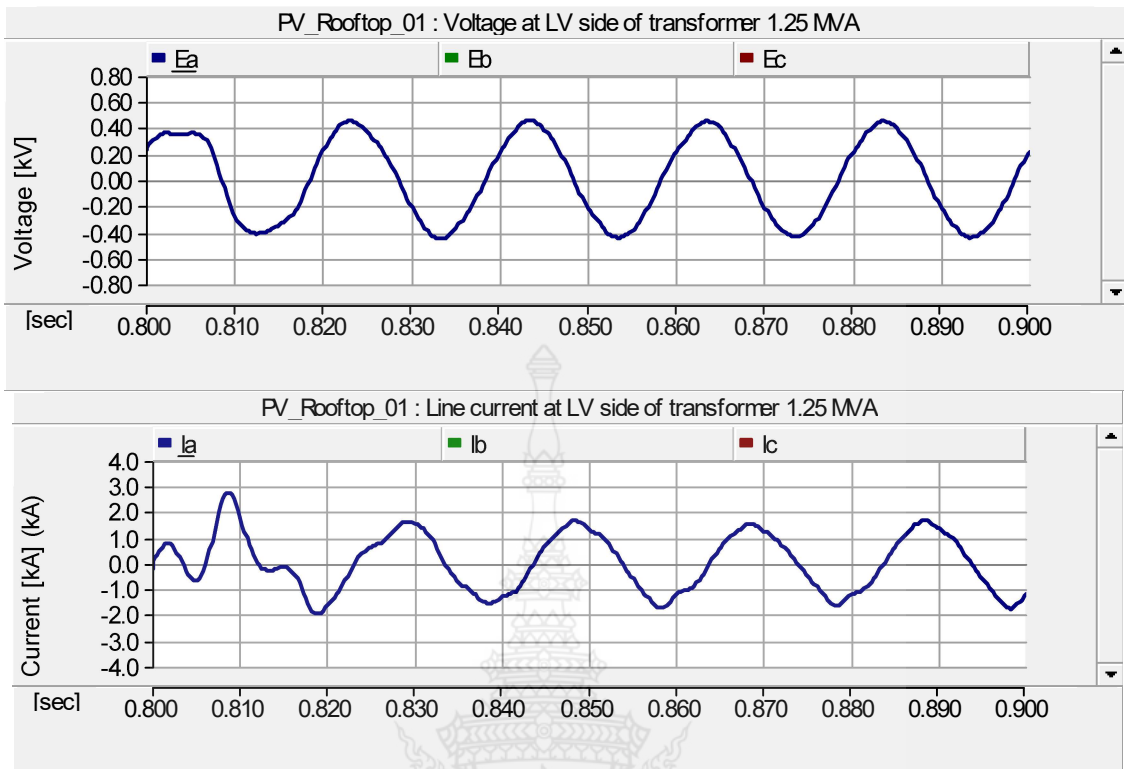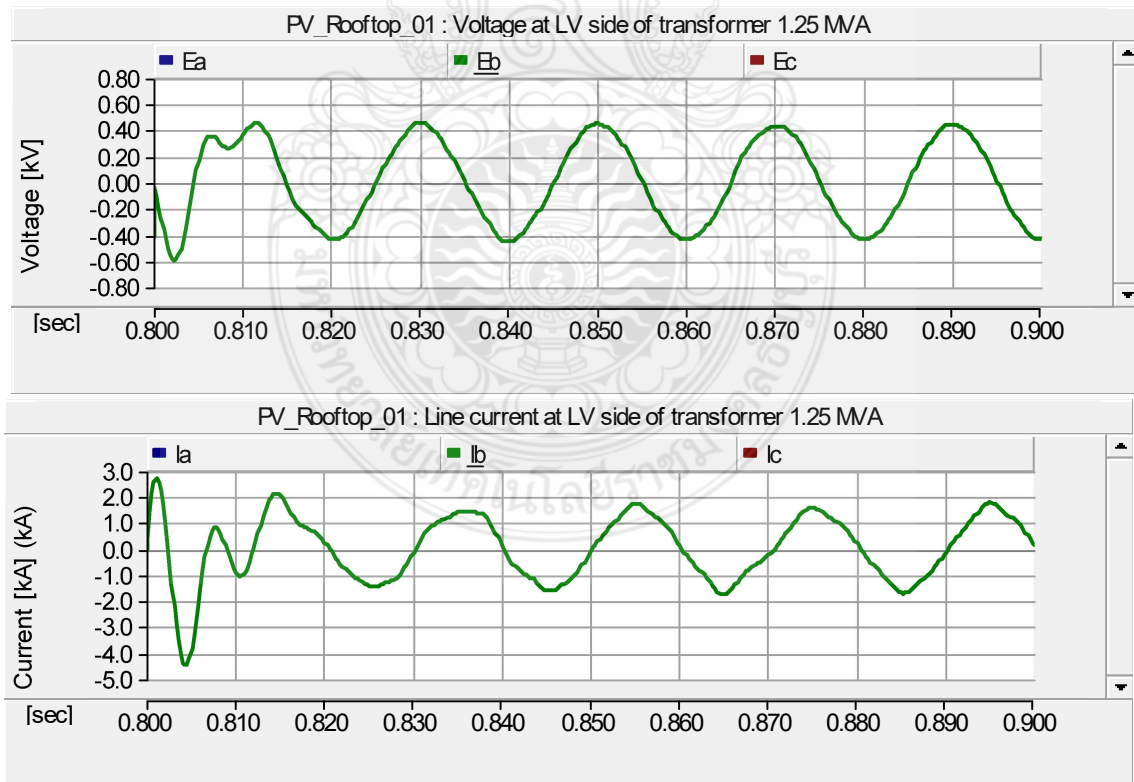
(a) Phase A

(b) Phase B
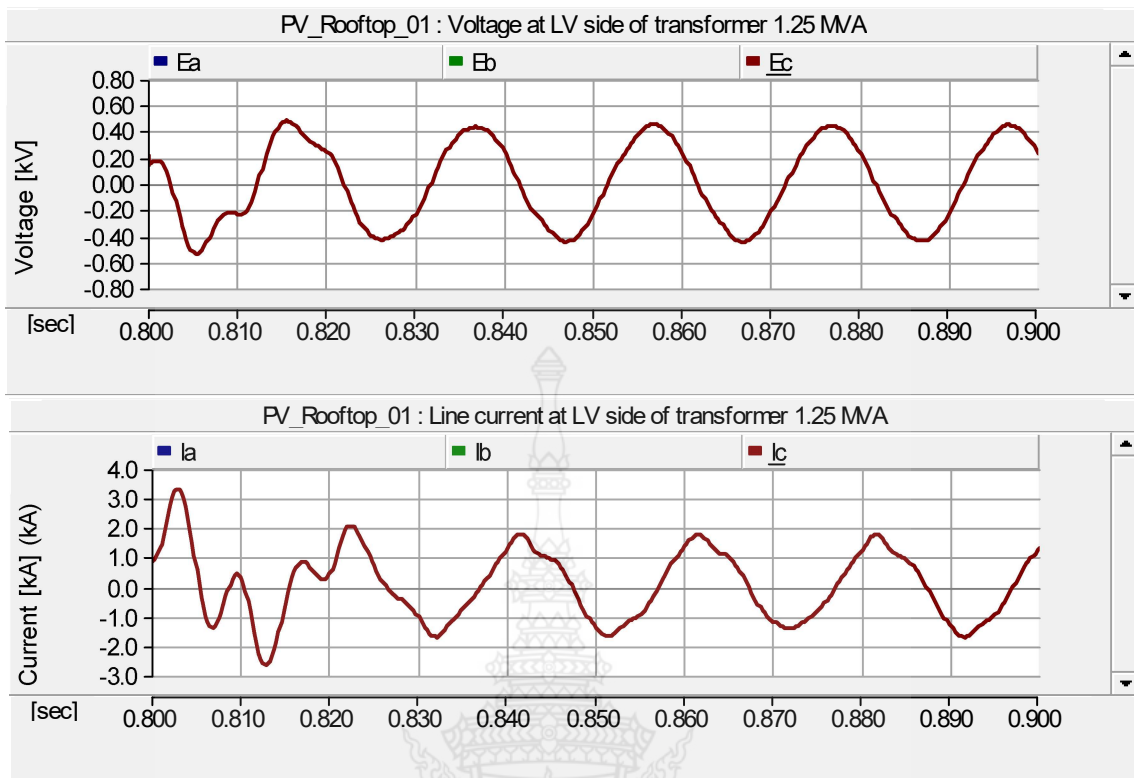
(c) Phase C

Figure 4.70 The Voltage and current waveform at LV side of transformer 1.25 MVA when BRKB connecting at 0.8 sec.

The simulation results in Figure 4.70 are definitely sighted that the ferroresonance affected to phase A, B and C. The voltage comprises of the fundamental mode ferroresonance and the current comprise of the cohesion of fundamental mode and quasi-periodic mode ferroresonance. However, this effect of ferroresonance goes out for a short time.

CHAPTER 5

CONCLUSION AND FURTURE WORK

5.1 Research Conclusion

The overall trends in the renewable energy, the PV rooftop system will be increasing, because it is clean energy and does not affect the environmental conditions. The government will encourage the integration of PV rooftop system into the distribution network of the Provincial Electricity Authority. However, its unstable nature condition and the problems discovered when systematizing the PV rooftop system into the distribution network system, these problems could continue to increase the power quality concern that could be the main concern in distribution systems. The poor power quality could incur disruption in the power system. Also it may cause interrupt in the protection system and will be damage. Therefore, the assessment power quality from the PV rooftop system is very important.

This thesis presents the assessment of power quality impact from the selected real PV rooftop power plant connected to the grid distribution PEA. In addition, this system was simulated by PSCAD/EMTDC and investigated under normal and abnormal case condition and can be summarized as follows.

The measurement results showed that the PV rooftop system can supply the electrical energy during the period of 6.30-18.30. The maximum output power is about 780 kW at the noon. The assessment power quality such as the voltage, current, frequency, voltage fluctuation in short term flicker and long term flicker, active power, and the total harmonic distortion of voltage and current meet the requirements of the electrical grid connection of PEA grid code and was also considered to pass the benchmark.

The Simulation Results by PSCAD/EMTDC. Firstly, the simulation model is validated and compared the data results from the manufacture in appendix A and confirm that the simulation model can simulate the I-V and P-V characteristic curve of solar module and PV array in any solar irradiance and temperature condition when the parameters were changed. Secondly, the simulation under steady state and vary temperature and solar irradiance is validated and confirm that all parameters of power quality meet the requirements of the electrical grid connection of PEA grid code and was also considered to pass the benchmark. Finally, the ferroresonance phenomenon simulation result explains that this simulation is to remind the Provincial Electricity Authority of Thailand (PEA) about the possible occurrence of ferroresonance in the low voltage side of the distribution transformer that is connected to PV rooftop system. Various situations have been introduced and simulated together with the analysis the

effect of the system parameters for instances, line capacitance, transformer's core inductance and PV source It is known that testing of ferroresonance in the transformer could lead the damage to the transformer or even completely destroy it if the resonance is in the unstable region. For these reason, in this thesis decided to use the simulation software for investigating this phenomenon by using the simulation software, which is flexible for arranging the experiment and collecting the data.

5.2 Suggestion and Future work

For the recommendation and future work, the energy storage system is one of alternative for reduced irregularity in the generated electricity from renewable energy especially battery system that could be recommended in parallel with the PV rooftop system. This investigation may examine a similar experiment as this thesis. In the event that the battery system can smooth out the electrical power control due sunlight irregularity in experiment and simulation while the inverter supply the fundamental active and reactive power as required to help an irregular network condition that mean, the energy storage system especially battery system can helpful for stabilize power quality in power system.
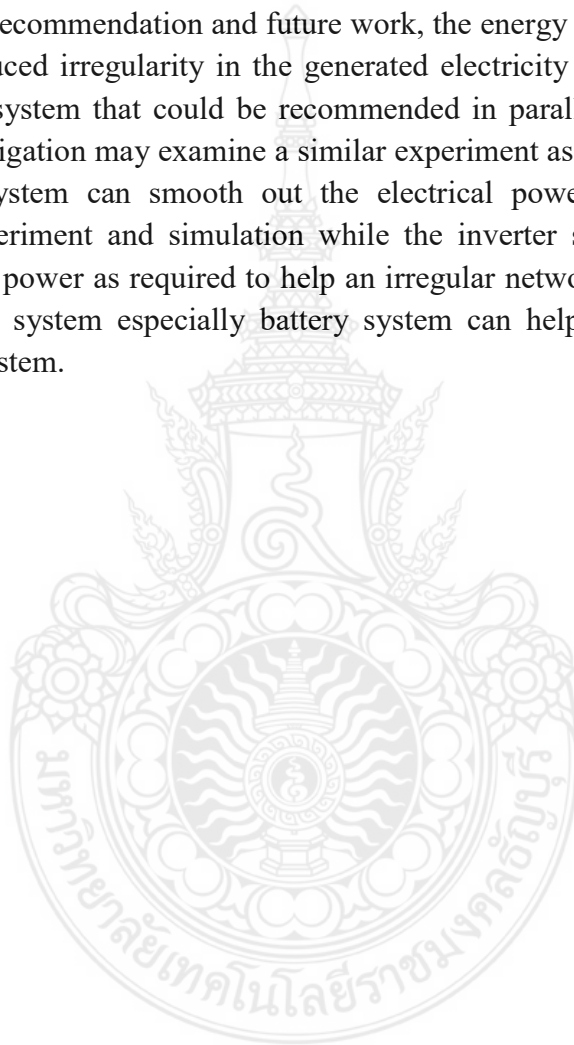
List of Bibliography

[1] Mario Vignolo, R. Z. **Transmission Networks or Distributed Generation?** Montevideo, Uruguay. (2002).

[2] Tammy Humphrey, **Fathoming Physics-E-book and Resources for HSC physics and the new Australian physics curriculum** access online; http://australiancurriculumphysics.com.au/fathoming-physics-hsc-textbook/motors-and-generators/chapter-9-transformers/, January 16, 2015.

[3] Philip P. Barker, R. W. **Determining the Impact of Distributed Generation on Power Systems: Part 1 - Radial Distribution Systems.** 12. IEEE. Retrieved 02 16, 2011, from IEEE.

[4] K Kauhaniemi, L. K. **Impact of Distributed Generation on the Protection of Distribution Networks.,** University of Vaasa, Finland, VTT Technical Research Centre of Finland, Finland. (2004).

[5] **Electricity Grid Schematic English**; access online; https://commons.wikimedia.org/wiki/File:Electricity_Grid_Schematic_English .svg, April 2017.

[6] Department of Renewable Energy Development and Energy Efficiency, Ministry of Energy, Thailand. **Alternative Energy Development Plan: AEDP2015**. access online; www.eppo.go.th/images/POLICY/ENG/AEDP2015ENG.pdf; online April 2017

[7] Vu Van Thong, J. D. **Interconnection of Distributed Generators and Their Influences on Power System.** Katholieke Univeristeit Leuven, Belgium. January 2004.

[8] E. V. Mgaya, Z. M. **The Impact of Connecting Distributed Generation to the Distribution System.** Czech Technical University. 2007.

[9] L.L. LOH and F.C. TZE. **Distributed Generation: Induction and Permanent Magnet Generators.** West Sussex, England, United Kingdom: John Wiley Y. & Sons, Ltd, 2007.

[10] Widén, J., **System Studies and Simulations of Distributed Photovoltaics in Sweden**. Digital Comprehensive Summaries of Uppsala Dissertations from Faculty of Science and Technology 711, ACTA Universitatis Upsaliensis Uppsala. 2010.

[11] **Alternative energy online tutorials** access online http://www.alternative-energy-tutorials.com/solar-power/grid-connected-pv-system.html January 2018.

[12] Mehmet E.M. and Furkan D., **A review of factors affecting operation and efficiency of photovoltaic based electricity generation systems.** Renewable energy and Sustainable energy reviews 15 (2011), P: 2176-2184.

[13] Kalogirou S. **Solar energy engineering: processes and systems: chapter 9**. Academic Press; 2009. p. 469–517.

[14] Pearsall NM, Hill R. **Clean electricity from photovoltaics: chapter 15.** Imperial College Press; 2001. pp. 1–42.

[15] J.H.R. Enslin and P.J.M. Heskes, **Harmonic interaction between a large number of distributed power inverter and the distribution network.** Vol.19, No.6 pp 15861593, Nov.2004

[16] E.Vasanasong and E.Spooner, **The prediction of net harmonic current produced by large number of residential PV inverters: Sydney Olympic village case study,** Vol.2 pp.1001-1006 Dec. 4-7 2000.

[17] M. Raoufi, and M. T. Lamchich, **Average current mode control of a voltage source inverter connected to the grid: Application to different filter cells.** Journal of Electrical Engineering, Vol. 55, No.3-4, pp. 77-82, 2004.

[18] **Australian Standard for Grid Connection of Energy System via Inverter – Part 2: Inverter Requirements,** Standards Australian Std. AS 47772.2-2002.

[19] **IEEE Standard for Interconnecting Distribution Resources with Electric Power Systems**, Standards Coordinating Committee 21 on Fuel Cells, Photovoltaics, Dispersed Generation and Energy Storage Std. IEEE Std. 5147 – 2003.

[20] **IEEE Recommended Practice for Utility Interface of Residential and Intermediate Photovoltaic (PV) System**, IEEE Standards Coordinating Committee 21 Photovoltaics Std. ANSI/IEEE std 929 – 1998.

[21] A. A. Latheef, **Harmonic Impact of Photovoltaic Inverter System on Low and Medium Voltage Distribution System**. M.Eng Thesis, School of Electrical Computer and Telecommunications Engineering, University of Wollongong, 2006.

[22] Kersting WH, Phillips WH. **Distribution feeder line models**. In: Proceedings of the 38th annual rural electric power conference. p. A4/1–A4/8; 1994.

[23] Willis HL. **Power distribution planning reference book.** CRC press; 2004.

[24] Muttaqi KM, Le AD, Negnevitsky M, Ledwich G. **A novel tuning method for advanced line drop compensator and its application to response coordination of distributed generation with voltage regulating devices.** IEEE Trans Ind Appl 2016; 52:1842–54.

[25] Shahnia F, Majumder R, Ghosh A, Ledwich G, Zare F. **Voltage imbalance analysis in residential low voltage distribution networks with rooftop PVs**. Electric Power System Res 2011;81(9):1805–14.

[26] Meersman B, Renders B, Degroote L, Vandoorn T, Vandevelde L. **Three-phase inverter-connected DG-units and voltage unbalance.** Electric Power System Res 2011;81(4):899–906.

[27] Yap WK, Havas L, Overend E, Karri V. **Neural network-based active power curtailment for overvoltage prevention in low voltage feeders.** Expert Syst Appl 2014;41(4):1063–70.

[28] Tonkoski R, Lopes LA, El-Fouly TH. **Coordinated active power curtailment of grid connected PV inverters for overvoltage prevention.** IEEE Trans Sustain Energy 2011;2(2):139–47.

[30] Bollen MH, Stockman K, Neumann R, Ethier G, Gordon JR, Van Reussel K. Et al. **Voltage dip immunity of equipment and installations-messages to stakeholders.** In: Proceedings of the IEEE15th international conference on harmonics and quality of power (ICHQP). p. 915-919; 2012.

[31] Martinez-Velasco J, Martin-Arnedo J. **Distributed generation impact on voltage sags in distribution networks.** In: Proceedings of the IEEE 9th international conference on electrical power quality and utilisation. p. 1–6; 2007.

[32] Van TL, Nguyen TH, Lee D-C. **Flicker mitigation in DFIG wind turbine systems.** In: Proceedings of the IEEE 14th European conference on power electronics and applications. p. 1–10; 2011.

[33] Zheng T, Makram EB. Wavelet. **Representation of voltage flicker.** Electr Power Syst Res 1998;48(2):133–40.

[34] Hernández J, Ortega M, De la Cruz J, Vera D. **Guidelines for the technical assessment of harmonic, flicker and unbalance emission limits for PV-distributed generation.** Electr Power Syst Res 2011;81(7):1247–57.

[35] **IEEE standard for interconnecting distributed resources with electric power systems**. IEEE Std. 1547–2003:1-28.

[36] Ding T, Kou Y, Yang Y, Zhang Y, Yan H, Blaabjerg F. **Evaluating maximum photovoltaic integration in district distribution systems considering optimal inverter dispatch and cloud shading conditions.** IET Renew Power Gener; 2016.

[37] Gulachenski E, Kern Jr E, Feero W, Emanuel A. **Photovoltaic generation effects on distribution feeders.** Electric Power Research Inst., Palo Alto, CA (United States); New England Power Service Co., Westborough, MA (United States); Ascension Technology, Lincoln Center, MA (United States); Electric Research and Management, Inc., State College, PA (United States); Worcester Polytechnic Inst., MA (United States); 1991.

[38] Woyte A, Van Thong V, Belmans R, Nijs J. **Voltage fluctuations on distribution level introduced by photovoltaic systems.** IEEE Trans Energy Convers 2006;21(1):202–9.

[39] Ari G, Baghzouz Y. **Impact of high PV penetration on voltage regulation in electrical distribution systems.** In: Proceedings of the IEEE international conference on clean electrical power (ICCEP). p. 744–748; 2011.

[40] Conti S, Raiti S, Tina G, Vagliasindi U. **Study of the impact of PV generation on voltage profile in LV distribution networks.** In: Proceedings of the IEEE Porto Power Tech; 2001. p. 6.

[41] Von Jouanne A, Banerjee B. **Assessment of voltage unbalance**. IEEE Trans Power Deliv 2001;16(4):782–90.

[42] ANSI C84. 1-1995, **Electrical power systems and equipment - voltage ratings (60 Hz)**, American national standards institute, NY 10036, USA.

[43] De La Rosa, F.C.,2006. **Harmonics and Power Systems**. CRC Press Taylor & Francis Group, Boca Raton.

[44] El-Samahy I, El-Saadany E. **The effect of DG on power quality in a deregulated environment.** In: Proceedings of the IEEE power engineering society general meeting. p. 2969–2976; 2005.

[45] D. Essah, E. Feiste, R. O'Connell, R.G. Hoft and G. Brownfield, **Harmonic effects of variable speed air conditioners on a single-phase lateral and on the distribution feeders in a typical residential power system. I,** in Proc. 1994 IEEE Applied Power Electronics Conference and Exposition, pp.622-627.

[46] A.B. Nassif, and X. Winsun, **Characterizing the Harmonic Attenuation Effect of Compact Fluorescent Lamps**, IEEE Trans. On Power Delivery, vol.24, no.3, pp.1748-1749, July 2009.

[47] Y. Zhou, **Harmonic sources in the city distribution system**, in Proc. 1997 IEEE Fourth International Conference on Advances in Power System Control, Operation and Management, vol.2, pp.549-551.

[48] H.O. Aintablian, and H.W. Jr. Hills, **Harmonic currents generated by personal computers and their effects on the distribution system neutral current**, in Proc. 1993 IEEE Industry Applications Society Annual Meeting, pp. 1483-1489.

[49] T.C. Shuter, H.T. Jr. Vollkommer and T.L. Kirkpatrick, **Survey of harmonic levels on the American Electric Power distribution system**, IEEE Trans. On Power Delivery, vol.4, no.4, pp.2204-2213, Oct 1989.

[50] C. D. Crites, R. K. Varma, V. Sharma and B. Milroy, **Characterization of Harmonics in a Utility Feeder with PV Distributed Generation**, in Proc. 2012 IEEE Electrical Power and Energy Conference, pp. 1-6.

[51] **IEEE Recommended Practice and Requirements for Harmonic Control in Electric Power Systems**, IEEE Standard 519-2014, 11 June 2014.

[52] G. Lemieux, **Power system harmonic resonance-a documented case**, IEEE Trans. on Industry Applications, vol. 26, no. 3, pp. 483-488, May/Jun. 1990.

[53] W. Xu, Z. Huang, Y. Cui and H. Wang, **Harmonic resonance mode analysis**, IEEE Trans. on Power Delivery, vol. 20, no. 2, pp. 1182- 1190, Apr. 2005.

[54] M. Contreras, H. Calleja and V. Cardenas, **Study of Harmonic Propagation in Ring Bus Distribution System,** in Proc. 2005 IEEE Power Electronics Specialists Conference, pp.1901-1907.

[55] Mehmet E.M. and Furkan D., **A review of factors affecting operation and efficiency of photovoltaic based electricity generation systems.** Renewable energy and Sustainable energy reviews 15 (2011), P: 2176-2184.

[56] Tonkoski R, Lopes LA. **Impact of active power curtailment on overvoltage prevention and energy production of PV inverters connected to low voltage residential feeders**. Renew Energy 2011;36(12):3566–74.

[57] Rahimi M, Assari H. **Addressing and assessing the issues related to connection of the wind turbine generators to the distribution grid**. Int J Electr Power 2017; 86:138–53.

[58] Conti S, Greco A, Messina N, Raiti S. **Local voltage regulation in LV distribution networks with PV distributed generation.** In: Proceedings of IEEE international symposium on power electronics, electrical drives, automation and motion. p. 519–524; 2006.

[59] Saad-Saoud Z, Lisboa M, Ekanayake J, Jenkins N, Strbac G. **Application of STATCOMs to wind farms**. IEE Proc- Gener, Transm Distrib 1998;145(5): pp.511–6.

[60] J. Arrillaga, D.A. Bradley and P.S. Bodger, **Power System Harmonics**: John Wiley and Sons, New York, 1985.

[61] Javier Marcos, Luis Marroyo, Eduardo Lorenzo, David Alvira, Eloisa Izco, **Power output fluctuations in large scale PV plants: One year observations with one second resolution and a derived analytic model.** Progress in Photovoltaics, Volume 19, Issue 2, March 2011, Pages 218–227.

[62] Woyte A, Belmans R, Nijs J., **Fluctuations in instantaneous clearness index: analysis and statistics.** Solar Energy 2007; 81, P.195–206.

[63] Garikoitz B., and et al., **Ferroresonance in three Phase Power Distribution Transformer: Sources, Con sequences and Prevention**. 19th International Conference on Electricity Distribution Vienna, 21-24 May 2007.

[64] D. A. N. Jacobson, **Examples of ferroresonance in a high voltage power system.** In Power Engineering Society General Meeting, 2003, IEEE, 2003, pp. 1206-1212.

List of Bibliography (Continued)

[65] Miličević, Kruno; Vulin, Dragan; Vinko, Davor. **Experimental Investigation of Symmetry-Breaking in Ferroresonant Circuit**. IEEE transactions on circuits and systems. I, Regular papers. 61 (2014), 5; 1543-1552

[66] Miličević, Kruno; Vinko, Davor; Vulin, Dragan. **Experimental Investigation of Impact of Remnant Flux on the Ferroresonance Initiation**. International journal of electrical power & energy systems. 61 (2014); 346-354

[67] Miličević, Kruno; Rutnik, Ivan; Lukačević, Igor. **Impact of Voltage Source and Initial Conditions on the Initiation of Ferroresonance.** WSEAS Transactions on Circuits and Systems. 7 (2008), 8; 800-810.

[68] V. Valverde, and et al., **Ferroresonance in Voltage Transformers: Analysis and Simulations.** Renewable Energy and Power Quality Journal Vol.1 No.5, March 2007. P.465-471

[69] J.R. Marti and A.C. Soudack, **Ferroresonance in power systems: Fundamental solutions.** IEE Proceedings C (Generation, Transmission and Distribution) Volume 138, Issue 4, July 1991. p. 321 – 329

[70] Slow Transients Task Force. **Modeling and Analysis Guidelines for Slow Transients-Part III: The Study of Ferroresonance.** IEEE Transactions on Power Delivery, vol. 15, no. 1, pp. 255-265, January 2000.

[71] Miličević, Kruno; Nyarko, Emmanuel Karlo; Biondić, Ivan. **Chua's model of nonlinear coil in a ferroresonant circuit obtained using Dommel's method and grey box modelling approach.** Nonlinear dynamics. 86 (2016), 1; 51-63

[72] Miličević, Kruno; Flegar, Ivan; Pelin, Denis. **Flux Reflection Model of the Ferroresonant Circuit.** Mathematical Problems in Engineering. 2009 (2009), 6; 693081-1-693081-13

[73] Gonen, T. **Electric Power Distribution System Engineering**; MaGraw-Hill College Div.: New York, NY, USA, 1985; Volume I.

[74] Ang, S.P. **Ferroresonance Simulation Studies of Transmission Systems**. Ph.D. Thesis, The University of Manchester, Manchester, UK, 2010.

[75] **EMTDC Manual**, Winntpeg: Manitoba HVDC Research Center,2003.

[76] Manitoba HVDC Research Centre Inc. (2005, April) **Users Guide on the use of PSCAD/EMTDC Document**.

[77] D. A. Woodford, A. M. Gole, R. W. Menzies, **Digital simulation of dc links and ac machines**, IEEE Trans. Power Apparatus and Systems, vol. PAS-102, no. 6, pp. t6l6-l623, June 1983.

[78] A. M. Gole, M. Meisingset, **An active filter for use at capacitor commutated HVDC converter,** IEEE Ttrans. Power Delivery,vol. 16, no. 2, pp. 335-341, April 2001.

[79] Qiuye Sun, Zhongxu Li, and Huaguang Zhang, **Impact of Distributed Generation on Voltage Profile in Distribution System,** in International Joint Conference on Computational Sciences and Optimization, 2009.

[80] Masato Oshiro, Kosuke Uchida, Tomonobu Senjyu, and Atsushi Yona, **Voltage Control in Distribution Systems Considered Reactive Power Output Sharing in Smart Grid,** in International Conference on Electric Machines and Systems, 2010, 97 pp. 458-463.

[81] S. A. Pourmousavi, A. S. Cifala, and M. H. Nehrir, **Impact of High Penetration of PV Generation on Frequency and Voltage in a Distribution Feeder,** IEEE, 2012.

[82] Edward J Coster, Johanna A Myrzik, Bas Kruimer, and Wil L Kling, **Integration Issues of Distributed Generation in Distribution Grids,** IEEE, vol. 99, January 2011.

[83] Yun Tiam Tan; Kirschen, D.S., **Impact on the Power System of a Large Penetration of Photovoltaic Generation,** Power Engineering Society General Meeting, 2007 IEEE, vol., no., pp.1-8, 24-28 June 2007.

[84] Yun Seng Lim, Jun Huat Tang1, **Experimental study on flicker emissions by photovoltaic systems on highly cloudy region: A case study in Malaysia,** Renewable Energy, Volume 64, April 2014, Pages 61–70.

[85] Y. Liu, J. Bebic, and B. Kroposki, **Distribution System Voltage Performance Analysis for High-Penetration PV**, Energy 2030 Conference, 2008. ENERGY 2008. IEEE. P.1-8.

[86] Srisaen, N.; Sangswang, A., **Effects of PV Grid-Connected System Location on a Distribution System,** Circuits and Systems, 2006. APCCAS 2006. IEEE Asia Pacific Conference on, vol., no., pp.852,855, 4-7 Dec. 2006.

List of Bibliography (Continued)

[87] Mitra, P.; Heydt, G.T.; Vittal, V., **The impact of distributed photovoltaic generation on residential distribution systems,** North American Power Symposium (NAPS), 2012, vol., no., pp.1,6, 9-11 Sept. 2012.

[88] Shayani, R.A.; de Oliveira, M.A.G., **Photovoltaic Generation Penetration Limits in Radial Distribution Systems,** IEEE Transactions on Power Systems. vol.26, pp.1625-1631, Aug. 2011

[89] Qiuye Sun, Zhongxu Li, and Huaguang Zhang, **Impact of Distributed Generation on Voltage Profile in Distribution System,** in International Joint Conference on Computational Sciences and Optimization, 2009.

[90] Danling Cheng, Barry A. Mather, Richard Seguin, Joshua Hambrick, and Robert P. Broadwater, **Photovoltaic (PV) Impact Assessment for Very High Penetration Levels**, IEEE Journal of Photovoltaics. Volume: 6, Issue: 1, Jan. 2016 P. 295 – 300.

[91] Papaioannou, I.T., Bouhouras, A.S., Marinopoulos, A.G., Alexiadis, M.C., Demoulias, C.S., Labridis, D.P., **Harmonic impact of small photovoltaic systems connected to the LV distribution network.** In: Proc. in. Conf. IEEE European Electricity Market, Lisboa, May 2008., P. 1–6.

[92] Batrinu, F., Chicco, G., Schlabbach, J., Spertino, F., **Impacts of grid-connected photovoltaic plant operation on the harmonic distortion.** In: Proc. in. Conf. IEEE, Melecon, May 2006, P. 861–864.

[93] Menti, A., Zacharias, T., Milias-Argitis, J., **Harmonic distortion assessment for a single-phase grid-connected photovoltaic system.** Renew. Energy 36 January 2011, P.360–368.

[94] Schlabbach, J., **Harmonic current emission of photovoltaic installations under system conditions.** In: Proc. in. Conf. IEEE European Electricity Market, Lisboan 2008, P. 1-5.

[95] M.Kesraoui and et al. **Grid connected solar PV system: modeling, simulation, and experimental tests.** Energy Procedia, Volume 95, 2016, Pages 181-188.

[96] Chen Qi and Zhu Ming, **Photovoltaic Module Simulink Model for a Stand-alone PV System.** Physics Procedia 24 (2012) 94 – 100.

[97] Miller N. and Z. Ye. 2003. **Distributed generation penetration study**. National Renewable Energy Laboratory.

List of Bibliography (Continued)

[98] V. H. M. Quezada, J. R. Abbad, and T. G. S. Roman, **Assessment of energy distribution losses for increasing penetration of distributed generation**, IEEE Trans. Power systems 21, 533-540 (2006).

[99] Thomson M. and Infield D. G. 2007. **Impact of widespread photovoltaics generation on distribution systems.** IET Renewable Power Gener. 1:33-40.

[100] S. Cobben, B. Gaiddon, and H. Laukamp, **Impact of photovoltaic generation on power quality in urban areas with high PV population**, PV upscale, 2008.

[101] F. Katiraei, K. Mauch, and L. Dignard-Bailey, **Integration of photovoltaic power systems in high penetration clusters for distribution networks and mini grids**, National Resources Canada, January 2009.
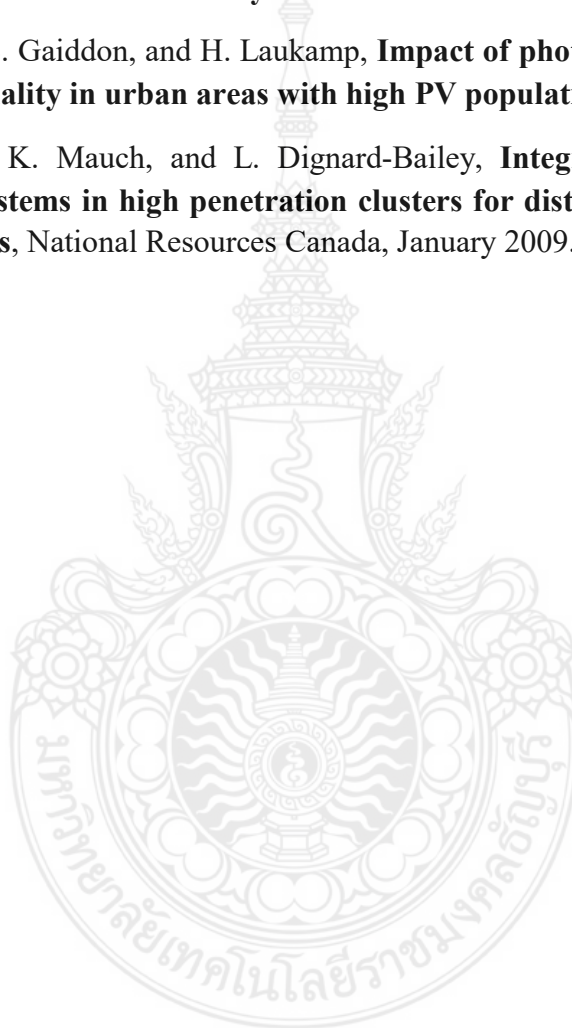
APPENDICES
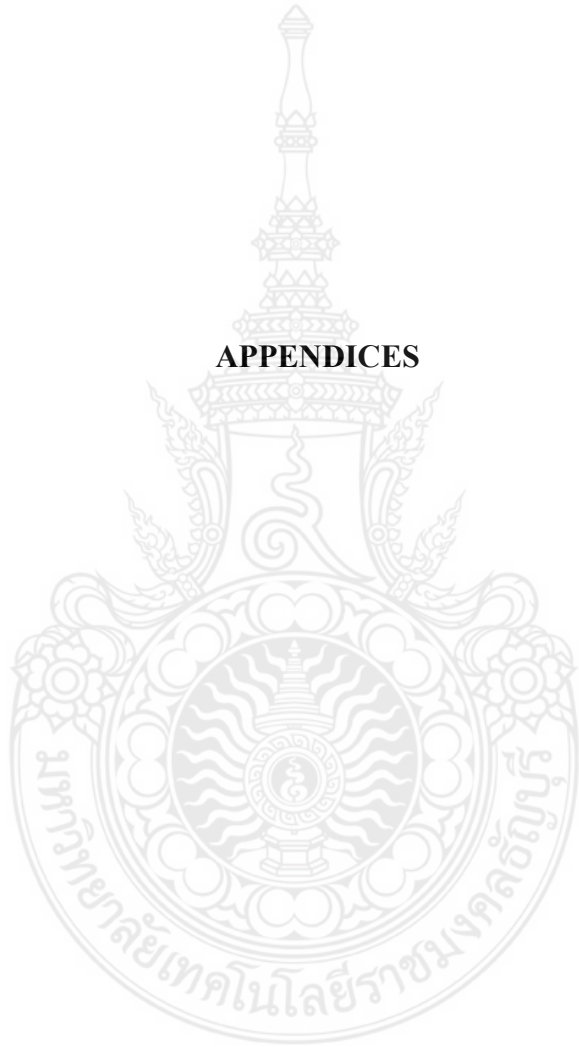
APPENDIX A

Datasheet of Solar Cell
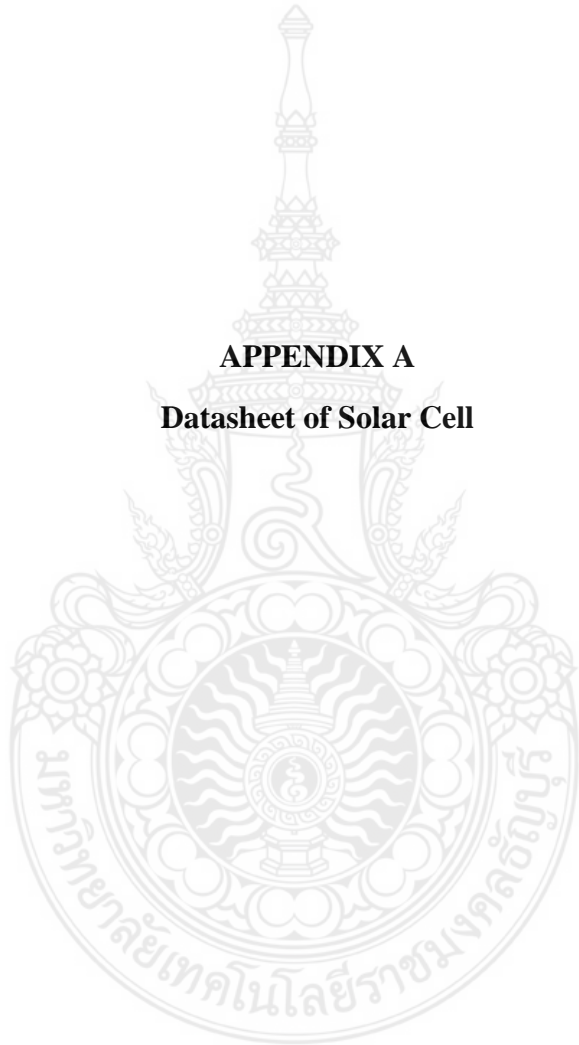
Jinko Solar

JKM265P-60
POLY CRYSTALLINE MODULE
245-265 Watt

Jinko Solar introduces a brand-newline of high performance modules in wide applicaton.

KEY FEATURES

High module conversion efficiency (up to 16.19%), through superior manufacturing technology

Anti-reflective coating improves light absorption and reduces surface dust

Excellent performance in low-light irradiance environment

Entire module certified to withstand high wind loads (2400 Pascal) and snow loads (5400 Pascal)

High salt mist and ammonia resistance

QUALITY&SAFETY

- Positive power tolerance of -0/+3% *
- 10 year warranty on material & workmanship *
- Industry leading power output warranty (12 years/90%, 25 years/80%)
- Premium linear performance warranty *

Premium Performance Warranty

New linear performance warranty
standard performance warranty

Additional value from Jinko Solar's linear warranty
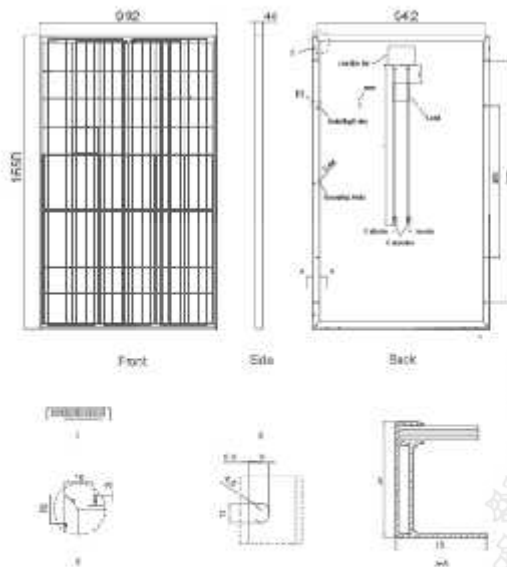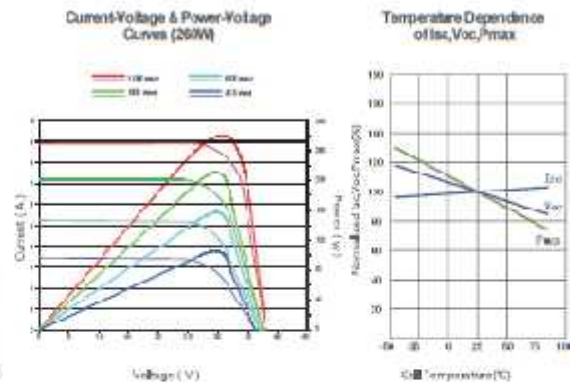
*Based on customer requirements and contract terms

ISO9001:2008、ISC14001:2004、CHSAS18001 certified factory
IEC61215、IEC61730、IEC61701、IEC62716 certified products

Engineering Drawings

Front   Side   Back

Packaging Configuration

(Two boxes = One pallet)

25pcs/ box, 50pcs/pallet, 700 pcs//0'4Q Container

Electrical Performance & Temperature Dependence

Current-Voltage & Power-Voltage Curves (260W)

Temperature Dependence of Isc, Voc, Pmax

Mechanical Characteristics

Cell Type	Poly-crystalline 156x156mm (6 inch)
No of cells	60 (6×10)
Dimensions	1650×992×40mm (65.00×39.05×1.57 inch)
Weight	18.5 kg (40.8 lbs)
Front Glass	3.2mm, High Transmission Low Iron Tempered Glass
Frame	Anodized Aluminium Alloy
Junction Box	IP67 Rated
Output Cables	TÜV 1~4.0mm², Length 900mm

SPECIFICATIONS

Module Type	JKM245P		JKM250P		JKM255P		JKM260P		JKM265P	
	STC	NOCT	STC	NOCT	STC	NOCT	STC	NOCT	STC	NOCT
Maximum Power (Pmax)	245Wp	181Wp	250Wp	184Wp	255Wp	188Wp	260Wp	193Wp	265Wp	197Wp
Maximum Power Voltage (Vmp)	30.1V	27.8V	30.0V	28.0V	30.8V	28.8V	31.1V	28.7V	31.4V	29.0V
Maximum Power Current (Imp)	8.14A	6.50A	8.20A	6.60A	8.28A	6.63A	8.37A	6.71A	8.44A	6.70A
Open-circuit Voltage (Voc)	37.5V	34.8V	37.7V	34.9V	38.0V	35.2V	38.1V	35.2V	38.6V	35.3V
Short-circuit Current (Isc)	8.76A	7.16A	8.85A	7.21A	8.92A	7.26A	8.98A	7.31A	9.03A	7.38A
Module Efficiency STC (%)	14.97%		15.27%		15.58%		15.89%		15.19%	
Operating Temperature(°C)	-40°C~+85°C									
Maximum system voltage	1000V/DC (IEC)									
Maximum series fuse rating	15A									
Power tolerance	0~+3%									
Temperature coefficients of Pmax	-0.41%/°C									
Temperature coefficients of Voc	-0.31%/°C									
Temperature coefficients of Isc	0.06%/°C									
Nominal operating cell temperature (NOCT)	45±2°C									

STC: Irradiance 1000W/m²   Cell Temperature 25°C   AM=1.5

NOCT: Irradiance 800W/m²   Ambient Temperature 20°C   AM=1.5   Wind Speed 1m/s

* Power measurement tolerance: ± 3%

APPENDIX B

PSCAD Application Note
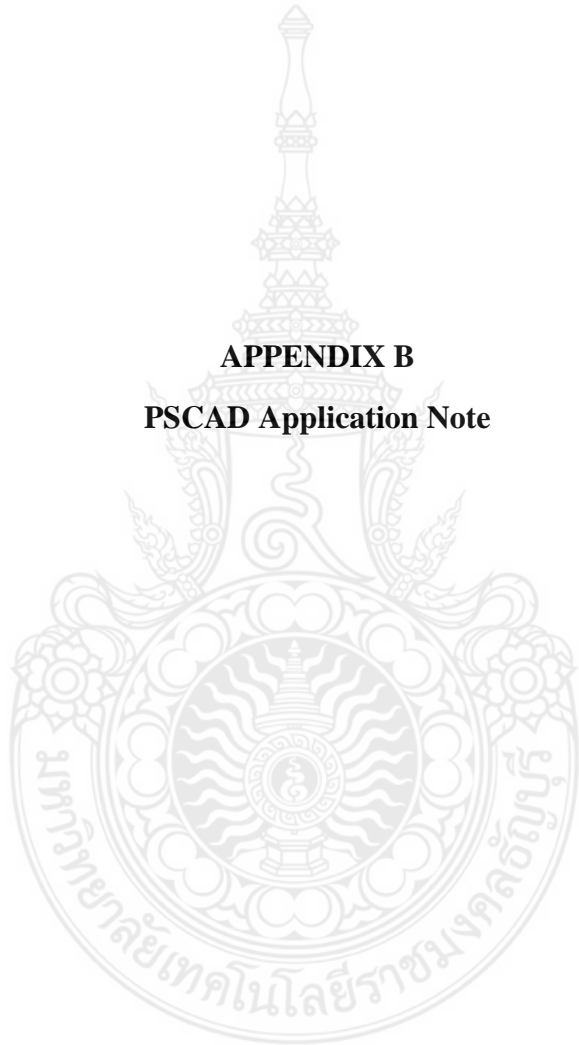
PSCAD Application Note

2-Quadrant AC-DC Conversion using VSC: The Active Rectifier Scheme

Original
September 2007

Revised
June 2016

1 Introduction

Bidirectional ac-dc conversion is applied when an ac system is linked to a dc system and needs to swap the role of source or load with the dc side; in other words, the direction of real power flow between the two systems may switch continually. Voltage-sourced converter (VSC) is one of the power electronics-based topologies employed in such applications. Variable-speed ac motor drives with energy-recovery regenerative braking[1], VSC-based HVDC transmission, FACTS devices such as STATCOMs[2], UPFCs, etc. are common examples of bidirectional ac-dc conversion. This application note explains this scheme through an example implemented in PSCAD™/EMTDC.

The converter links a 3-phase ac source to a dc load/source through a voltage-sourced converter (VSC). The VSC employs a voltage-sourced converter and

2 System Description

2.1 Power Circuit

Figure 2-1 illustrates the layout of the model in PSCAD™. The ac side of the converter is supplied by a voltage source 3-phase 208V 60Hz. The VSC comprises 6 IGBT-diode pairs, which form a 2-level 3-pole bridge, as shown in Figure 2-1. The electrical characteristics
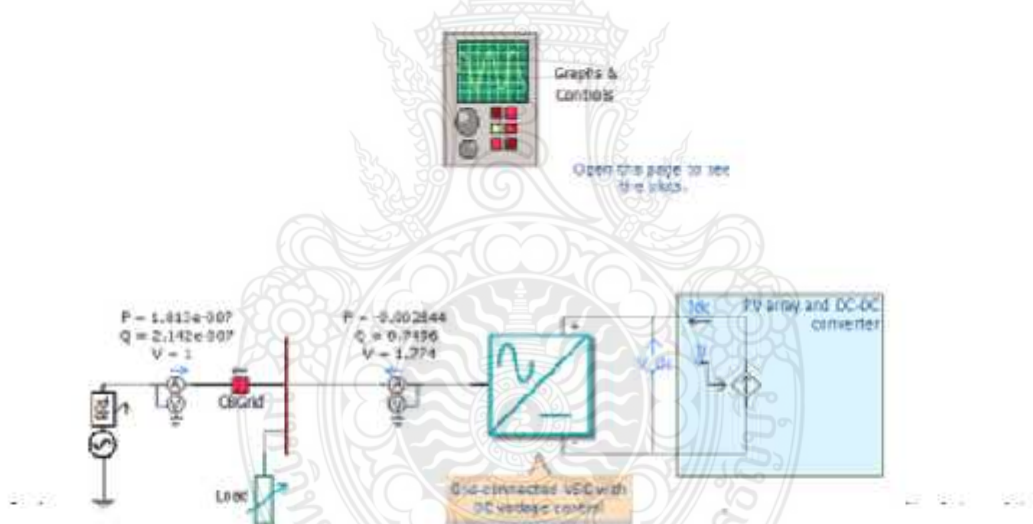

Figure 2-1. VSC-based ac-dc converter

1- In this type of regenerative braking, power is returned to the ac source through the braking period.

2- In a STATCOM, real power is exchanged between the ac and dc sides to regulate the dc-link voltage.
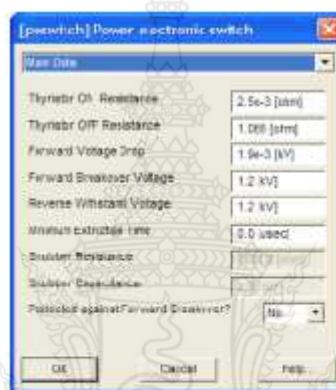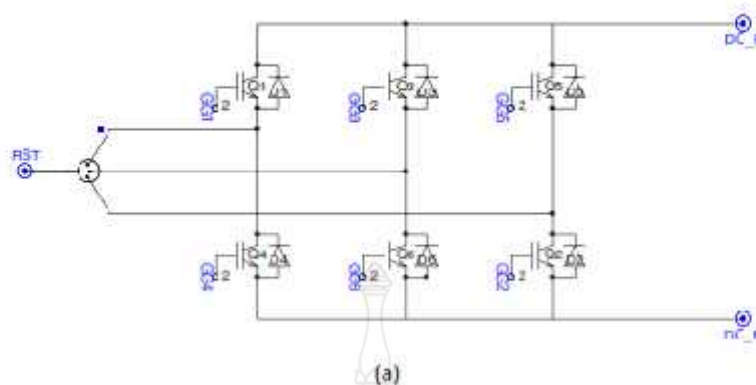
(a)

(b)

Figure 2-2: a) 3-pole IGBT-diode bridge; b) The electrical characteristics of the switching components.

The dependent current source at the dc side represents the dc system, which can either absorb or produce power, depending on the sign of the signal I.

Sinusoidal pulse-width modulation (SPWM) switching technique was chosen in this example. The carrier frequency has been set to 7kHz. Designed for a cutoff frequency of 1.55kHz, the low-pass LCL filter unit at the ac side of the VSC eliminates high-frequency switching disturbances from the 60 Hz current and voltage waveforms. Figure 2-3 displays the 3-line layout of the filter.
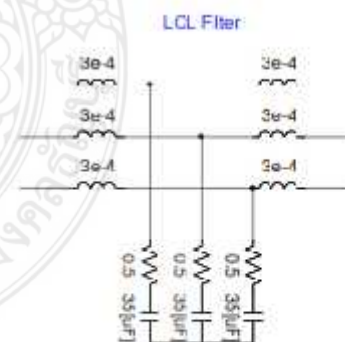

Figure 2-3: The LCL low-pass filter.

2.2 Control Algorithm

Vector control strategy is used in this example. In this technique, the ac current of the VSC is controlled to adjust active power exchange between the ac and dc sides, as well as the reactive power level at the ac terminals of the VSC [1]. The control system block diagram of the model can be found in the *Rectifier Control* function block in Figure 2-1.

The block diagram of the control strategy is presented in Figure 2-4-b. The ac current phasor of the VSC (I_C signal in Figure 2-1) is decomposed into direct (d) and quadrature (q) components, which are in-phase with, and perpendicular to, the ac **phase** voltage E, respectively. The direct component of the ac current i_d regulates the active power transfer between the ac and dc sides. Hence, the dc-link voltage can be adjusted by controlling i_d. The reactive power level at the ac terminals of the VSC can be regulated by controlling of the quadrature component i_q.
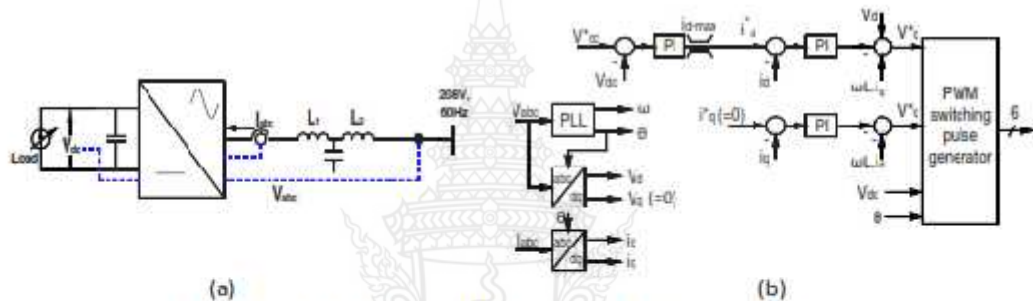

Figure 2-4: The current control strategy for the 2-quadrant VSC:
a) The converter and the measured quantities; b) The control algorithm.

Decomposition of the ac current vector d and q components is carried out by applying the Park transform. The Park transform requires a reference phase angle to map 3-phase quantities onto the d-q coordinates. In this application, the ac phase voltage is chosen as the reference vector, whose phase angle information can be obtained using a phase-locked loop (PLL). Figure 2-5 shows the PLL block in PSCAD™. This block is available in Master Library\CSMF.
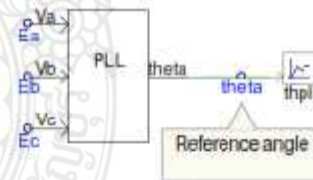

Figure 2-5: The PLL block in PSCAD™ extracts the phase angle information of the phase voltage vector.

The output of the PLL (i.e. $\angle E_a$) is applied to the Park transform blocks. The 3-phase ac currents are mapped onto the d-q reference frame as depicted in Figure 2-6. The function blocks shown in this figure are user-defined components and are provided in the attached library file ABC_DQ_Transforms.psl'.

117

The three regulators in the control algorithm are implemented using PSCAD™ standard Master Library components, such as summation, PI controller, gain, etc. (see Figure 2-7). The Optimum Run feature of PSCAD/EMTDC can be employed to tune the parameters of the regulators.
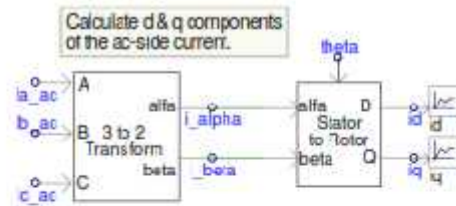

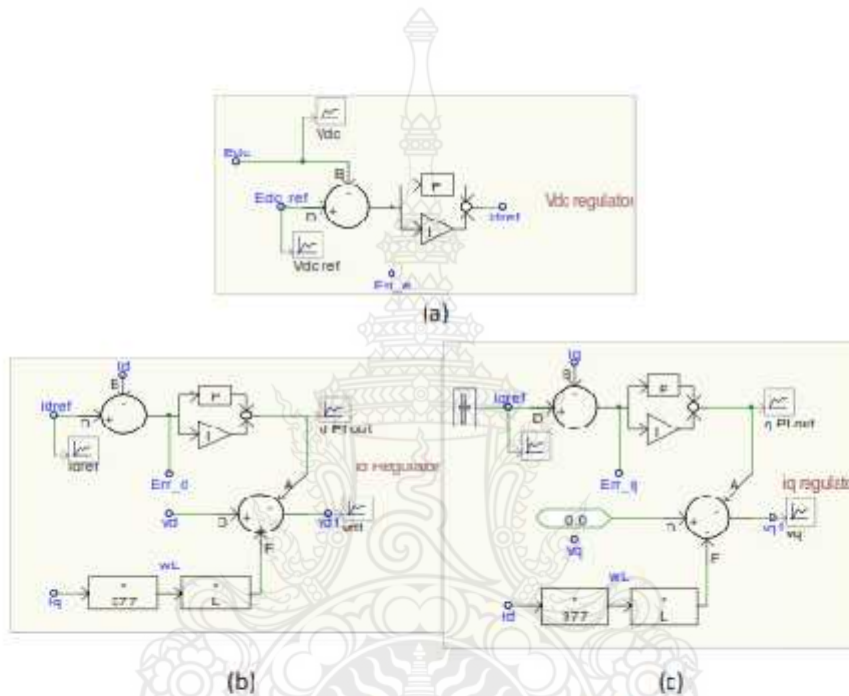Figure 2-6: Park transform, applied to the VSC 3-phase currents.

Figure 2-7: Three control loops of Figure 2-4, modeled in PSCAD.

The regulators provide the set points v_d^* and v_q^*. Modulation waveforms Ref_a, Ref_b and Ref_c are obtained by applying Inverse Park transform to v_d^* which are subsequently applied to inverse Park transform blocks to v_d^* and v_q^*, as depicted in Figure 2-8.
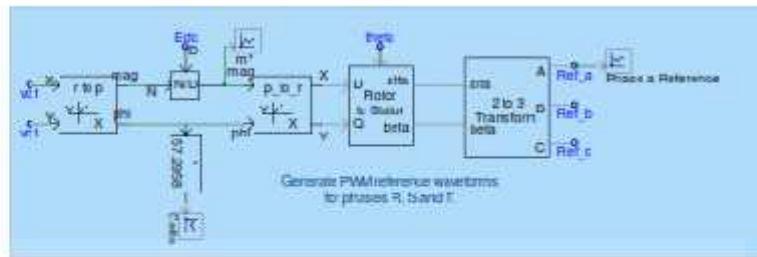
Figure 2-8: Generation of modulation waveforms

PWM switching pulses are produced by comparing the modulation waveforms (Ref_a, Ref_b and Ref_c in Figure 2-8) with a triangular carrier signal, through six 'Interpolated Firing Pulses' blocks, found in Master Library/HVDC_FACTS_PE.

The 'Variable-Frequency Saw-tooth Generator' block (in Master Library/CSMF) produces the carrier signal.
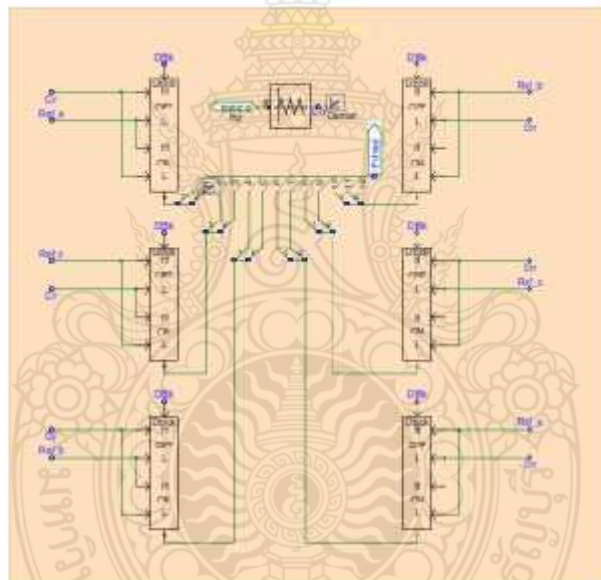

Figure 2-9: PWM switching pulse generation

Responses of the system to a few dc load disturbances are shown in Figure 2-10. In this simulation, the dc-link voltage has been set to 370V.

In Figure 2-10-a, the VSC starts and raises the dc voltage to 370V. In Figure 2-10-b, a 28A load is applied to the dc link. It can be observed that the converter's control system restores the dc-link voltage. Similar response is presented in Figure 2-10-c, where the dc-side current switches from +28A to -28A, causing the VSC to transfer power from the dc link to the ac system. Again, one can notice that the dc-link voltage is maintained at 370V.
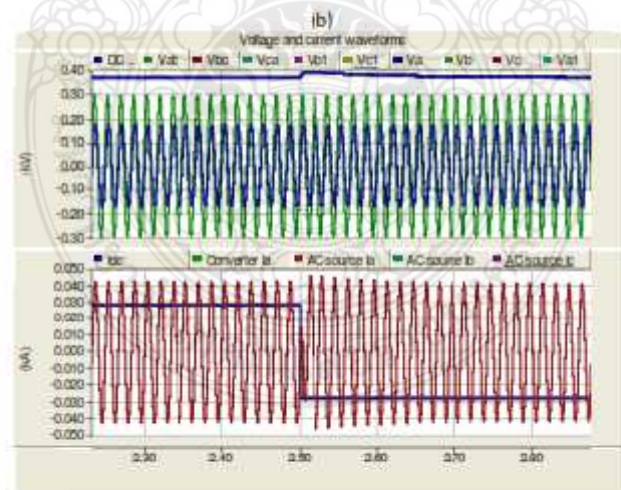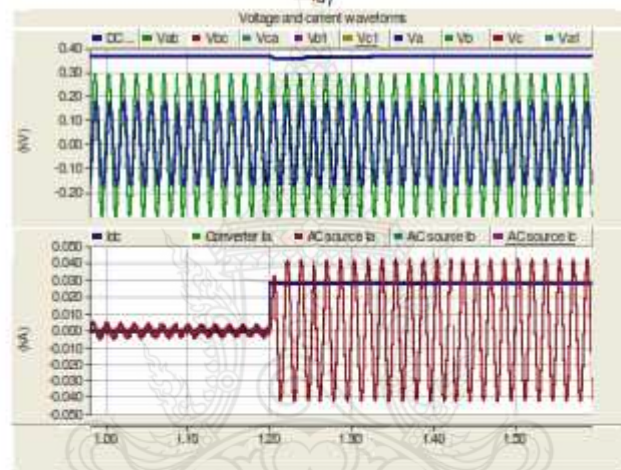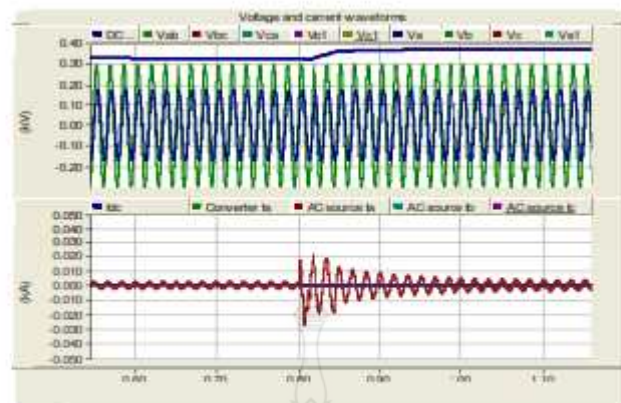
Figure 2-10: Response of the ac-dc converter to dc load disturbances.
a) Startup: The dc voltage is adjusted to 370V;
b) Response of the VSC to a +28A dc load;
c) Response of the VSC to a -56A dc load disturbance

3 References

[1] R. Peña et al. 'Doubly Fed Induction Generator Using Back-to-Back PWM Converters and its Application to Variable-Speed Wind-Energy Generation', IEE Proc. Electrical Power Applications, Vol. 143, No. 3, May 1996, pp. 231-241.

APPENDIX C

List of Publications

List of Publications

International Journal

Thanomsat, N.; Plangklang, B.; Ohgaki, H. **"Analysis of Ferroresonance Phenomenon in 22 kV Distribution System with a Photovoltaic Source by PSCAD/EMTDC."** Energies 2018, 11, 1742. Impact Factor 2017= 2.676, Quartiers 2017 = Q1, https://www.mdpi.com/

Nattapan Thanomsat, Boonyang Plangklang. **"Modelling of a micro grid PV rooftop system by PSCAD."** Applied Mechanics and Materials 2016-02-08, Vol. 839, pp 34-38. Impact Factor 2016 = 0.12, Quartiers 2017 = Q4, https://www.scientific.net/AMM.839.34

International Conference

N.Thanomsat, B.Plangklang. **"Analysis of Power Output Impact on PV Rooftop System Under Different Installation Positions by PSCAD."** The 12th EMSES 2015. Energy Procedia Volume 89, June 2016, Pages 149-159.
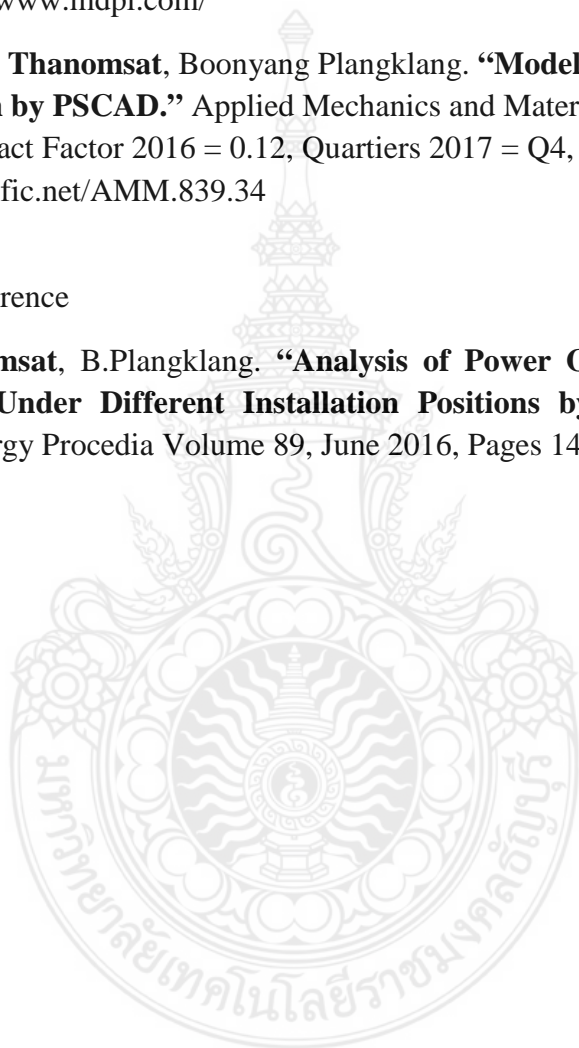
Biography

Name - Surname	Mr. Nattapan Thanomsat
Date of Birth	12 February 1975
Address	139/137 M.1, Samedt District, Muang, Chonburi, Thailand, 20000
Education	B.E. in Electrical Power, Mahanakorn University of Technology.
	Dipl.-Ing. Energiesystemtechnik, Technische Universitaet Clausthal, Germany.
	Doctor of Engineering Program in Energy and Materials Engineering (International Program) Faculty of Engineering, Rajamangala University of Technology Thanyaburi.
Experiences Work	Senior Electrical Engineer and Radiation Safety Officer, Autoclaved Aerated Concrete Product CO., Ltd.
	Lecturer, Department of Electrical Engineering, Faculty of Engineering, Burapha University.
Telephone Number	086 777 1511
Email Address	nattapan@eng.buu.ac.th